NOTE TO USERS

This reproduction is the best copy available.

RICE UNIVERSITY

Metal Ion Interactions with Single Walled Carbon Nanotubes

by

Jonathan Joseph Brege

A THESIS SUBMITTED
IN PARTIAL FULFILLMENT OF THE
REQUIREMENTS FOR THE DEGREE

Doctor of Philosophy

APPROVED, THESIS COMMITTEE:

Andrew R. Barron, Chair
Charles W. Duncan, Jr. – Welch Chair of Chemistry and Professor of Materials Science

Lon J. Wilson, Professor of Chemistry

Kevin Kelly, Associate Professor of Electrical and Computer Engineering

HOUSTON, TEXAS

January 2009

ABSTRACT

Metal Ion Interactions with Single Walled Carbon Nanotubes

by

Jonathan J. Brege

The optical properties of single walled carbon nanotubes were probed for their various responses in the presence of a wide range of metal ion compounds. The effects of both the metal ion and the counter ion on the fluorescence of SDBS-surfacted single walled carbon nanotubes (SWNTs) have been investigated for solutions of Group 2, 12, and 13 metal salts with a $[M^{n+}]$ of between 0.5 - 5 mM per 15 $mg.L^{-1}$ of SWNT. The decrease in fluorescence is found to be due to quenching. The Stern-Volmer quenching constants are found to depend on the identity of the metal ion, the anion, and the diameter (related to the n,m value) of the SWNT. Overall there is a dependence on the ionic radius of the metal: ions with a radius less than 1 Å exhibit little quenching, but those with radii greater than 1 Å show increasing quenching efficiency with increased size. The Stern-Volmer quenching constants for a particular metal/anion combination show a linear correlation with the SWNT band gap and an inverse, but equal, relationship for the diameter of the SWNT. We propose that the SWNT exciton formed from light absorption is sensitive to its local environment, and that the field around metal ions has a significant effect on the exciton facilitating non-radiative decay paths

The ability of cobalt, copper, and nickel salts to quench SDBS surfacted SWNTs has been studied. Increased quenching is observed with transition metal ions as compared to their Group 2 and 12 analogs. This differs from the established charge versus ionic-volume trend observed with the latter. Some of this apparent increase is due to absorption by aggregates formed between the metal ions and the surfactant; however, these effects can be mitigated by centrifugation. Despite removal of any aggregates, the transition

metals still show greater quenching efficiency than their main group homologs. This observed effect is proposed to be due to a strong $M^{2+}\cdots$SDBS attractive interaction causing a large concentration of ions near the nanotube surface compared to their Group 2 and 12 counterparts.

To further understand metal ion interactions with SWNTs, a comparative study between the surfactant SDS and SDBS was conducted, which allowed for an indirect observation of the structure of the surfactant-SWNT conjugates. Greater quenching by Group 2 ions (higher K_{sv}) was observed for SDBS-SWNTs as compared to SDS-SWNTs, which is consistent with the metal being held closer to the SWNT surface. Group 12 metal ions cause ground state changes for SDS-SWNT conjugates indicating a rearrangement of the surfactant micelle.

The observation of an enhanced quenching mechanism characteristic found in transition metal quenching led to the development of a hydrophobically immobilized surfactant template for the synthesis of ultra-small copper nanoparticles. The particles are produced by N,N,N',N'-tetramethyl-*p*-phenylenediamine (TMPDA) reduction of aqueous Cu^{2+} on a hydrophobically immobilized sodium dodecylbenzene sulfonate (SDBS) surfactant template in the presence of sodium citrate at room temperature. Single walled carbon nanotubes (SWNTs) act as a scaffold controlling the size of the SDBS micelle, which in-turn confines a limited number of copper ions near the nanotube surface. TMPDA reduction forms copper nanoparticles that are less than 2 nm. Particles formed in the absence of the SWNT immobilizer range from 2 to 150 nm.

"Other things may change us, but we start and end with family."

-Anthony Brandt

Acknowledgments

First and foremost I need to thank my advisor, Dr. Andrew Barron. Dr. Barron has supplied me with every educational and financial resource that I have needed during my tenure at Rice and has helped mold me into the chemist that I am today. His never-ending passion for nanotechnology and insatiable work ethic has inspired me to apply those qualities to my own professional development and for that I will be forever grateful.

I would also like to thank my other two committee members, Dr. Kelly and Dr. Wilson. Both outstanding faculty members have generously given their time to guide me during the thesis writing period. Dr. Wilson, in particular, has been an inspiration to me before I began my time at Rice. During my visitation it was his down to earth, laid back and caring personality that ultimately led me to choose Rice as my institution for higher learning. Even though he may not have realized it, he continued to mentor me through his course instruction and "elevator talks" during all my years of study. I will never forget his contributions to my maturity as a chemist and as a person.

An educator is of vital importance for they not only teach you material but they ultimately teach you how to teach what you have learned to others. A key person in my development as a future educator was Dr. Mc Hale. Her generous support and calm nature have shown me what a good educator acts like and the patience that they have towards their students. I hope to parlay her teachings into a future career as a professor.

Family provides you with a foundation for all the decisions you make in your life. I have been fortunate to be surrounded by several families that have supported me throughout my time in higher education. First and foremost, I thank my biological family for inspiring, supporting, and loving me through my doctoral journey. Specifically; Mom, Dad, Jane, John, Jill, Kevin, Ben, Christina, Josh and Rachel. My family has gone above and beyond with emails, cards, letters and visits to Texas to show their support of my educational pursuits. I also thank the little ones- Daniel, Austin, Isaac, Katelyn, Kylee

and Chelsea for motivating me to pursue my absolute potential. I hope that my accomplishments inspire them to seek higher education in the future.

The second family that has been instrumental in my education is my Barron Lab Family. Together we have grown and transformed not only as chemists, but as people. I could not be where I am today without the immense help and encouragement of Chris Crouse, Chris Hamilton, Amanda, Nadjmeh and Huma. My bartending partner, Alvin, has helped me in good times and bad and my drinking partner Eoghan was always there to pick me up on an off day. My times hunting and fishing with Chris Crouse and JT are some of my fondest memories of my time at Rice and I thank them both immensely for giving me the opportunity to share in their lives. My Texas families have supported me daily and during all major holidays. The Mayos and the Alexanders have helped me start my home away from home. Though it is difficult to be so far from immediate family, life is a lot easier when you feel like a part of one where you live. I thank both families for including me in all events and generously inviting me to all their family holiday gatherings.

I spent many sleepless nights working vigorously with my writing companion Truman, and I thank him for keeping me company during those tiring times. My greatest appreciation goes to Kelley, the love of my life. You were always there to lift my spirits during the difficult times and smile with me during the joys and celebrations. It has been an amazing journey with you that I am looking forward to continuing.

Table of Contents

List of Figures

Introduction

Chapter 1

Chapter 2

Chapter 3

Chapter 4

List of Tables

Abbreviations and Glossary

Å	angstrom(s), 10^{-10} m
AFM	atomic force microscopy
°C	degrees centigrade
ca.	*circa*, approximately
cm	centimeter, 10^{-2} m
δ	delta, chemical shift (NMR)
e.g.	*exempli gratia*, for example
Eq.	equation
et al.	*et alia*, and others
g	gram
ICP-AES	inductively couple plasma atomic emission spectroscopy
i.e.	*id est*, that is (to say)
IR	infrared spectroscopy
K	Kelvin
λ	lamda, wavelength
L	liter(s), ligand
M	molar, $mol.L^{-1}$
MWNT	multi-walled carbon nanotube
μm	micrometer(s), 10^{-6} m
mg	milligram(s), 10^{-3} g
mL	milliliter(s), 10^{-3} L
mM	millimolar, 10^{-3} M
M_W	molecular weight
min	minute(s)
mol	mole(s)

mmol	millimole(s), 10^{-3} mol
nm	nanometer(s), 10^{-9} m
n,m	single-walled carbon nanotube chirality vector
rpm	revolutions per minute
SWNT	single-walled carbon nanotube
SDBS	sodium dodecyl benzene sulfonate
SDS	sodium dodecyl sulfate
SV	Stern-Volmer
TEM	transmission electron microscopy
UV-vis	ultraviolet/visible spectroscopy
XRD	X-ray diffraction
UV-vis	ultraviolet/visible spectroscopy

Introduction

One of the seminal discoveries in nanotechnology is of the parent fullerene, C_{60}, three decades ago by Smalley, Kroto, and Curl.[1] Fullerenes are a carbon allotrope composed entirely of sp^2 carbon to form either a hollow sphere, ellipsoid, or tube. Single walled carbon nanotubes (SWNTs), double walled carbon nanotubes (DWNTs), and multiple walled carbon nanotubes (MWNTs) are all examples of tubular fullerenes. Of all the carbon allotropes, SWNTs are now at the forefront of nanotechnology, materials, and chemical research. Since their discovery by Iijima in 1991,[2,3] their unique physical (e.g., hardness, thermal and electrical conductivity, and high Young's modulus) and optoelectronic (fluorophores, semiconducting, or metallic) properties have made these materials very popular for applications in the areas of medicine, electronics, optics, energy, health, and sensing. As with the discovery of any new science field, much work needs to be put into researching the fundamental properties of the materials.

Single walled carbon nanotubes. A SWNT can be envisioned by rolling a two dimensional graphene sheet into a seamless tube such that all the carbon atoms align. A typical tube is 1 to 2 nm in diameter with varied lengths into the micron region. This restriction in the diameter with long lengths yields a virtually one-dimensional system or quasi-one-dimensional system. The high aspect ratio material has a similar electronic structure to graphene. All the carbon atoms are sp^2 hybridized, forming 3 σ-bonds with adjacent carbons and a p electron that is part of the extended π-electron system. As one can imagine, there are multiple (but not infinite) ways to construct a SWNT depending on the angle at which the graphene sheet is rolled. To better classify SWNTs, a nomenclature is employed where a chiral vector (n,m) designates the angle of rolling, also known as the chiral angle (θ). There are three designated SWNT types: zigzag, armchair, and chiral as depicted in Figure I.1. Zigzag tubes are formed when the

graphene sheet is rolled at $\theta = 0°$; these easily identified by their $(n,0)$ or $(0,m)$ index. Armchair SWNTs are recognized by the n = m index with $\theta = 30°$. Armchair SWNTs have symmetry through a mirror plane; therefore, they are considered achiral. Last of the named SWNTs are chiral, where $n \neq m$ and angles are formed in the range of $0° < \theta < 30°$. Depending on their chiral angle, SWNTs can be either metallic or semiconducting.[4] Nanotubes are metallic when $n - m = 3k$ and k is an integer. Thus, all armchair SWNTs and one-third of zigzag SWNTs are metallic. All other SWNTs, roughly two-thirds, are semiconducting; the valence and conduction bands of these SWNTs are dependent on the chiral angle. The plot in Figure I.2 depicts the different n,m rolling vectors on a graphene sheet used to obtain the various chiralities of SWNTs. The metallic tube indices are highlighted in red while the semiconducting tubes are in black. There is an inverse but not linear relationship between the diameter and bandgap of semiconducting nanotubes.

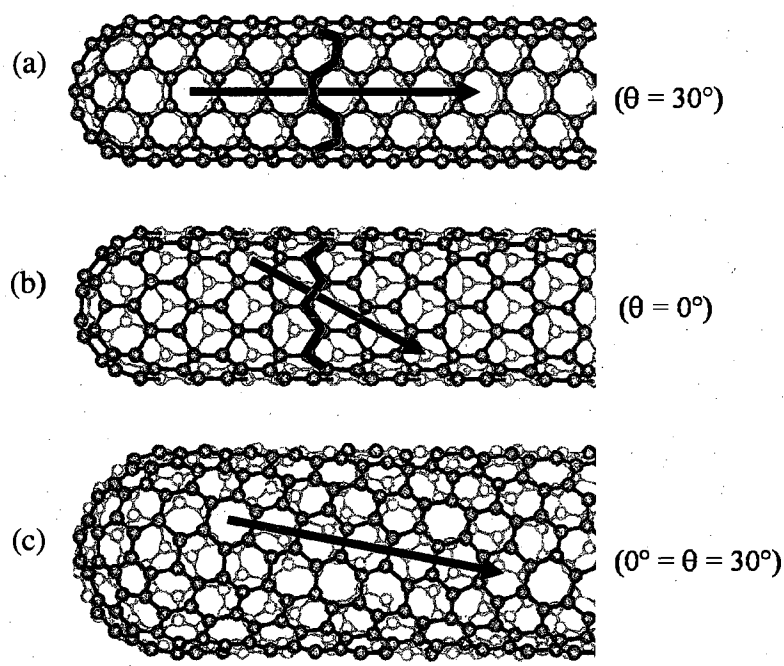

Figure I.1. Models of the various types of SWNTs: (a) armchair, (b) zigzag, and (c) chiral structures.[5]

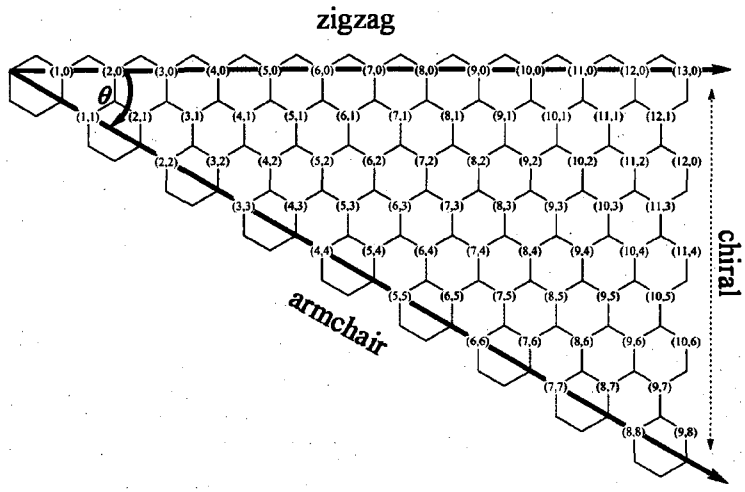

Figure I.2. Visualization of the different vectors to obtain the various (*n*, *m*) chiral SWNTs.

The unique physical structure of SWNTs gives rise to distinctive electronic properties. The quasi-one-dimensionality of the nanotube causes the overlap of partially filled orbitals along the axis to be extremely long compared to the perpendicular direction forming distinct van Hove singularities. A schematic for the density of states for a semiconducting tube is shown in Figure I.3. The optical transitions depicted reveal possible absorption ($V_2 \rightarrow C_2$) and emission ($C_1 \rightarrow V_1$) pathways in semiconducting SWNTs. The mechanism of emission in SWNTs was first elucidated by Weisman and coworkers in 2002.[6] This revelation led to the detection of individual semiconducting SWNTs in solution using fluorescence spectrometry. Later work utilized calculations to assign optical transition energies to specific structures.[7] By using a 2-dimension excitation/emission scan, it is possible to detect a plethora of semiconducting *n,m* species as shown in Figure I.4. Monitoring the emission intensities of a large number of SWNTs is appealing but very time consuming and not viable for many experimental processes. Careful investigation of the spectra reveals that over 43 different semiconducting species can be observed by exciting at just two wavelengths, 660 nm and 785 nm. Furthermore, by deconvoluting the spectra as in Figure I.5, one can determine the intensity contribution

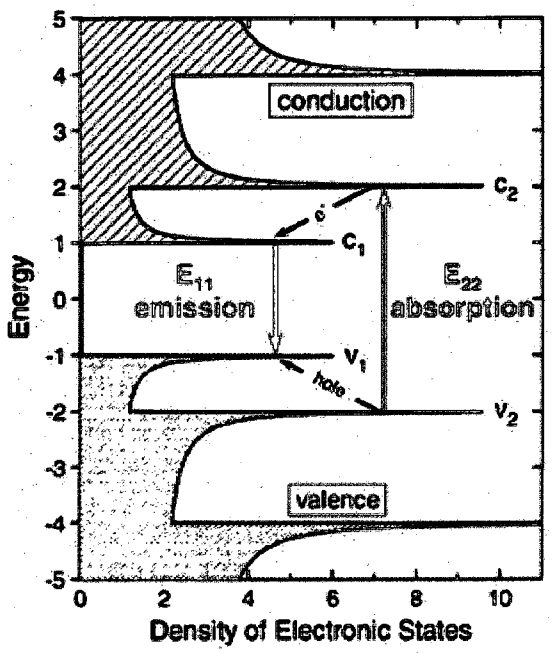

Figure I.3. The electronic density of states with van Hove singularities for a semiconducting SWNT showing absorption and emission pathways.[8]

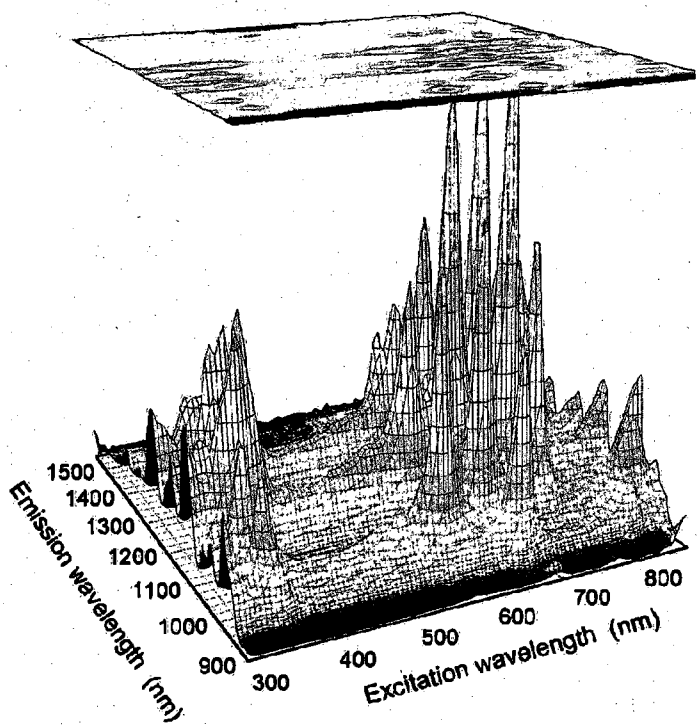

Figure I.4. The photoluminescence map of semiconducting tubes when a full two-dimension scan is conducted.[9]

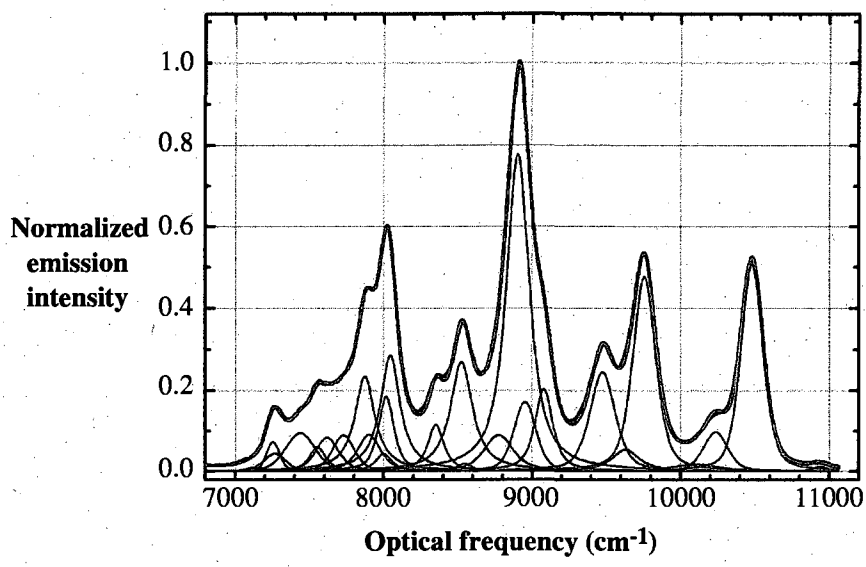

Figure I.5. Deconvoluted fluorescence spectra (660 nm excitation) of SDBS-SWNTs showing the measured (blue line), simulated (red line) spectra, and the basis functions (black lines).[10]

from each individual tube. Through this new technology, the emission properties of over 43 different chiralities can be monitored simultaneously and quantitative data can be obtained for individual chirality SWNTs.

A few areas of the mechanism of fluorescence for carbon nanotubes can be deciphered from our knowledge of surfactant interactions with graphene. First, surfactant preferentially exists at any liquid/air or liquid/solid surface boundary to minimize hydrophobic repulsions. For this system, it includes surfactant adsorbed onto the surface of the hydrophobic nanotube and the air/water interface. Additional surfactant molecules will be free in solution or will form spherical micelles that are not interacting with the nanotubes. It is possible for free molecules in solution to exchange with surfactant molecules on the surface of the nanotube or exchange with molecules within the micelles. The rate of exchange of free molecules with surfactant molecules hydrophobically

immobilized on the surface should be much slower than exchange with the surfactant molecules in a micelle. Therefore, surfactant molecules near the nanotube surface are "static" while those in solution are "dynamic." Surfactant–nanotube interactions play a vital role in the fluorescence of SWNTs because without good solubilization, no fluorescence is observed.

Fluorescence Quenching of SWNTs. Several processes must take place for an emission event in the form of fluorescence to occur. First, the molecule must absorb a photon of sufficient energy to promote an electron to an excited state (see Figure I.3). When the molecule relaxes, an electron radiatively decays to the ground state through the emission of a photon of lower energy. When a fluorophore's emission ceases, it is said to have been quenched. General fluorescence quenching can occur through a variety of pathways.[11] Ground state quenching occurs when some interaction prevents the molecule from absorbing an electron; therefore no radiative decay can occur. This type of quenching is most easily detected by a change in the absorption spectra. In excited state quenching, the fluorophore absorbs a photon, but instead of radiatively decaying, the ground state is reached by some other non-radiative relaxation process. The exact mechanism varies depending on the fluorophore and the quencher. In addition to the two aforementioned general mechanisms of fluorescence quenching, there are a few de-excitation pathways that are unique to SWNTs.

Fluorescence can be perceived as an electron transfer process (in the form of photon emission), and quenching can be envisioned as the disruption of this process. Therefore, any circumstance that affects an electron transfer event can cause quenching in SWNTs. A sample of raw SWNTs, dispersed in solution, contains both metallic tubes with no bandgap and semiconducting tubes with varied bandgaps. Lack of sufficient surfactant or disruption of the micelle around the SWNTs causes nanotubes to bundle. Fluorescent semiconducting tubes bundle with non-emissive metallic tubes, allowing

intertube energy transfer. Upon excitation, an electron in a semiconducting SWNT is promoted to a higher energy level. Instead of radiative decay, the excited state transfers its energy to a metallic tube which is in physical contact with the semiconducting SWNT, and non-radiative decay occurs. This ground state process is easily observed by absorption spectroscopy, where a broadening and shifting of the absorption bands is prominent.

As promising as SWNTs are for use as fluorophores, there is relatively little work published concentrating on their quenching or electron transfer processes. For example, it has been reported that the bleaching of nanotube fluorescence and absorbance spectra from the reaction of surfacted SWNTs with small organic electron-acceptor molecules depends solely on the reduction potential of the organic molecule.[12] The quenching ability of a particular organic species for a specific chirality tube is controlled by the reduction potential of the dye and the bandgap of the tube. In this example, there is the possibility of specific detection of a particular compound since only SWNTs with bandgaps above a threshold-energy are affected while those under the threshold are unaffected.

A quenching event that is somewhat unique to SWNTs is their sensitivity to pH. Smalley and coworkers have shown that SWNT fluorescence is suppressed in an acidic medium.[13] Also, dissolved oxygen can cause a reduction in SWNT fluorescence, but only when H^+ ions are present.[14] While acid quenching of SWNTs is reversible by simple pH adjustment or removal of dissolved oxygen, other quenching processes are not. Utilizing SWNTs for their physical attributes often involves chemically modifying the structure so that it can be more easily dispersed in a matrix or attached to a surface. Forming covalent bonds to SWNTs transforms their sp^2 carbon atoms to sp^3 atoms by removing an electron from the extended π-electron system. Thus, functionalized SWNTs do not exhibit fluorescence.

Electron transfer processes are common in metals and their ions have been used in emission studies to quench the fluorescence of various organic molecules including pyrenes, anthracenes, flavins, bipyridines, and acridinium ions.[15,16,17,18] Single walled carbon nanotubes are extended polyaromatic molecules and may behave in a manner similar to organic fluorophores. It is crucial to fully discern any metal ion interactions with SWNTs before using them in specific applications.

SWNTs as sensors. Unlike most single molecules[19] or other nanomaterials such as quantum dots,[20] SWNTs exhibit no fluctuations in fluorescence intensity or spectral changes making them attractive fluorophores for sensing applications.[21] Moreover, SWNTs have attractive physical properties for sensing as well. While they typically only have an average diameter of 1 nm and lengths greater than a micron, SWNTs still have a tensile strength up to 60 GPa. Furthermore, all of the atoms of the nanotube are on the periphery, exhibiting a surface area greater than 1000 m^2g^{-1}, making them extremely sensitive to their local environment. The first SWNT-sensor concepts appeared in the literature in 2000.[22,23] The simple system detected electron donor-electron acceptor molecules by monitoring changes in resistance through the bare SWNTs as they came in contact with O_2, NO_2, and NH_3. These initial works set the foundation for using SWNTs as field effect transitors (FETs) to detect a variety of molecules. Recently, a SWNT based sensor utilizing peptides has been developed for the detection of heavy metal ions, in particular, copper (II) and nickel (II).[24] By varying the type of peptide sequences functionalized on the nanotube, a differential preference for metal ions is achieved. The selectivity and sensing in this study are actually achieved through the peptide sequence, which translates to changes in the conductance in the SWNT-FET. During competitive ion experiments with Pb^{2+} and Zn^{2+}, the authors note interference due to a direct interaction between the positive charge of the Pb^{2+} or Zn^{2+} and the nanotube rather than competitive binding of the metal ions with the peptide. This was further observed by a

change in the p-type conductance in the semiconducting SWNT. Due to the interdependency of the electronic and optical properties of SWNTs, it is important to investigate any fundamental interactions that affect the SWNT's fluorescence before they can be applied in electronic applications.

Unfortunately, there appears to be other issues that could complicate any SWNT-based sensor system. The addition of NaCl or $MgCl_2$ to sodium dodecylsulfate (SDS) surfacted SWNTs promotes the selective aggregation of the SWNTs which in-turn results in the quenching of fluorescence.[25] While researchers have probed nanotubes for specific sensing applications, no one has investigated various metal ion effects on nanotubes. Other work has shown that metal salts can interfere with the fluorescence through a bundling mechanism[25] or through a direct interaction with SWNTs.[24] Before SWNTs can be used in sensing applications, a complete understanding of these metal ion interactions is paramount. Therefore, we have investigated fundamental metal ion interactions with SWNTs to quantify quenching events and then applied those concepts to develop a new synthesis technique.

References

1 H. W. Kroto, J. R. Heath, S. C. O'Brien, R. F. Curl, and R. E. Smalley, *Nature*, 1985, **318**, 162.

2 S. Iijima, *Nature*, 1991, **354**, 56.

3 S. Iijima and T. Ichihashi, *Nature*, 1993, **363**, 603.

4 S. M. Bachilo, M.S. Strano, C. Kittrell, R. H. Hauge, R. E. Smalley, and R. B. Weisman, *Science,* 2002, **298**, 2361.

5 Adapted from http://nano.gtri.gatech.edu/Images/MISC/figure4.gif, accessed December 2008.

6 S. M. Bachilo, M.S. Strano, C. Kittrell, R. H. Hauge, R. E. Smalley, and R. B. Weisman, *Science,* 2002, **298**, 2361.

7 R. B. Weisman and S. M. Bachilo, *Nano Lett.,* 2003, **3**, 1235.

8 Image modified from R. B. Weisman and S. M. Bachilo, *Nano Lett.,* 2003, **3**, 1235.

9 http://www.appliednanofluorescence.com/products.html accessed December 2008.

10 Image adapted from J. J. Brege, C. Gallaway, and A. R. Barron, *J. Phys. Chem. C,* 2007, **111**, 17812

11 B. Valeur, *Molecular Fluorescence: Principles and Applications.* Wiley-VCH, Chichester (2002).

12 M. J. O'Connell, E. E. Eibergen, and S. K. Doorn, *Nature Mater.* 2005, **4**, 412.

13 M. S. Strano, C. B. Huffman, V. C. Moore, M. J. O'Connell, E. H. Haroz, J. Hubbard, M. Miller, K. Rialon, C. Kittrell, S. Ramesh, R. H. Hauge, and R. E. Smalley, *J. Phys. Chem. B,* 2003, **107**, 6979.

14 G. Dukovic, B. E. White, Z. Zhou, F. Wang, S. Jockusch, M. L. Steigerwald, T. F. Heinz, R. A. Friesnew, N. J. Turro, and L. E. Brus, *J. Am. Chem. Soc.,* 2004, **126**, 15269.

15 C. Hariharan, V. Vijaysree, and A. K. Mishra, *J. Lumen.,* 1997, **75**, 205.

16 C. Hariharan and A. K. Mishra, *Radiation Measurements,* 1998, **29**, 473.

17 F. Grieser and R. Tausch-Treml, *J. Am. Chem. Soc.,* 1980, **102**, 7258.

18 A. W. Varnes, R. B. Dodson, and E. L. Wehry, *J. Am. Chem. Soc.,* 1972, **94**, 946.

19 J. K. Trautman, J.J. Macklin, L. E. Brus, and E. Betzig *Nature,* 1994, **369**, 40.

20 M. Nirmal, B. O. Dabbousi, M. G. Bawendi, J. J. Macklin, J. K. Trautman, T. Harris, and L. E. Brus, *Nature,* 1996, **383**, 802.

21 J. Kong, M. G. Chapline, and H. J. Dai, *Adv. Mater.,* 2001, **13**, 1384.

22 J. Kong, N. R. Franklin, C. Zhou, M. G. Chapline, S. Peng, K. Cho, and H. Dai, *Science,* 2000, **287**, 622.

23 P. G. Collings, K. Bradley, M. Ishigami, and A. Zettle, *Science,* 2000, **287**, 1801.

24 E. S. Forzani, X. Li, P. Zhang, N. Tao, R. Zhang, I. Amlani, R. Tsui, and L. A. Nagahara, *Small,* 2006, **2**, 1283.

25 S. Niyogi, S. Boukhalfa, S. B. Chikkannanavar, T. J. McDonald, M. J. Heben, and S. K. Doorn, *J. Am. Chem. Soc.,* 2007, **129**, 1898.

Chapter 1

Fluorescence Quenching of Single Walled Carbon Nanotubes in SDBS Surfactant Suspension by Diamagnetic Metal Ions

Introduction

Single walled carbon nanotubes (SWNTs) exhibit fluorescent properties similar to other polyaromatic analogs containing conjugated π systems such as pyrene, anthracene, graphene, etc. In those systems, the fluorescence is sensitive to ionic strength, pH, self-quenching, paramagnetic effects, and metal ion quenching. Much work has gone into observing this phenomena and quantifying it for practical applications such as sensing and metal ion detection. Carbon nanotubes possess many of the same fluorescent properties as other organic fluorophores but also have the added benefit of simultaneously being a scaffold. This is ideal because unlike the others, a secondary support is not necessary for practical applications. To date, no work has concentrated on the interactions between SWNTs and metal ions even though a few studies appear to have investigated this.

Doorn and coworkers[1] have reported that the addition of NaCl or $MgCl_2$ to sodium dodecylsulfate (SDS) surfacted SWNTs promotes the selective aggregation of the SWNTs. This is not a direct interaction of the metal ions with the SWNTs but rather an interaction between the metal ions and the surfactant. The salts are added until they pull the surfactant off of the nanotubes causing the surfactant to be below the critical micelle concentration (CMC) around the nanotube. The nanotubes bundle and cause a quenching effect of the fluorescence. The SWNT is simply used as a fluorescent probe to give insight to the surfactant absorption onto the different nanotube species. The metal ions act as a way to remove surfactant below the CMC. The same results could be obtained by diluting the SWNT solution to the point where it is below the CMC.

Group 2 and Group 12 metal ions with a +2 oxidation state are similar in many ways. The chloride, sulfate, and acetate salts of each are very soluble in basic solutions. They both have filled outer valence shells. The Group 2 ions have a filled s-orbital in the highest energy state and the Group 12 ions have a filled d-orbital that is at a similar energy. Most interesting for this comparative study, both Groups have similar ionic radii yielding similar charge densities for the +2 oxidation state as outlined in Table 1.1. Also important within a particular Group is a systematic increase in ionic radii allowing for a mechanistic approach in understanding the interactions between these metal ions and SWNTs. In addition, all of these metals ions are diamagnetic in nature, eliminating the possibility of paramagnetic quenching interactions common with other fluorophores.[2,3] In order to further explore this phenomenon and determine the generality of M^{n+} quenching of SWNT fluorescence, we have investigated the charge transfer reaction between sodium dodecylbenzensulfonate (SDBS) surfacted SWNTs with Group 2, 12 and 13 metal ions. Stern-Volmer constants were obtained for each of the metals with 18 different chirality nanotubes.

Table 1.1. Comparison between Group 2 and Group 12 metal ions by size and charge.[4]

Group 2	r (Å)	Charge density ($Z.Å^{-3}$)	Group 12	r (Å)	Charge density ($Z.Å^{-3}$)
Mg^{2+}	0.66	3.03	Zn^{2+}	0.74	2.70
Ca^{2+}	0.99	2.02	Cd^{2+}	0.97	2.06
Sr^{2+}	1.12	1.79	Hg^{2+}	1.10	1.82
Ba^{2+}	1.34	1.49			

Results and Discussion

Individual semiconducting SWNTs dispersed in SDBS surfactant exhibit fluorescence from 660 and 785 nm irradiation.[5] In agreement with our prior studies,[6] the addition of cadmium acetate solution with a [Cd^{2+}] between 0.5 – 5.0 mM per 15 mg.L^{-1} of SWNTs results in the reduction of the fluorescence of the SWNTs. As shown in Figure 1.1, each of the different fluorescing (n,m) nanotubes is affected by the presence of the Cd^{2+} ions, and all of the semiconducting nanotubes exhibit a decrease in fluorescence intensity with increasing metal ion concentration. The three-dimensional plots indicate that the decay is monotonic and appears to be independent of the excitation energy (see below). Weisman and co-workers have shown that the fluorescence spectra may be fitted for the contributions from each particular (n,m) SWNT.[7] Each individual spectrum was therefore fitted to determine the intensity contributions of 43 different fluorescing tubes (see Experimental). Analysis of a spectrum in the presence and absence of Cd^{2+} shows that there is no shift in the emission wavelengths, see Figure 1.2.

Given the well behaved decrease in fluorescence of the SWNTs by Cd^{2+} using $Cd(OAc)_2$, we have investigated the effects of both the metal ion and the counter ion for metal salt solutions with a [M^{n+}] between 0.5 - 5 mM per 15 mg.L^{-1} of SWNT. The following metal salts cause an analogous decrease in fluorescence of the SWNTs (albeit with varying efficiencies per mM of M^{n+}): $MgCl_2$, $Mg(SO_4)$, $Mg(OAc)_2$, $CaCl_2$, $Ca(OAc)_2$, $SrCl_2$, $BaCl_2$, $Ba(OAc)_2$, $Zn(SO_4)$, $CdCl_2$, $Cd(SO_4)$, $Cd(OAc)_2$, $HgCl_2$, and $Hg(OAc)_2$. In contrast, $Ga_2(SO_4)_3$, and $Al(NO_3)_3$ show no reduction in fluorescence over the concentration range studied.[8]

A decrease in fluorescence of a SWNT can be caused by any of several possible effects: inter-tube energy transfer from bundling, acid suppression of fluorescence, changes in the absorption (spectral bleaching), and quenching via either static or dynamic mechanisms. Prior to further studies of metal, counter ion, and SWNT n,m effects, it is worth discussing the possibility each of these alternatives.

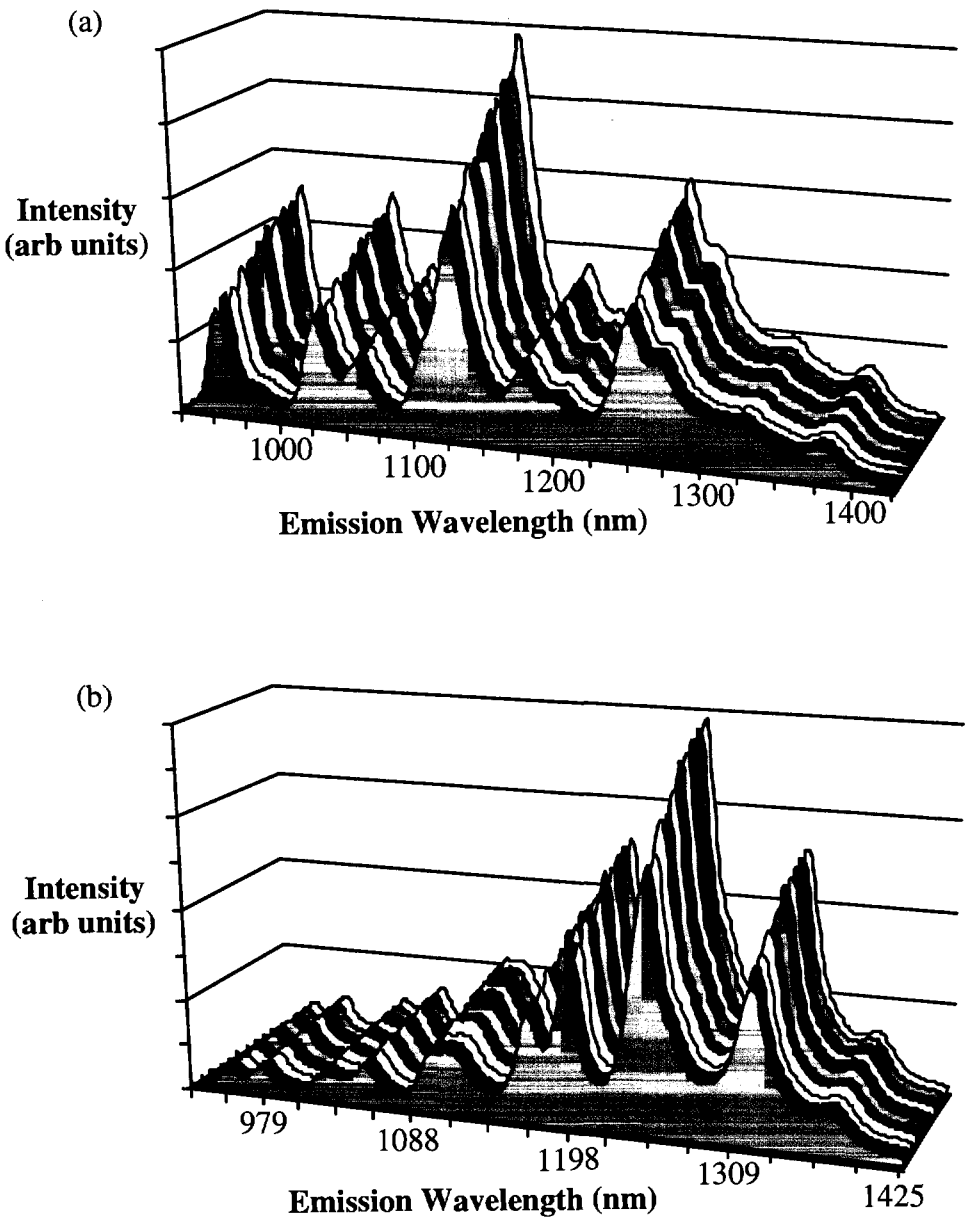

Figure 1.1. Fluorescence spectra of SDBS-SWNTs in the presence of $Cd(OAc)_2$ with (a) 660 nm and (b) 785 nm excitation showing the decrease in fluorescence with increased Cd^{2+} concentration (0 – 5.0 mM in 0.5 mM steps).

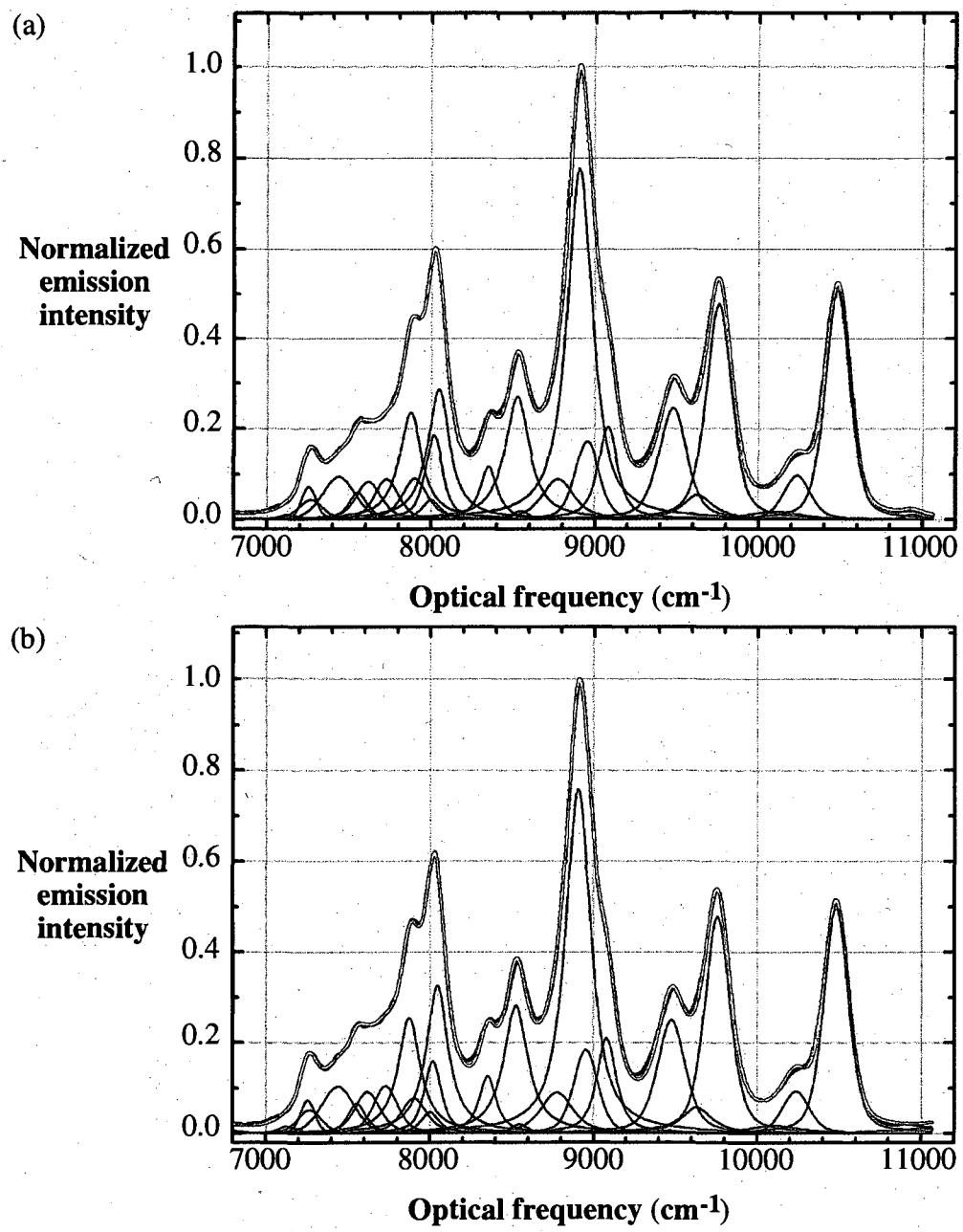

Figure 1.2. Deconvoluted fluorescence spectra using Applied NanoFluorescence Software (660 nm excitation) of (a) SDBS-SWNTs and (b) SDBS-SWNTs in the presence of $Cd(OAc)_2$ (4.0 mM), showing the measured (blue line) and simulated (red line) spectra, and the basis functions (black line). The spectra are normalized to allow comparison of the spectral deconvolutions.

Individual semiconducting SWNTs suspended in solution fluoresce when a sufficient micellar layer is present to provide isolation from other SWNTs (in particular the metallic ones).[14] Disruption of the micelle structure allows for van der Waals attractions to dominate resulting in bundling of the SWNTs and thus a decrease in fluorescence intensity. Subsequent bundling is irreversible without extreme physical treatment such as sonication.[9] Based upon these observations, we propose that in the present case bundling does not occur. Firstly, at extreme ionic strengths, the surfactant micelle structure can be perturbed. However, addition of Na^+, Cs^+, Al^{3+}, or Ga^{3+} does not change the fluorescence even though they were used in the same concentration as the other metals that do affect fluorescence (i.e., Cd^{2+}). Secondly, a characteristic of bundling of SWNTs is a red shift and broadening of the bands in the UV-vis spectrum.[14]

As can be seen from Figure 1.3, no such effects occur with the addition of Cd^{2+} suggesting that that the ground state electronic structure of the SWNTs is not perturbed. Finally, in our original report on the formation of CdS coated SWNTs, we observed that

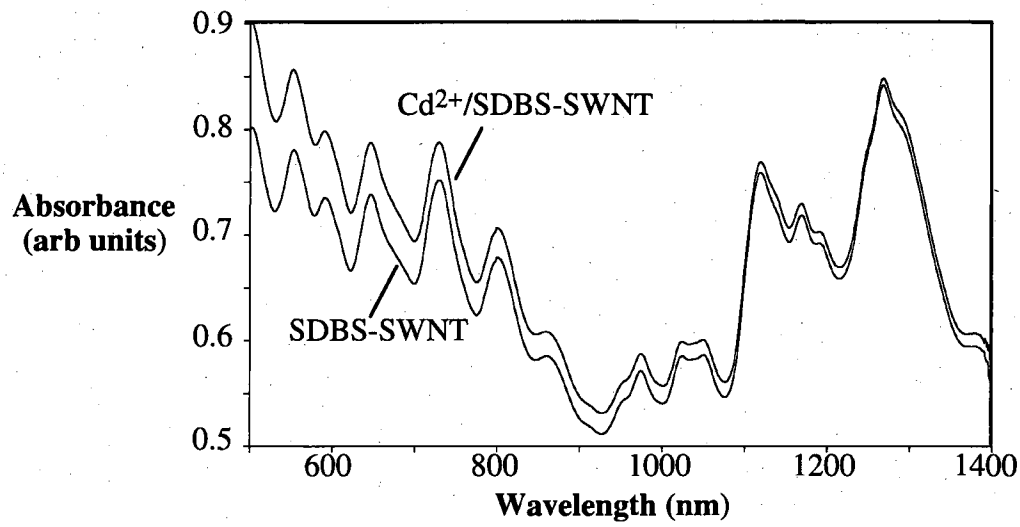

Figure 1.3. UV-vis absorption spectra of (a) SDBS-SWNTs and (b) SDBS-SWNTs in the presence of $CdCl_2$ (2.0 mM).

the fluorescent intensity was regained upon addition of the sulfur source (thiourea), which we proposed was due to the removal of the Cd^{2+} ion from the surface of the SWNT. As an alternative to reacting the metal ion, complexation with a chelate agent should have the same effect. Indeed, fluorescence loss due to the presence of M^{n+} ions can be recovered by adding EDTA. For example, as may be seen from Figure 1.4, addition of 3.0 mM $SrCl_2$ to SDBS-SWNTs results in a reduction in fluorescence. Subsequent addition of an excess of EDTA results in the recovery of fluorescence (Figure 1.4). It is important to note that if the SWNTs did bundle, the binding energy of ~0.5 $eV.nm^{-1}$ of SWNT contact is difficult to overcome and treatment with EDTA would not separate them. Based on the foregoing, it is clear that the observed fluorescence loss is not due to nanotubes bundling.

Smalley and coworkers have shown that SWNT fluorescence is suppressed in an acidic medium.[10] In addition, dissolved oxygen can cause a reduction in SWNT fluorescence, but only when H^+ is present.[5,11] Both of these issues are overcome by the use of basic conditions. In this study, we adjusted the solution with NH_4OH for several reasons. Firstly, the basic medium eliminates large quantities of hydronium ion being present in solution prohibiting fluorescence loss from dissolved oxygen, allowing the reactions to be run in air. Secondly, the use of NaOH as a source of base resulted in a significant change in pH with the addition of the metal ions. For example, addition of 5.0 mM $CdCl_2$ to a NaOH/SDBS-SWNT solution results in a reduction of pH from 10.5 to 7.5. Such a change in pH results in a significant decreases in the fluorescence of the SWNTs. We are interested in the fluorescence decrease caused by the presence of the M^{n+} ions, therefore using NH_4OH resulted in the pH remaining constant (pH = 10.5) with the addition of M^{n+} indicating that fluorescence loss is not due to a pH change.

A loss of SDBS-SWNT fluorescence can be caused by changes in the absorption properties of the fluorophores. Previous reports indicate that there is an absorbance reduction (in concert with fluorescence decay) when organic molecules react with

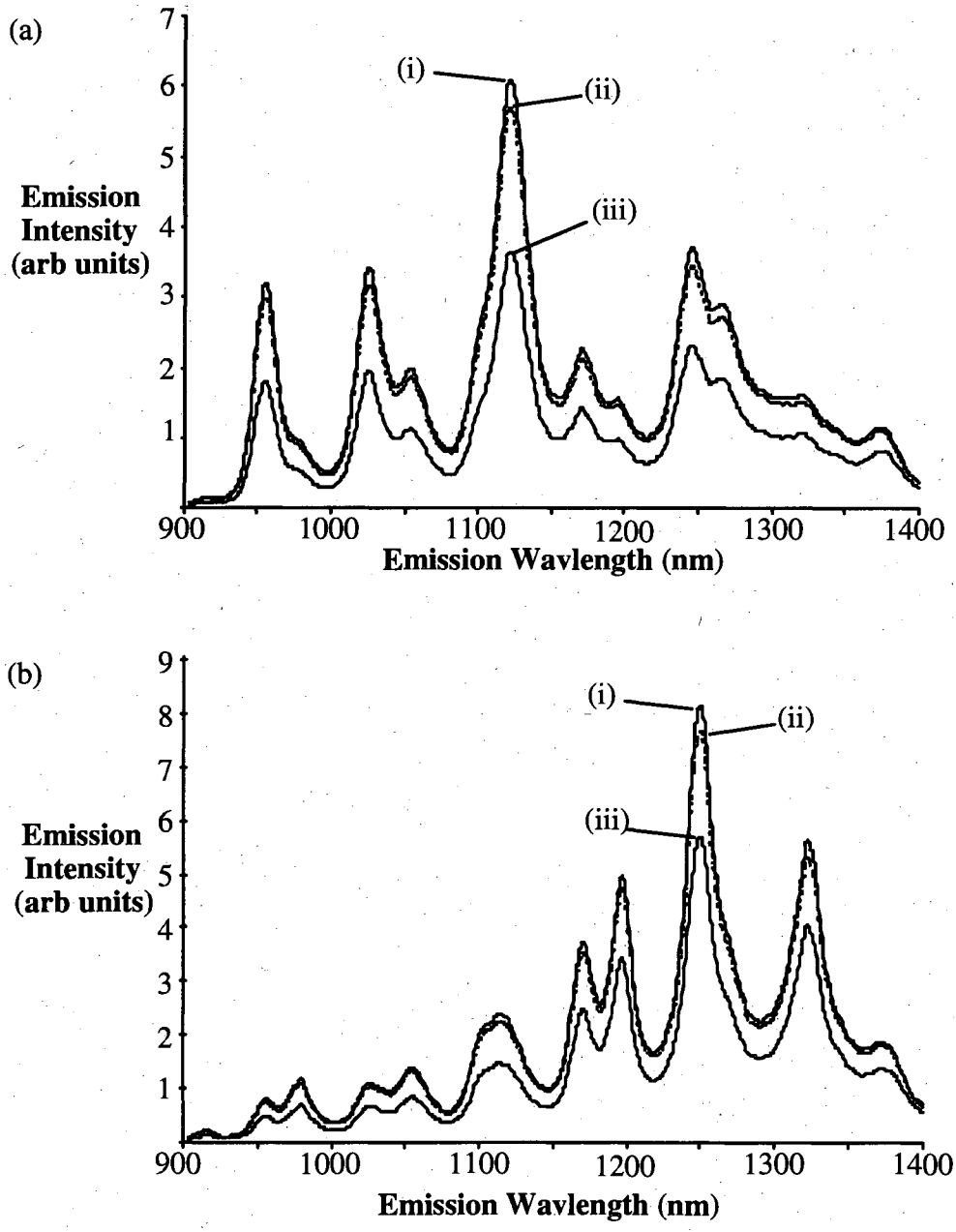

Figure 1.4. Fluorescence of SDBS-SWNTs using (a) 660 nm and (b) 785 nm excitation in the presence of $SrCl_2$ (3.0 mM) before (i) and after (ii) the addition of EDTA (15 mM) showing the recovery of fluorescence with the addition of EDTA. The fluorescence spectrum with EDTA (15 mM) in the absence of quencher molecules is shown for comparison (iii).

SWNTs.[7] This process is ordinarily classified as "spectral bleaching". As may be seen from Figure 1.3, there is no change in the absorbance spectra accompanying fluorescence decay with the addition of metal ions (Cd^{2+} in Figure 1.3), indicating that spectral bleaching is not the source of fluorescence decay.

Based upon the above evidence, we propose that the decrease in fluorescence of the SDBS-SWNTs in the presence of M^{n+} is not caused by bundling, acid suppression, or spectral bleaching, and must therefore be due to quenching. The fluorescence quenching of SDBS-SWNTs by M^{n+} is consistent with Stern-Volmer behavior and therefore we can characterize the quenching of individual nanotubes. Fluorescing species with intensity I_o, quenched by a species M^{n+}, to give a reduced intensity I, follow Eq. 1, where K_{SV} is the Stern-Volmer quenching constant.

$$I_o/I = K_{SV}[M^{n+}] + 1 \qquad (1)$$

In this manner we can obtain the Stern-Volmer quenching constants using a linear regression least squares fit for each metal, counter ion and SWNT (n,m) combination (Tables 1.1 and 1.2). Figure 1.5 shows a representative Stern-Volmer plot for quenching of 6,5-SWNT by $Hg(OAc)_2$. Some of the (n,m) SWNTs are either absent from the sample, not strong emitters with the excitation energies used, or are in a low percentage and have a minimal intensity contribution to the overall spectrum. Consequently, preparing meaningful Stern-Volmer plots from these n,m SWNTs is not possible. For these reasons, we analyzed the 18 most intense nanotubes present in the sample.

It has been previously reported that there is an excitation wavelength dependence on the fluorescence quenching of functionalized SWNTs by nitroaromatic molecules.[12] We observe minimal excitation dependence with only slight variations in the quenching processes from 660 and 785 nm excitation (see Tables 1.1 and 1.2). This is expected

enching constants for Group 2 metal complexes from 660 and 785 nm irradiation.[a]

SWNT n.m															
9,7	13,2	14,0	8,7	10,5	9,5	8,6	12,1	9,2	7,6	8,4	9,4	10,2	7,5	6,5	8,3
27	11	19	30	27	6.1	24	33	21	31	35	26	28	31	36	30
26	***11***	***19***	***30***	***26***	***5.2***	***23***	***32***	***21***	***30***	***34***	***26***	***28***	***30***	***35***	***29***
18	22	18	21	21	14	30	18	15	43	20	26	33	39	36	36
12	***16***	***13***	***16***	***15***	***8.0***	***24***	***12***	***9.3***	***36***	***14***	***20***	***27***	***32***	***30***	***30***
31	34	33	27	33	32	43	29	23	55	34	42	47	50	51	54
26	***29***	***28***	***21***	***27***	***27***	***37***	***23***	***18***	***48***	***29***	***36***	***41***	***44***	***45***	***48***
40	40	13	32	41	26	43	28	38	61	26	39	43	51	48	51
34	***34***	***7.9***	***26***	***35***	***21***	***37***	***23***	***33***	***54***	***21***	***33***	***37***	***45***	***42***	***45***
67	30	19	55	61	19	43	65	30	51	53	39	39	46	46	43
64	***28***	***18***	***53***	***58***	***17***	***42***	***62***	***28***	***49***	***51***	***37***	***38***	***45***	***45***	***43***
203	295	244	211	224	258	313	229	240	377	293	385	382	398	402	392
190	***281***	***231***	***199***	***211***	***245***	***298***	***216***	***227***	***361***	***278***	***368***	***366***	***381***	***385***	***375***
323	460	363	294	361	431	481	382	305	611	464	603	596	637	613	640
301	***433***	***340***	***274***	***338***	***406***	***454***	***358***	***285***	***579***	***437***	***572***	***565***	***604***	***581***	***607***
352	577	413	344	385	509	568	383	364	661	483	683	669	710	688	688
330	***548***	***389***	***322***	***362***	***482***	***539***	***360***	***341***	***630***	***457***	***650***	***637***	***677***	***655***	***655***

n bold and italics.

enching constants for Group 12 metal complexes from 660 and 785 nm irradiation.[a,b]

SWNT n.m															
9,7	13,2	14,0	8,7	10,5	9,5	8,6	12,1	9,2	7,6	8,4	9,4	10,2	7,5	6,5	8,3
b	b	6.5	b	b	3.3	13	b	24	19	4.8	7.1	12	13	21	12
b	***b***	***5.8***	***b***	***b***	***2.6***	***12***	***b***	***23***	***18***	***4.1***	***6.4***	***11***	***12***	***21***	***12***
47	45	30	49	50	38	58	51	70	72	56	63	64	69	79	73
41	***39***	***25***	***43***	***44***	***33***	***52***	***45***	***64***	***66***	***50***	***57***	***58***	***63***	***73***	***67***
54	49	37	56	57	41	65	57	64	80	60	66	69	76	83	80
49	***44***	***31***	***51***	***52***	***35***	***59***	***52***	***58***	***73***	***54***	***60***	***63***	***70***	***76***	***74***
82	74	48	77	85	67	91	91	70	111	95	99	98	107	118	114
75	***68***	***42***	***70***	***78***	***61***	***84***	***84***	***64***	***103***	***88***	***91***	***90***	***99***	***110***	***106***
b	6.6	13	15	b	b	17	b	24	27	b	15	20	23	24	17
b	***3.9***	***10***	***12***	***b***	***b***	***14***	***b***	***21***	***23***	***b***	***12***	***17***	***20***	***21***	***14***
55	69	66	72	58	50	82	54	95	90	60	82	86	89	97	88
47	***61***	***58***	***64***	***50***	***42***	***73***	***46***	***86***	***81***	***52***	***73***	***77***	***80***	***88***	***79***

n bold and italics.

tained due to low emission intensities.

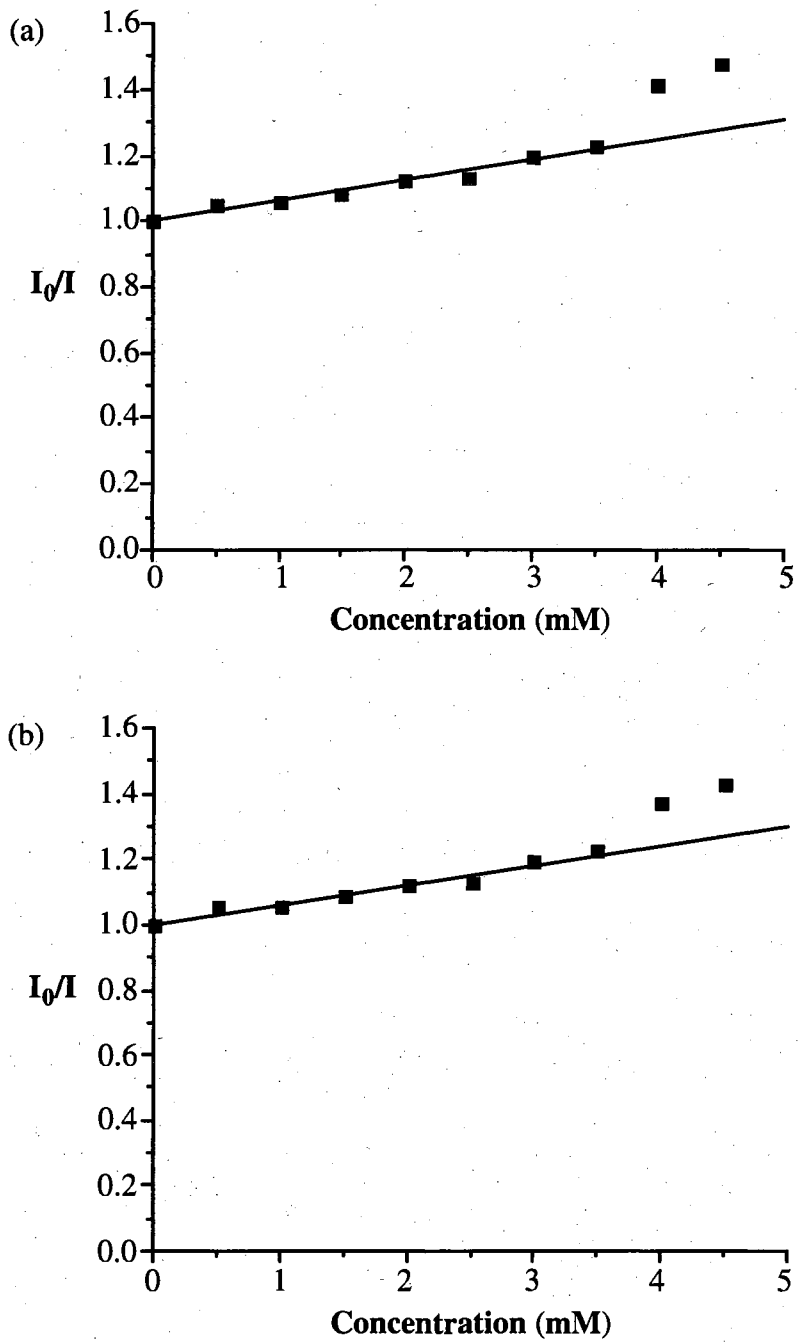

Figure 1.5. A representative Stern-Volmer plot for quenching of 6,5 SDBS-SWNT by $Hg(\dot{O}Ac)_2$ measured using 660 nm excitation (top) (R^2 = 0.969) and 785 nm excitation (bottom) (R^2 = 0.968) .

however, as the dependence is most prominent at low excitation wavelengths and diminishes at high wavelengths. Noticeable in Figure 1.5 is the deviation from linearity of the Stern-Volmer plot at the high concentrations of 4.0 mM and 4.5 mM. This is expected because the solution has become too concentrated allowing for simultaneous static and dynamic quenching.

Dependence on Metal. As may be seen from Tables 1.1 and 1.2, the quenching constant for a particular n,m SWNT is highly dependant on the choice of metal ion and counter ion. A comparison of the data for the chloride salts (thus eliminating counter ion effects) for the quenching of the 10,2 SDBS-SWNT (Figure 1.6) shows that within the Group 2 metals the quenching efficiency follows the trend of increasing atomic number

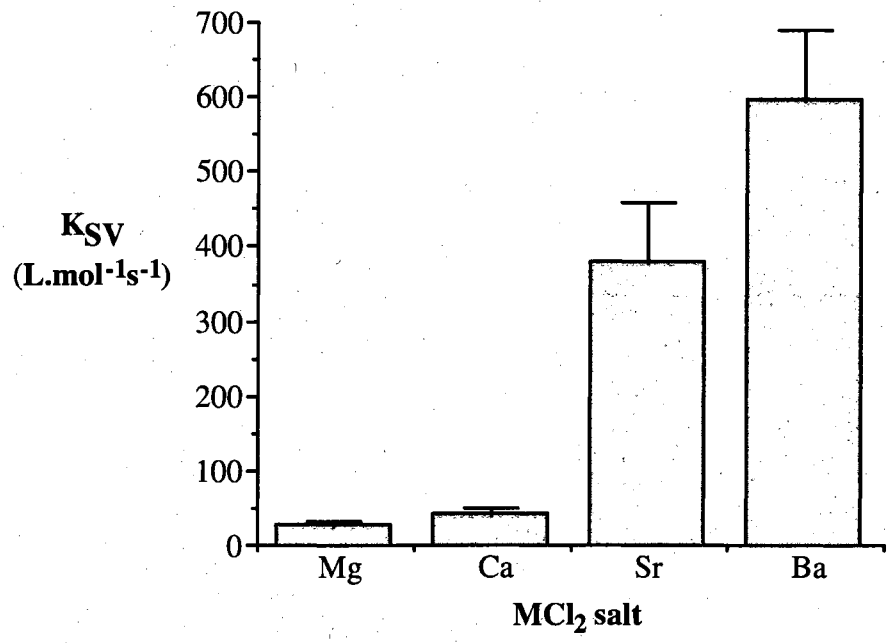

Figure 1.6. Comparison of Stern-Volmer quenching constant for the 10,2 SDBS-SWNT with Group 2 chlorides measured using 660 nm excitation.

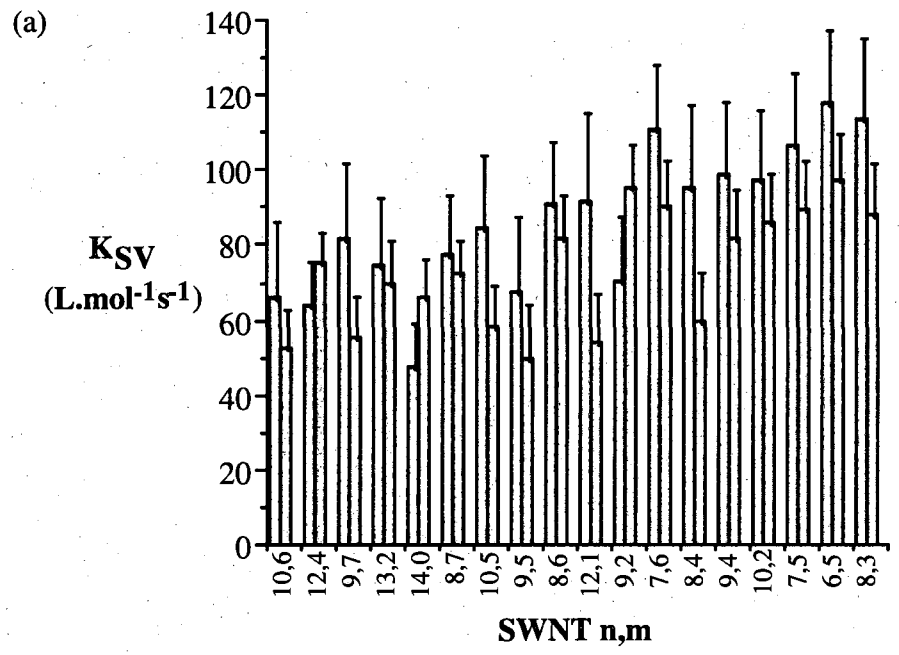

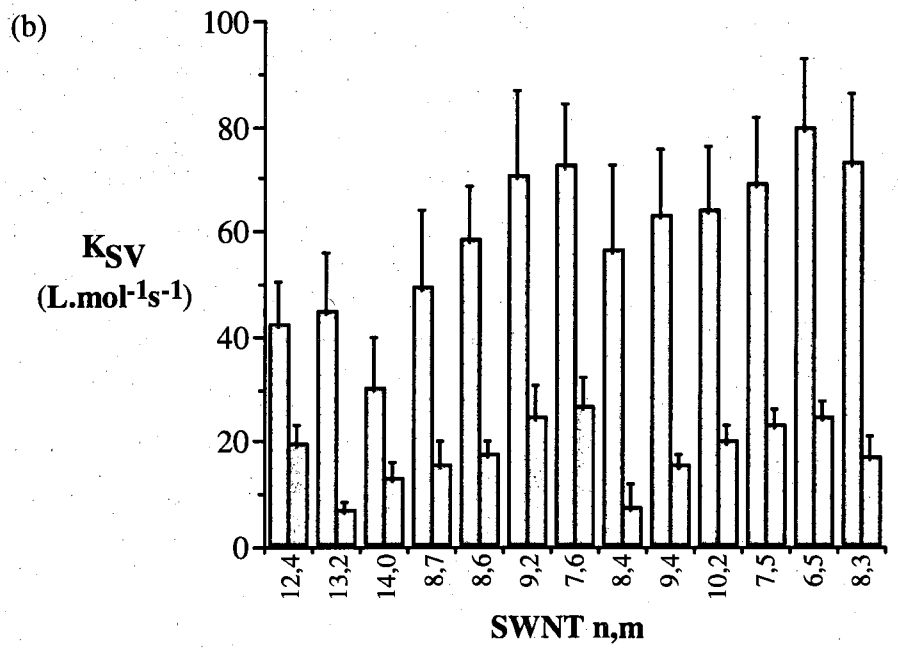

Figure 1.7. Comparison of Stern-Volmer quenching constant for selected SDBS-SWNTs n,m values (using 660 nm excitation) with (a) chlorides and (b) acetates of cadmium (□) and mercury (□).

(i.e., Mg < Ca < Sr < Ba). The relationship between the Group 12 metals is a little more complex. While the Stern-Volmer quenching constants for $Zn(SO_4)$ are all significantly less than the analogous values for $Cd(SO_4)$, the values for $Hg(OAc)_2$ are within experimental error of those of $Cd(OAc)_2$ (Figure 1.7a) rather than larger as would be expected by the trend observed for the Group 2 metals. Furthermore, the quenching constants for $HgCl_2$ are significantly lower than those for $CdCl_2$ (Figure 1.7b). Comparing the data for all the n,m values, it is apparent that there is no correlation between Stern-Volmer quenching constant and the atomic number, diffusion coefficient, UV-vis spectral overlap, or the reduction potential. As may be seen from Figure 1.8, there is, however, an apparent dependence of on the ionic radius of the quenching metal. Importantly, ions with a radius less than 1 Å exhibit little quenching, but those with radii greater than 1 Å show increasing quenching efficiency with increased size. The slight

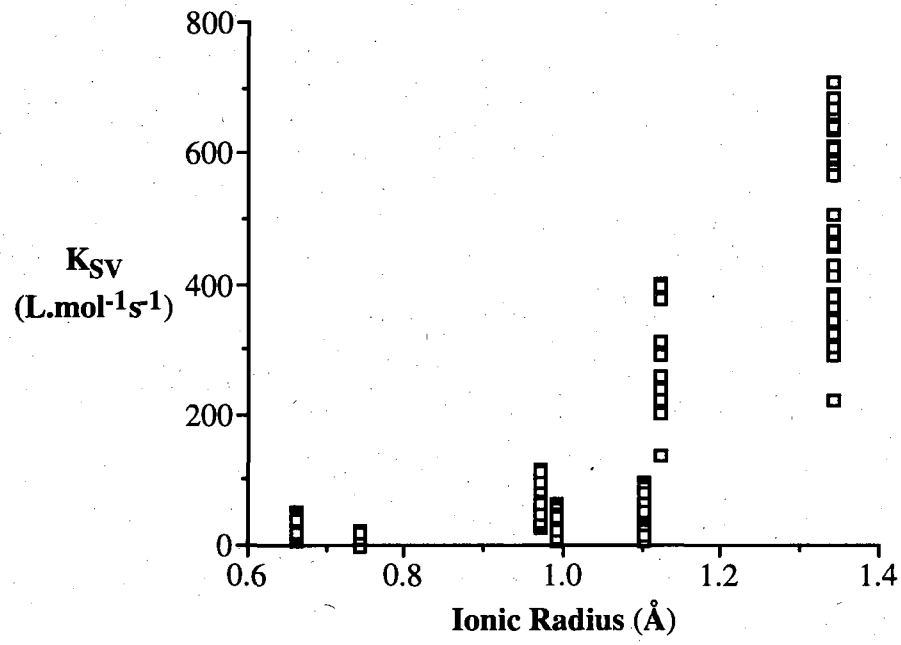

Figure 1.8. Stern-Volmer quenching constant for SDBS-SWNTs using 660 nm excitation as a function of the M^{2+} ionic radius for MCl_2, $M(OAc)_2$, and $M(SO_4)$.

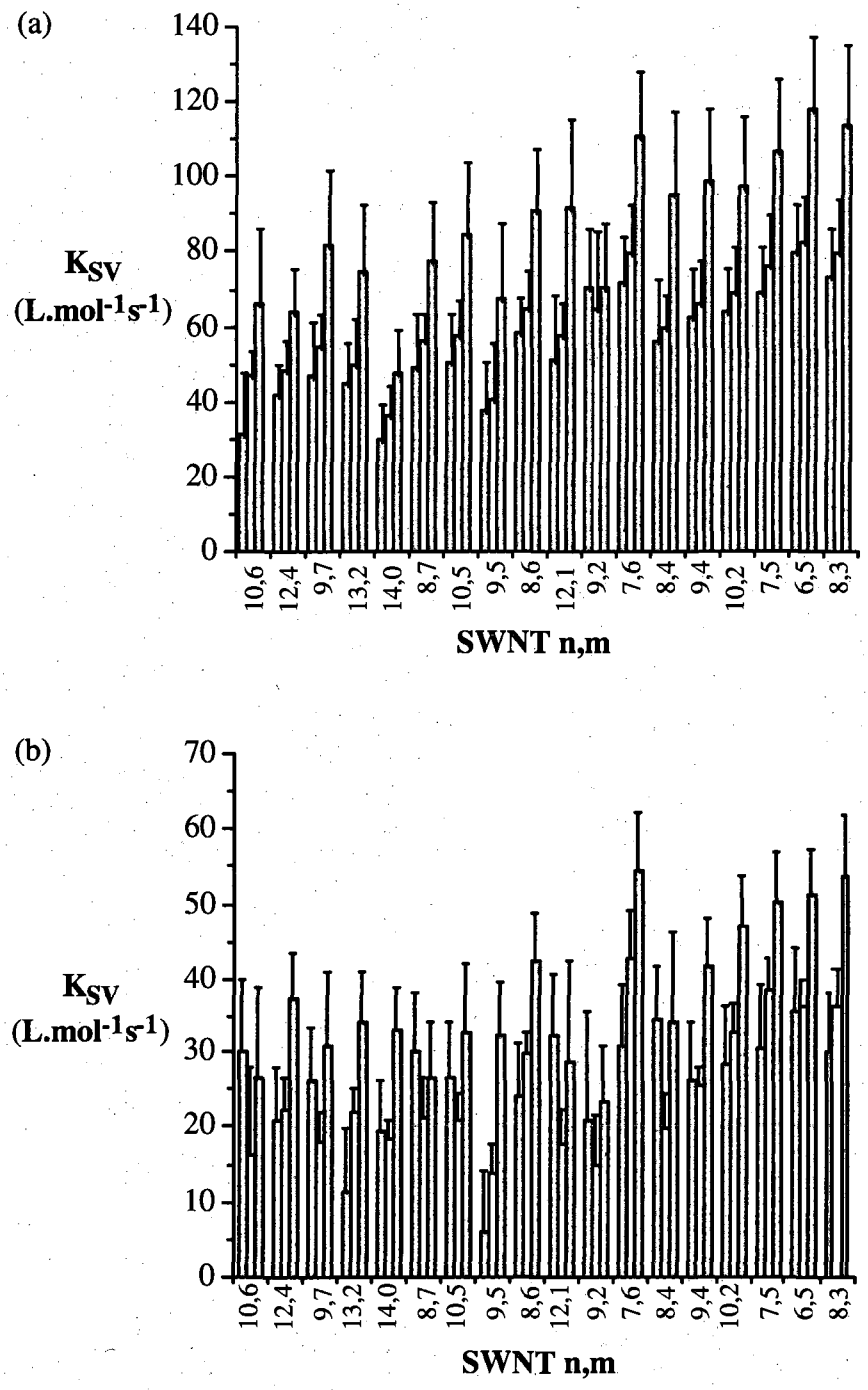

Figure 1.9. Stern-Volmer quenching constants for SDBS-SWNTs (using 660 nm excitation as a function) of the X^{n-} counter ion (a) CdX_n and (b) MgX_n: X = Cl^- (□), SO_4^{2-} (□), and OAc^- (□).

anomaly of this trend is the mercury derivatives that appear to be consistent with an apparent decrease in the effective radius of the Hg^{2+} ion. Given the greater covalent nature of mercury compounds as compared to their Zn and Cd analogs, this may be a possible rational for the reduced efficacy of the mercury compounds.

Dependence on Anion. In addition to the variation in the Stern-Volmer quenching constants with the identity of the metal ion, there is a lesser, but significant, dependence on the anion. As seen in the representative plots in Figure 1.9, the quenching efficiency follows the trend of $Cl^- \approx SO_4^{2-} < OAc^-$. Although it is unclear as to what the difference can be assigned to, we propose that whereas chloride and sulfate are non-coordinating anions (especially under the pH conditions employed herein), acetate would be expected to retain some coordination to the metal. The dependence on the identity of the counter ion is distinct from quenching of organic fluorophores (e.g., 2,5-

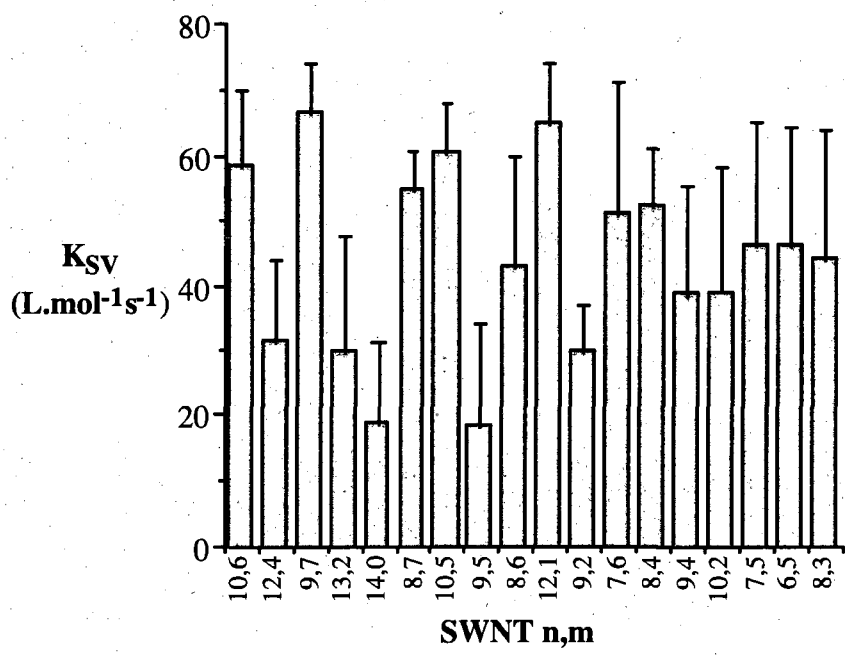

Figure 1.10. Stern-Volmer quenching constants for SDBS-SWNTs (using 660 nm excitation) as a function of SWNT n,m value in the presence of $Ca(OAc)_2$.

diphenyloxazole) by metal ions.[8]

Dependence on SWNT n,m. Figure 1.10 shows the Stern-Volmer quenching constants for SDBS-SWNTs as a function of SWNT n,m value in the presence of $Ca(OAc)_2$. It is clear that there is a dependence of quenching on the identity of the SWNT, i.e., the n,m value. In previous studies it has been reported that selective quenching between organic dyes and SWNTs of particular n,m values. This quenching occurs where the valance band of the SWNT is above a threshold value associated with the reduction potential of the dye.[7] Thus, for a particular SWNT/organic combination, SWNTs with a valance band above a certain value quench, while those with a valance band below that value do not. Such a situation does not occur for the quenching of SDBS-SWNTs by metal salts; however, as may be seen from Figure 1.11a, a plot of the Stern-Volmer quenching constants for a particular Group 2 metal/anion combination as a function of the SWNT band gap shows that within the error of the measurements a linear correlation exists. SWNTs with larger band gaps are quenched more efficiently that those with small band gaps. The variation between SWNTs of particular n,m values (i.e., the slope of the lines in Figure 11a) appears to depend on the relative ability of the metal as a quencher. Given that there is a near inverse relationship between SWNT band gap and diameter, an inverse but equal relationship between the quenching constant and diameter of the SWNTs (Figure 1.11b). This trend holds true for both 660 nm and 785 nm excitation, both Group 2 and Group 12 metal ions, and all counterions as shown in Figure 1.12.

Possible Mechanisms of Quenching. From the above discussion, we have found that the efficiency of a metal salt to quench the fluorescence of a SWNT depends on the ionic radius of metal, the identity of the counter anion, and the band gap and/or the

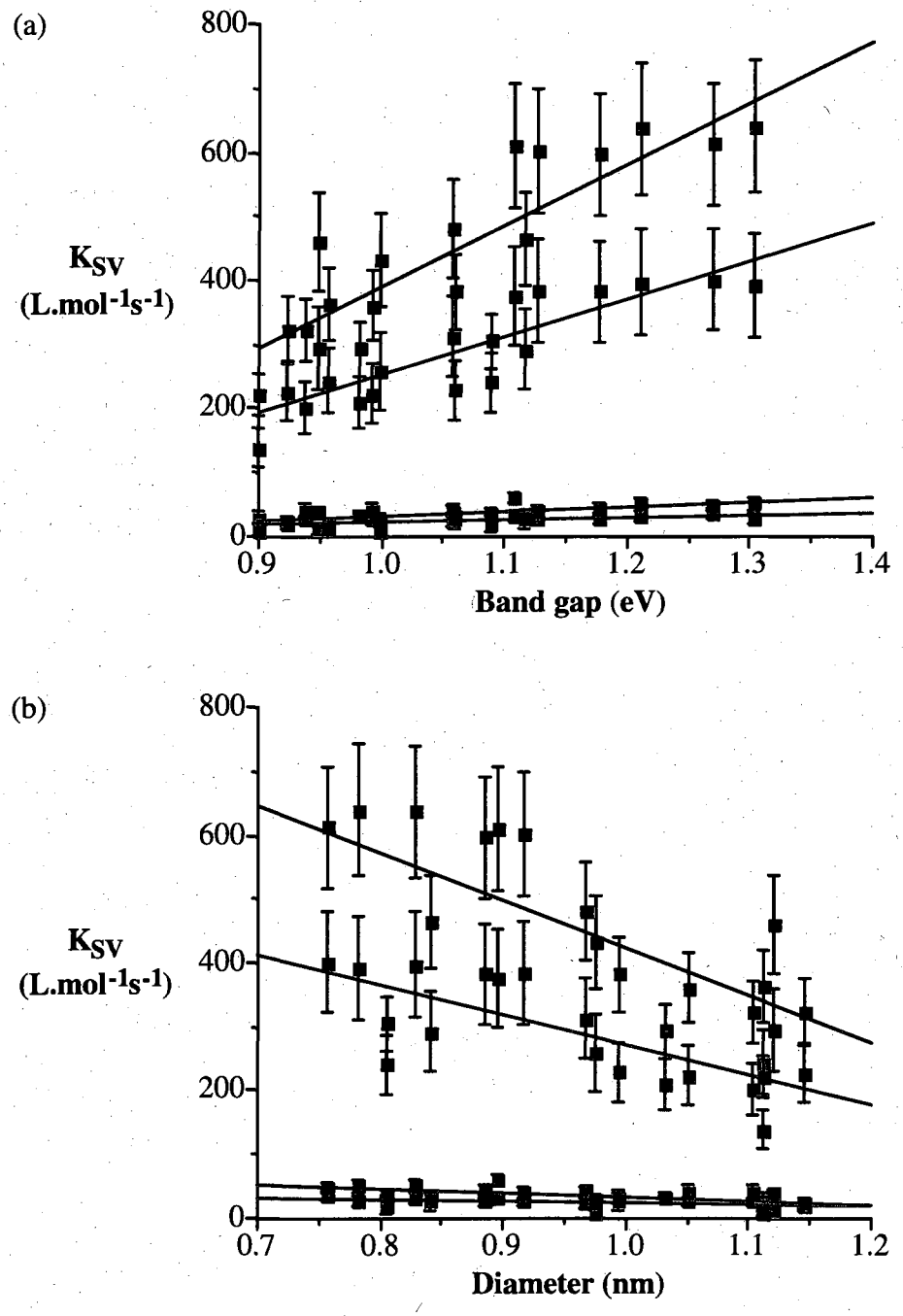

Figure 1.11. Stern-Volmer quenching constants using MCl_2 for selected SDBS-SWNT (using 660 nm excitation) as a function of (a) SWNT band gap and (b) SWNT diameter. M = Mg (■), Ca (■), Sr (■), and Ba (■).

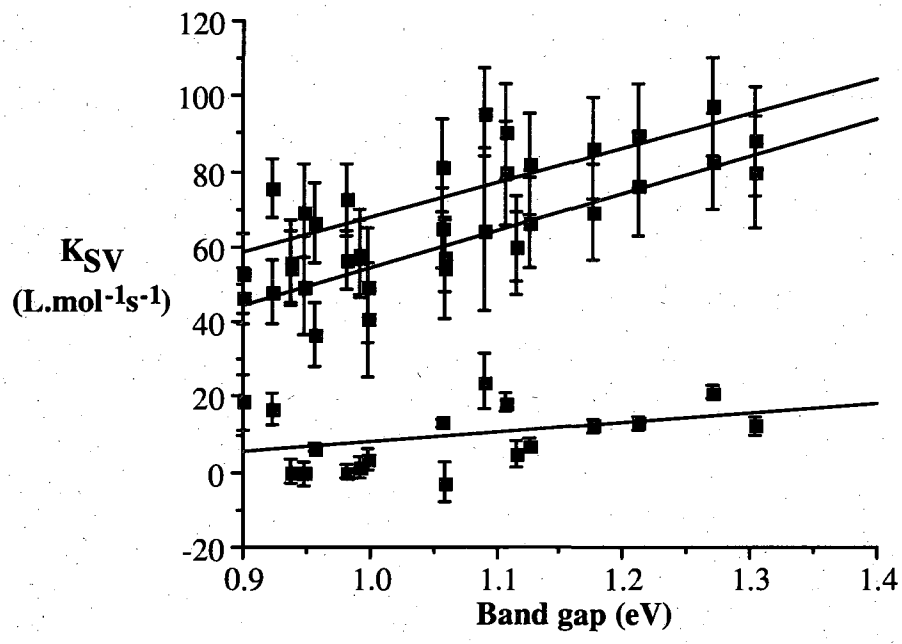

Figure 1.12. Stern-Volmer quenching constants for SDBS-SWNTs (using 785 nm excitation as a function) of the SWNT band gap using $M(SO_4)$. M = Zn (■), Cd (■), and Hg (■).

diameter of the SWNT. Quenching reactions can be generally classified as either dynamic or static processes (or a combination of both).[13] Static quenching can be attributed to either the formation of a non-florescent ground state complex or through a sphere of effective quenching. As noted above, the concentration dependence of the quenching follows a classic Stern-Volmer plot that is consistent with either static or dynamic mechanisms. We note that for some of the SWNT n,m/M^{n+}/anion combinations there appears a positive deviation from linearity at high concentrations of the metal salt (see Figure 1.5). Such a deviation is suggestive of a more complex mechanism, making a definitive assignment of the mechanism difficult. However, we can preclude a simple

static quenching mechanism involving the formation of a non-florescent ground state complex.

If the SWNT and metal ion formed a non-florescent ground state complex then the electronic structure of the SWNT would be perturbed resulting in a red shift in the absorbance (e.g., Figure 1.3) and fluorescence spectra (e.g., Figures 1.1 and 1.2). As may be seen from Figures 1.1-1.3 there is no such red shift upon addition of M^{n+}. Thus, we propose that the quenching process does not involve the formation of a complex between the metal ion and the SWNT.

The reduced fluorescence reported for the dye-SWNT is attributed to spectral bleaching caused by electron transfer from the valance band of the SWNT to an acceptor molecule.[7] For such a ground state process, electron transfer is expected to occur from the top of the SWNT valence band to the metal complex. Such an interaction would be particularly evident by changes in the characteristic first van Hove transitions.[14] As may be seen from Figure 1.3, the addition of a quenching M^{n+} does not result in any alteration of either the first (830 - 1600 nm) or second (600 - 800 nm) van Hove transitions,[15] indicating that the quenching process does not involve electron transfer from the valance band of the SWNT to an acceptor ion. Indeed, if it was a simple electron transfer process, then the quenching ability of the Group 2 and 12 metal complexes would involve reduction of the metal centers or electron transfer into the lowest appropriate unfilled orbital on the metal···solvate complex, most probably a σ^* orbital (i.e., $M\text{-}NH_3$ or $M\text{-}OH_2$). The reduction potentials of each metal studied are significantly higher than the Fermi levels of the SWNTs.[23] *Ab initio* calculations of the relative energy of these orbitals indicate that these are also much higher than necessary to facilitate SWNT-to-M^{n+} electron transfer.

In summary, the quenching process does not involve the formation of a complex between the metal ion and the SWNT or electron transfer from the valance band of the

SWNT; however, there is clearly a perturbation of the electronic structure of the SWNTs. The intensity of the radial breathing mode (RBM) is an indication of the electron density on the SWNT. In Figure 1.13, the addition of Ba^{2+} shows a reduction in the radial breathing mode (RBM) at 236 cm^{-1} caused by a loss of electron density in the nanotube.[16,17] The intensity of the RBM undergoes recovery upon the removal of the metal ions. The addition of EDTA (Figure 1.13c) promotes the formation of a M[EDTA] complex that is sterically hindered from being sufficiently close to the nanotube. Based on the foregoing, we propose that the quenching of the fluorescence of SWNTs is caused, not by a particular electron transfer process, but rather the distortion of the SWNT's electronic structure by the presence of a charged species in close proximity (contact) to the SWNT.

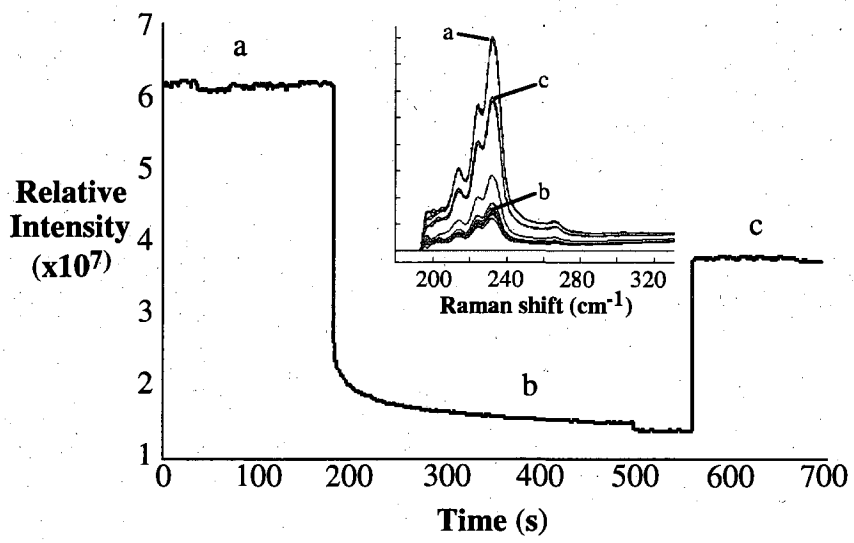

Figure 1.13. Intensity of the radial breathing mode (RBM) as a function of time for (a) SDBS-SWNTs after (b) addition, at t = 200 s, of 0.3 mL 40 mM $Ba(OAc)_2$ solution, and (c) subsequent addition, at t = 550 s, of 0.3 mL excess EDTA solution. The difference in intensity between (a) and (c) is consistent with the dilution of the sample.

The optical transitions in SWNTs provide insight into the nature of the excited states in these 1-D systems. There has been increasing evidence that light absorption produces strongly correlated electron-hole states in the form of excitons.[1,18,19,20] Swan and co-workers have demonstrated that the local environment around a SWNT shifts the exciton level and also has an effect on the bandgap itself.[21] Most of the electric field of the exciton actually flows outside of the SWNT itself, and are therefore sensitive to local electric effects. It is also known that the excitons are affected by magnetic fields.[22] There are actually several exciton energy levels, but only one has an emitting decay path; the others are dark. The magnetic field shifts the relative levels, and can alter the fluorescence intensity. Thus, it is clear that the exciton is exquisitely sensitive to its local electric and magnetic environment. This is so, even if the perturbing field is uniform. Highly anisotropic fields around metal ions should have an even more profound and chaotic effect on the exciton and therefore facilitate non-radiative decay paths. We propose that even a close approach of such ions should, and indeed does, quench fluorescence. This idea is born out in recent work by Strano and co-workers,[23] where they use physisorbed ferro/ferricyanide ions to detect peroxide from glucose peroxidase via quenching of fluorescence. In this case the high charge state quenches fluorescence, yet there is clearly not a direct reaction with the SWNT (i.e., covalent bond); the system is reversible and retains the $[Fe(CN)_6]^{n-}$ structure.

If the quenching involves distortion of the SWNT's electronic structure by a charged species, then this would explain why it is the size of the metal ion and the diameter of the SWNT that appear to be the controlling factors. Furthermore, this would also be consistent with the trend that the greatest effect in quenching of fluorescence occurs with the biggest metal ion (i.e., Ba^{2+}) and the smallest diameter SWNT (8,3), where the greatest volume of the SWNT's exciton would be affected by the charge of the metal ion. Conversely, the smallest metal ion (Mg^{2+}) would affect only a small fraction

of the exciton of the largest diameter SWNT (12,4). A schematic representation of this is shown in Figure 1.14. If the quenching of a M^{2+} is due to the volume of the charge that subtends the exciton of the SWNT, then for a given SWNT n,m there should be a correlation between the ionic volume (rather than simply diameter) of the M^{2+} ion and the Stern-Volmer quenching constant. Figure 1.15 shows an example of just such a correlation for the 10,5 SDBS-SWNT.

It should be noted that if charge volume was the only parameter, the Al^{3+} (r_{ionic} = 0.51 Å) and Ga^{3+} (r_{ionic} = 0.81 Å) should have quenching efficiencies approaching that for Mg^{2+} (0.66 Å) and Cd^{2+} (0.97 Å), respectively. Given that neither of the Group 13 metals shows any appreciable quenching then an alternative reason for their lack of efficacy must be found. At this time, we can propose two possible rationales for the behavior of the Group 13 metals. First, if the perturbation of the SWNT's exciton is due to the localization of charge field near the SWNT, then both the size of the ion and the magnitude of the charge should be important. In this regard, a plot of Stern-Volmer quenching constant as a function of the M^{n+} charge density (Figure 1.16) shows that the quenching efficiency of Al^{3+} and Ga^{3+} would be expected to be minimal, as indeed is observed. A second explanation may involve the predominant speciation of aluminum and gallium salts in aqueous solution at pH = 10.5. Under basic conditions, $M(OH)_4^-$ is a significant fraction of the Group 13 metal in solution. If the major quenching effect is due to the cationic nature of the metal ions (since the excess NH_3 dopes the SWNTs with electrons making a SWNT···M^{n+} interaction favored), then the $M(OH)_4^-$ would not be expected to quench the fluorescence of the SWNTs. Further studies will be required to elucidate the exact nature of these effects.

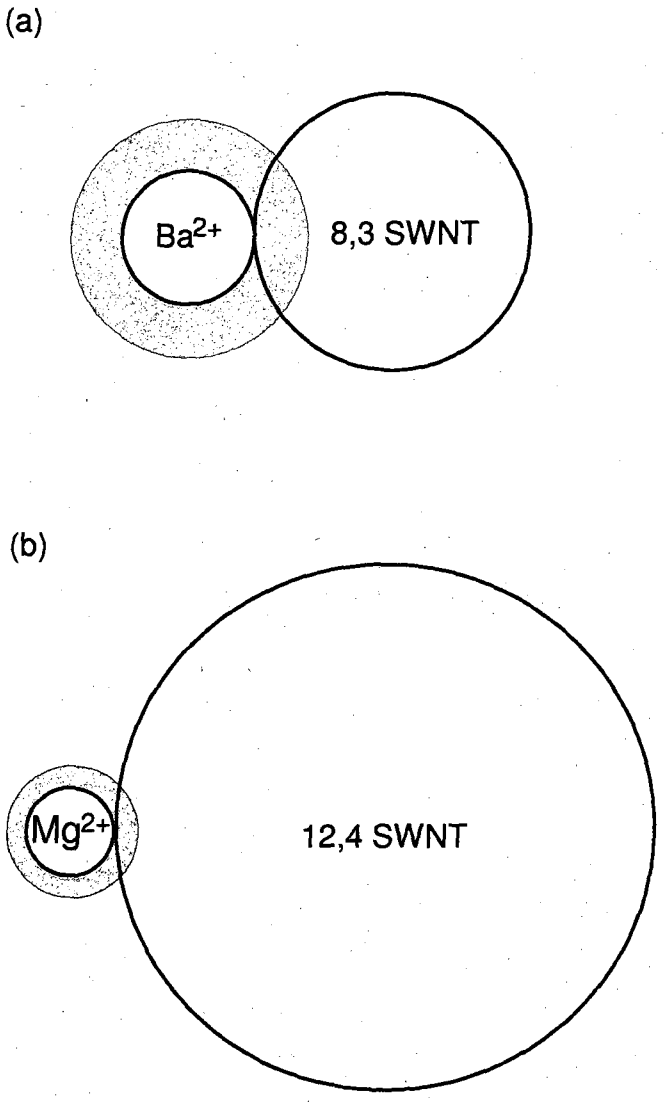

Figure 1.14. Schematic representation of the extent of influence of the charge on the metal ion on the electronic structure of the SWNT as a function of the relative sizes of ion and SWNT. The (a) largest metal ion with smallest diameter SWNT and (b) the smallest metal ion with largest diameter SWNT.

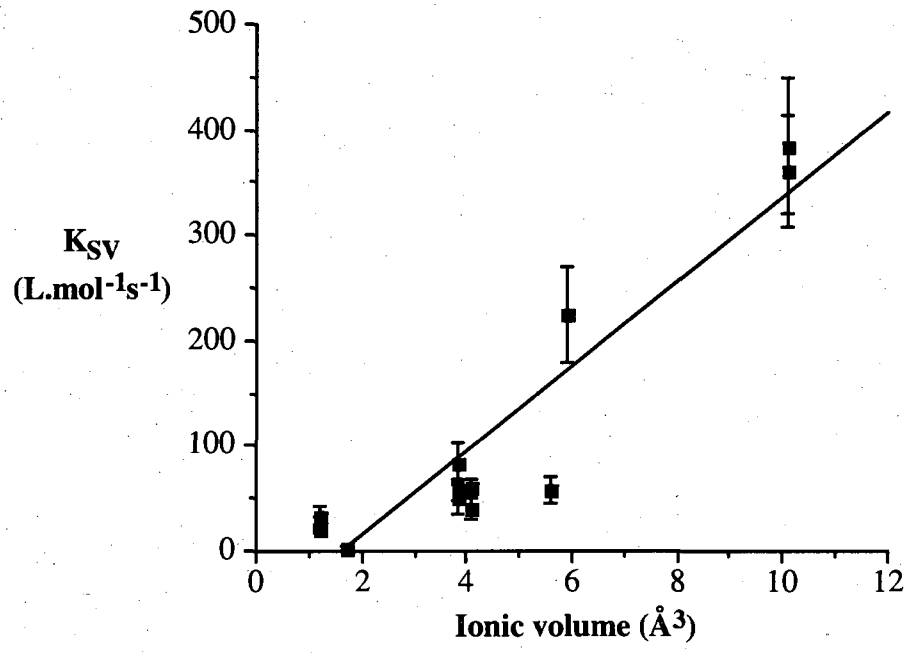

Figure 1.15. Stern-Volmer quenching constant for the 10,5 SDBS-SWNT using 660 nm excitation as a function of the M^{2+} ionic volume for MCl_2, $M(OAc)_2$, and $M(SO_4)$ (R^2 = 0.859).

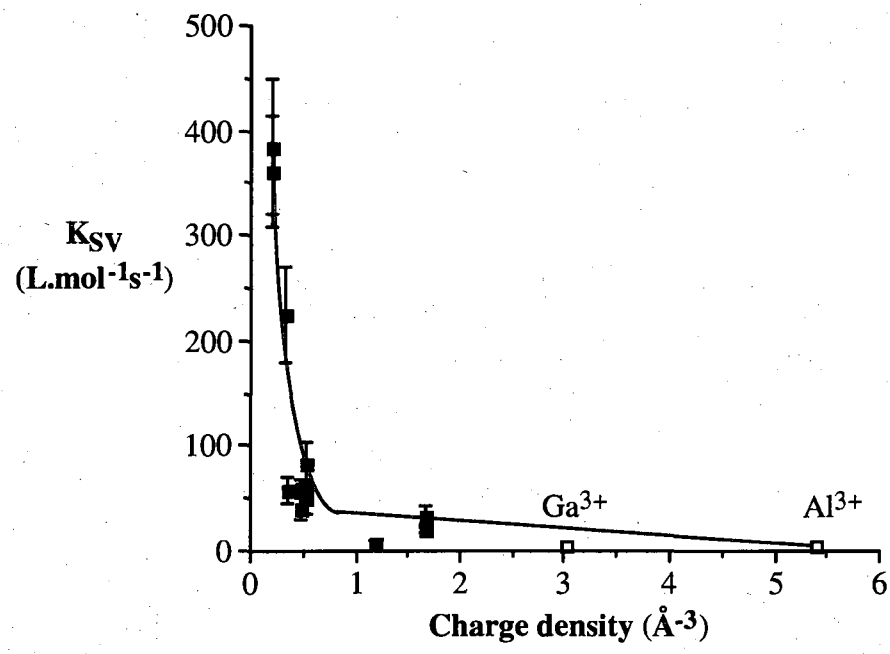

Figure 1.16. Stern-Volmer quenching constant for the 10,5 SDBS-SWNT using 660 nm excitation as a function of the M^{n+} charge density for M^{2+} (■) and M^{3+} (□).

Conclusions

We have demonstrated that diamagnetic Group 2 and 12 metal ions quench SDBS-surfacted SWNTs with varying degrees of efficiency. The larger the ionic radii (lower charge density) of the ion, the greater the efficiencies of quenching that occurs; the smaller the SWNT, and the greater the quenching effect of a particular M^{2+} ion. The identity of the anion has a lesser effect than that of the metal ion or the diameter (band gap) of the SWNT. We can preclude both the formation of a non-florescent ground state complex or spectral bleaching, and instead propose that the SWNT excitons formed by light absorption are affected by the presence of the metal ion facilitating non-radiative decay paths.

Our work categorizing metal ions by their charge and radius, and proposing a correlation between the field···SWNT interactions and quenching rate is consistent with other researcher's views that the SWNT exciton is sensitive to its local environment. We suggest that the highly anisotropic field around metal ions has a significant effect on the exciton and facilitates non-radiative decay paths. In addition, our data provides a basis for estimating the sensitivity of the fluorescence based on the size and charge density of the various ions employed. We propose that even a close approach of such ions should, and indeed does, quench fluorescence.

Finally, we note that Wang et al.,[29] suggested that the excitonic character of optically excited SWNTs "raises the possibility of modifying the SWNT transitions through external perturbations, thus facilitating new electro-optical modulators and sensors." In this regard, we are continuing our studies of the effects of metal ions on the fluorescence of SWNTs and in particular the effect of combining electrostatic charge with magnetic field in paramagnetic transition metal ions.

Experimental

All chemicals were obtained commercially and used without further purification. All solutions used contained ultra pure (UP) water from a Millipore Milli-Q UV water filtration system. HiPco SWNTs (batch 162.10) were obtained from the Carbon Nanotube Laboratory (Rice University, Houston, TX). Metal salts used were $Al(NO_3)_3$ (Mallinckrodt Chemical), $Ga_2(SO_4)_3$ (Strem Chemicals), $HgCl_2$ (EM Science), $BaCl_2$ (Merck), $Hg(OAc)_2$ and $MgCl_2$ (J.T. Baker Chemical Company), $CdCl_2$, $Cd(SO_4)$, $Cd(OAc)_2$, $Ca(OAc)_2$, and $Zn(SO_4).7(H_2O)$ (Sigma-Aldrich), and $Ba(OAc)_2$, $CaCl_2$, $Mg(SO_4)$, $Mg(OAc)_2$, and $SrCl_2$ (Fisher Scientific Company). Technical grade sodium dodecylbenzensulfonate (SDBS) and 99.5% EDTA (Sigma-Aldrich), and 14.8 N NH_4OH (Fisher Scientific Company) were used as received. Fluorescence spectra were collected on a NanoSpectralyzer (Applied NanoFluorescence, LLC) with 660 and 785 nm excitation sources, Raman data was obtained using a Kaiser Process Raman spectrometer (Kaiser Optical Inc.) with 785 nm excitation. Absorption spectra were collected on a Varian Cary 400 spectrophotometer. All measurements were taken at room temperature (298 K).

Preparation of Surfacted Nanotubes. Solutions of SDBS surfacted SWNTs (SDBS-SWNTs) were prepared using a modification of previously published procedures.[24] Raw HiPco SWNTs were dispersed in SDBS solution (225 mL, 1%) and sonicated for 15 minutes in a cup-horn sonicator (Cole Palmer CPX-600, 540 W). The solution was centrifuged (Sovall 100S Discovery Ultracentrifuge with Surespin 630 swing bucket rotor) for 4 hours at 122,000 G. The top 2/3 of the solution was decanted off (referred to as surf-tubes) and diluted with 1% surfactant solution to obtain a concentration of 24 $mg.L^{-1}$ as determined by UV-Vis spectroscopy.

Fluorescence Quenching of Surfacted Nanotubes. NH_4OH (4 M, 0.4 mL per 1.0 mL of surf-tubes) was added to the surf-tubes and stirred for 24 hours. The NH_4OH/SDBS-SWNTs were placed in a cuvette (2.8 mL) and 0.4 mL of metal solution (concentration varying from 0 to 40 mM in 4 mM increments) was added. The solution was inverted several times to induce mixing. Final concentrations are 15 $mg.L^{-1}$ surfacted nanotubes, 1 M NH_4OH, and 0 – 5 mM (in 0.5 mM increments) of metal ions. After 1 hr, fluorescence measurements were obtained by 660 and 785 nm excitation and absorption spectra were collected. The pH of each NH_4OH/SDBS-SWNT/M^{n+} combination was obtained using pH-indicator strips to ensure that the pH had not changed by more than 0.5 pH units. Fluorescence spectra were automatically fitted with ANF NanoSpectralyzer software to yield excitation profiles of 43 different nanotubes. The 18 most intense peaks were chosen for analysis. Stern-Volmer plots were prepared by graphing (I_o/I)-1 versus $[M^{n+}]$ where I_o is the intensity of the NH_4OH-tubes in absence of the metal ion, I is the intensity of the NH_4OH-tubes with the metal ion present, and $[M^{n+}]$ is the concentration of the metal solution in moles/liter. A linear least squares regression was preformed to obtain the Stern-Volmer constants.

Sodium hydroxide (pH = 12.5, 0.4 mL per 1.0 mL of SDBS-SWNTs) was added to the SDBS-SWNT solution and stirred for 24 hours. The NaOH/SDBS-SWNTs solution (2.8 mL) was placed in a cuvette and the appropriate metal solution (0.4 mL, concentration varying from 0 - 40 mM in 4 mM increments) was added. The solution was inverted several times to induce mixing. Final concentrations are 15 $mg.L^{-1}$ surfacted nanotubes, and 0 - 5 mM in 0.5 mM increments of metal ions. After 1 hr, fluorescence measurements were obtained by 660 and 785 nm excitation and absorption spectra were collected. The pH of each NaOH/SDBS-SWNT/M^{n+} combination was obtained using pH-indicator strips. It was found that the metal ions reacted with the strong base changing

the pH. In addition to the metal ions, the change in pH also causes quenching (see below) therefore NaOH was found to not a suitable base for these quenching studies.

Nanotube Fluorescence as a Function of pH. To ensure that the pH did not play a role in the quenching mechanism, SDBS-SWNTs (2.0 mL, 24 $mg.L^{-1}$) were placed in a cuvette. NH_4OH solution (0.8 mL, pH = 7.5) was added and the solution was inverted several times to mix. Fluorescence measurements were taken after 24 hrs. The process was repeated for NH_4OH solutions pH = 7.5 - 12.5 in 0.5 pH unit increments, and the fluorescence intensity was monitored.

Fluorescence Recovery. For fluorescence recovery experiments, three solutions were prepared. A blank was prepared by placing NH_4OH/SDBS-SWNTs (2.1 mL, 1:0.4 ratio) in a cuvette. Millipore water (0.3 mL) was added and the cuvette was inverted several times to induce mixing. After 30 minutes, EDTA solution (0.3 mL, 100 mM in 1 M NH_4OH) was added and the solution mixed. Fluorescence measurements were obtained 30 minutes later. Samples of metal ion quenched SWNTs were obtained by combining NH_4OH/SDBSSWNT (2.1 mL, 1:0.4 ratio) with metal solution (0.3 mL) in a cuvette, where the concentration of the solution dependent on the type of metal. Concentration was chosen to quench the fluorescence of the SWNTs to approximately 2/3 of their original intensity. The cuvette was inverted several times and stood for 30 minutes. NH_4OH solution (0.3 mL, 1 M) was added, and the solution was mixed. Fluorescence measurements were obtained after 30 minutes. Fluorescence recovered samples were made by combining NH_4OH/SDBS-SWNT (2.1 mL, 1:0.4 ratio) with metal solution (0.3 mL) in a cuvette, where the concentration of the solution dependent on the type of metal. The cuvette was inverted several times and set for 30 minutes. EDTA solution (0.3 mL, 100 mM in 1 M NH_4OH) was added, the cuvette was inverted

several times, and fluorescence measurements were obtained after another 30 minutes. Spectra were compared to the blank to the metal ion quenched SWNTs.

Quenching Mechanism. Fluorescence quenching processes are described by the Stern-Volmer equation ($I_0/I = K_{sv}[Q] + 1$), where $K_{sv} = k_q\tau_0$, K_{sv} is the Stern-Volmer (SV) quenching constant, k_q is the quenching rate constant ($M^{-1}sec^{-1}$), and τ_0 is the excited singlet lifetime of the fluorophore in the absence of a quencher.

Raman Monitoring. The fluorescence of NH_4OH/SDBS-SWNTs with the metal ion solutions was monitored over time using Raman spectroscopy. NH_4OH/SDBS-SWNTs (2.1 mL, 1:0.4 ratio) were placed in a cuvette. While stirring, in-situ Raman measurements were taken every 45 s (1 second exposure, 5 accumulations). After 5 minutes, the appropriate metal solution (0.3 mL, 20 mM) was added to the cuvette and spectra were collected for 6 hrs. Changes in electron density in the SWNTs were monitored using Raman spectroscopy. NH_4OH/SDBS-SWNT's (2.1 mL, 1:0.4 ratio) were placed in a cuvette. While stirring, in-situ Raman measurements were taken every 45 s (with 1 s exposure, 5 accumulations). After five minutes, the metal solution (0.3 mL, 20 mM) was added to the cuvette and spectra were collected for 30 minutes. EDTA solution (0.3 mL, 100 mM in 1 M NH_4OH) was added and spectra were taken for five additional minutes.

References

1 S. Niyogi, S. Boukhalfa, S. B. Chikkannanavar, T. J. McDonald, M. J. Heben, and S. K. Doorn, *J. Am. Chem. Soc.,* 2007, **129**, 1898.

2 B. Brocklehurst, *Radiat. Res. Rev.,* 1970, **2**, 149.

3 E. J. Marshall, N. A.Philipson, and M. J. Pilling, *J. Chem. Soc., Faraday Trans. 2* 1976, **72**, 830.

4 *CRC Handbook of Chemistry and Physics,* 84th ed.; CRC Press: Boca Raton, FL., 2003.

5 S. M. Bachilo, M. S. Strano, C. Kittrell, R. H. Hauge, R. E. Smalley, and R. B. Weisman, *Science*, 2002, **298**, 2361.

6 R. Loscutova, and A. R. Barron, *J. Mater. Chem.*, 2005, **15**, 4346.

7 Applied NanoFluorescence, Houston TX.

8 We note that the addition of significantly higher concentrations of NaCl has been reported to result in spectral bleaching. See reference 1.

9 Y. Tan and D. E. Resasco, *J. Phys. Chem. B,* 2005, **109**, 14454.

10 M. S. Strano, C. B. Huffman, V. C. Moore, M. J. O'Connell, E. H. Haroz, J. Hubbard, M. Miller, K. Rialon, C. Kittrell, S. Ramesh, R. H. Hauge, and R. E. Smalley, *J. Phys. Chem. B,* 2003, **107**, 6979.

11 G. Dukovic, B. E. White, Z. Zhou, F. Wang, S. Jockusch, M. L. Steigerwald, T. F. Heinz, R. A. Friesnew, N. J. Turro, and L. E. Brus, *J. Am. Chem. Soc.,* 2004, **126**, 15269.

12 It has been observed that K_{SV} for SWNTs can be dependent on the excitation wavelength, generally weaker at longer excitation wavelength. This has been ascribed to the intrinsic luminescence quantum yield (in the absence of any quencher) decreasing with increasing excitation wavelength, M. E. Kose, B. A. Harruff, Y. Lin, L. M. Veca, F. Lu, and Y.-P. Sun, *J. Phys. Chem. B,* 2006, **110**, 14032.

13 B. Valeur, *Molecular Fluorescence: Principles and Applications.* Wiley-VCH, Chichester (2002).

14 M. Zheng and B. A. Diner, *J. Am. Chem. Soc.,* 2004, **126**, 15490.

15 We note that in Figure 1.2 there appears a slight increase in the intensity of the second van Hove transitions with the addition of Cd^{2+}; however, this is due to the overlap of the SWNT absorption with the tail of the Cd^{2+} absorption.

16 L. Kavan, P. Rapta, L. Dunsch, M. J. Bronikowski, P. Willis, and R. E. Smalley, *J. Phys. Chem. B,* 2001, **105**, 10764.

17 K. Okazaki, Y. Nakato, and K. Murakoshi, *Phys. Rev. B,* 2003, **68**, 035434/1.

18 H. Htoon, M. J. O'Connell, P. J. Cox, S. K. Doorn, and V. I. Klimov, *Phys. Rev. Lett.,* 2004, **93**, 0027401/1

19 Y.-Z.. Ma, J. Stenger, J. Zimmermann, S. M. Bachilo, R. E. Smalley, R. B. Weisman, and G. R. Fleming, *J. Chem. Phys.*, 2004, **120**, 3368.

20 F. Wang, G. Dukovic, L. E. Brus, and T. F. Heinz, *Science,* 2005, **308**, 838.

21 Y. Yin, S. B. Cronin, A. Walsh, A. Stolyarov, M. Tinkham, A. Vamivakas, W. Bacsa, M. S. Ünlü, B. B. Goldberg, and A. K. Swan, *IEEE J. Sel. Top. Quantum Electron.*, 2006, **12**, 1083.

22 S. Zaric, G. N. Ostojic, J. Kono, J. Shaver, V. C. Moore, M. S. Strano, R. H. Hauge, R. E. Smalley, and X. Wei, *Science*, 2004, **304**, 1129.

23 P. W. Barone, S. Baik, D. A. Heller, and M. S. Strano, *Nature Materials,* 2005, **4**, 86.

24 M. J. O'Connell, S. M. Bachilo, C. B. Huffman, V. C. Moore, M. S. Strano, E. H. Haroz, K. L. Rialon, P. J. Boul, W. H. Noon, C. Kittrell, J. Ma, R. H. Hauge, R. B. Weisman, and R. E. Smalley, *Science,* 2002, **297**, 593.

Chapter 2

Transition Metal Ion Interactions with SDBS-Surfacted Single Walled Carbon Nanotubes

Introduction

In Chapter 1 we reported that diamagnetic Group 2 and 12 metal ions quench sodium dodecylbenzenesulfonate (SDBS) surfacted SWNTs with varying degrees of efficiency.[1] This quenching occurs in the absence of aggregation, and the quenching efficiency is not only dependant on the identity of the metal ion but also the diameter (band gap) of the SWNT as well as, to a lesser extent, the identity of the anion. The larger the ionic radius of the ion, the greater the efficiency of quenching that occurs for a particular n,m SWNT. The smaller the diameter of the SWNT, the greater the quenching effect of a particular M^{2+} ion. Through a systematic study, we were able to eliminate contributions from pH effects, bundling, acid suppression, reduction-oxidation events, and surfactant desorption phenomena. Purposefully, we did not investigate any effects from paramagnetic contributions by only choosing Group 2 and Group 12 metal ions. To examine the paramagnetic effect of metal ions on SDBS surfacted SWNTs, metal ions with unpaired spins must be used. Taking into account charge density parameters, it is imperative to choose metal ions with similar radii and charge to that of the Group 2 and Group 12 metal ions with varying degrees of unpaired spin. To accomplish this goal, we have chosen to investigate copper, cobalt, and nickel salts. An examination of Table 2.1 shows the radii of the ions in relation to the metal ions already studied in Chapter 1.

The fluorescence quenching of large aromatic molecules by transition metal ions is well documented, and in several cases, an increased quenching has been observed in comparison to main group analogs due to their paramagnetic nature.[2,3] With this in mind, we have investigated the quenching effects of both paramagnetic and diamagnetic

Table 2.1. Comparison between Group 2 and 12 metal ions and transition metals by size and charge density.[4]

Metal	r (Å)	Charge density ($Z.Å^{-3}$)	Metal	r (Å)	Charge density ($Z.Å^{-3}$)
Mg^{2+}	0.66	1.66	Ni^{2+}	0.69	1.45
Ca^{2+}	0.99	0.49	Cu^{2+}	0.72	1.28
Sr^{2+}	1.12	0.34	Co^{2+}	0.72	1.28
Ba^{2+}	1.34	0.20			
Zn^{2+}	0.74	1.18			
Cd^{2+}	0.97	0.52			
Hg^{2+}	1.10	0.36			

transition metal ions (M^{2+}) on the fluorescence of SDBS surfacted SWNTs. In particular, we are interested in any difference between paramagnetic and diamagnetic cations because small polyaromatic molecules have been shown to exhibit an increased sensitivity to paramagnetic metal ions. The potential for similar effects to exist with extended aromatic systems such as SWNTs has yet to be investigated.

Results and Discussion

Individual semiconducting SWNTs dispersed in SDBS surfactant exhibit fluorescence at 660 and 785 nm irradiation. Consistent with our prior studies,[1,5] the addition of divalent transition metal salts with a concentration between 0.5-5 mM per 15 $mg.L^{-1}$ of SWNTs results in the reduction of the fluorescence of the SWNTs. The M^{2+}

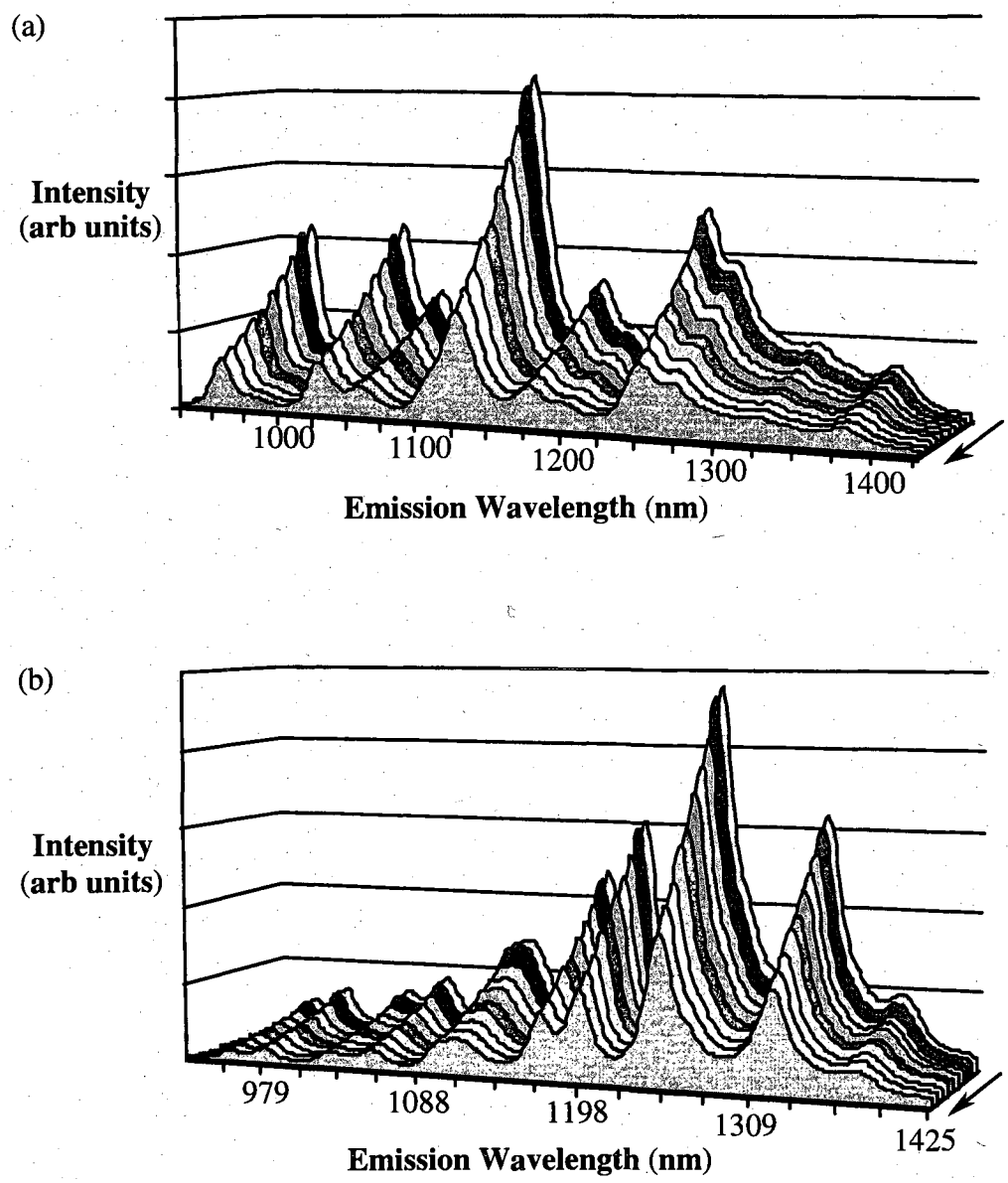

Figure 2.1. Fluorescence spectra of SDBS-SWNTs in the presence of $Cu(OAc)_2$ with (a) 660 nm and (b) 785 nm excitation showing the decrease in fluorescence with increased Cu^{2+} concentration (0 – 4.5 mM in 0.5 mM steps). The arrows indicate increasing Cu^{2+} ion concentration.

systems studied include $Cu(SO_4)$, $Cu(OAc)_2$, $CuCl_2$, $Co(SO_4)$, $Co(OAc)_2$, $CoCl_2$, $Ni(SO_4)$, $Ni(OAc)_2$, and $NiCl_2$.

The interaction between the metal ions and nanotubes is non-preferential in that all of the semiconducting nanotubes show a decrease in fluorescence with an increase in metal concentration. Displayed in Figure 2.1 is a representative three-dimensional plot, using $Cu(OAc)_2$, where fluorescence decay is observed irrespective of excitation energy, either 660 nm or 785 nm. Fluorescence spectra may be fitted for the contributions from each particular (n,m) SWNT.[6] Fitting the spectra and deconvoluting the intensity contributions from the 43 different fluorescing nanotubes were used to determine if any shifts in emission wavelengths were occurring. The emission spectra of the nanotubes in the presence of M^{2+} salts maintain the same line shape (albeit with a lesser intensity) as the nanotubes in the absence of the metal salt reaffirming that each of the different chirality nanotubes are affected to some degree.[1] In addition to maintaining the same line shape, none of the peaks shift during the reduction in fluorescence.

Stern-Volmer plots can be prepared and quenching constants for each *n,m* SWNT may be calculated.[1] Three representative plots are shown in Figure 2.2. A summary of the quenching constants for the 15 most intense nanotubes from 660 nm and 785 nm excitation are shown in Table 2.2. As may be seen from comparing the data in this table, there is a significant variation of quenching constants as a function of excitation wavelength. We have previously observed that the quenching constants for main group metal ions with SDBS-SWNTs show virtually no dependence on the excitation wavelength, which is in good agreement with similar studies.[1,7] Since the current study contradicts these observations, there must be another reason why transition metal ions quenching constants show excitation wavelength dependence.

The fluorescence quantum yield by a particular nanotube should remain constant in this system and is defined as the ratio of the number of photons emitted to the number of photons absorbed. The intensity of emission can be reduced if the number of photons absorbed by the nanotube is decreased. Unlike the Group 2 and 12 metals studied in our

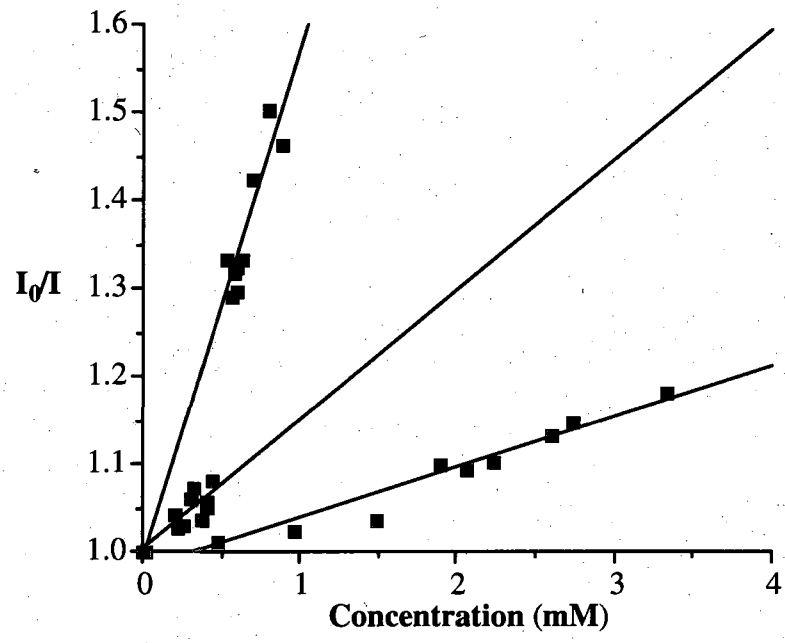

Figure 2.2. Representative Stern-Volmer plots for quenching of 12,5 SDBS-SWNT by $CuCl_2$ (▪, $R^2 = 0.951$), $CoCl_2$ (▪, $R^2 = 0.654$), and $NiCl_2$ (▪, $R^2 = 0.948$) measured using 785 nm excitation.

previous work,[1] the transition metals studied can absorb visible light via d→d transitions.

It is possible that a decrease in fluorescence for the SWNTs is observed because the absorption by the M^{2+} complex reduces the incident intensity effectively decreasing the quantum yield. By this reasoning, only metals that absorb at the excitation energy (660 or 785 nm) should be affected. This appears not to be the case since the absorption for each metal at 660 and 785 nm is minimal (Figure 2.3a). However, the UV-visible spectra for each metal salt is significantly altered in the presence of SDBS (Figure 2.3b) resulting in a shift in the spectra. This increases the absorbance at 785 nm and even more so at 660 nm. Furthermore, the subsequent absorption correlates with the relative effects on the quenching constant for each metal (see Table 2.2). Based upon this result, it is possible that the observed reduction of fluorescence of SDBS-SWNTs

enching constants for transition metal complexes from 660 and 785 nm irradiation.[a,b]

				SWNT n.m									
4	9,7	13,2	8,7	10,5	9,5	8,6	7,6	8,4	9,4	10,2	7,5	6,5	8,3
5	260	311	166	236	246	226	267	156	192	199	213	213	198
5)	(246)	(295)	(154)	(222)	(232)	(212)	(253)	(145)	(179)	(187)	(200)	(200)	(186)
1	476	566	304	456	418	474	580	336	409	440	488	502	499
3)	(449)	(535)	(284)	(430)	(393)	(447)	(548)	(314)	(385)	(415)	(461)	(474)	(471)
2	211	233	107	191	174	182	221	99	139	154	170	178	174
2)	(198)	(220)	(97)	(179)	(162)	(170)	(207)	(90)	(128)	(143)	(158)	(166)	(162)
	57	73	59	63	54	80	106	64	79	86	98	97	96
)	(48)	(63)	(50)	(54)	(45)	(70)	(94)	(54)	(69)	(75)	(87)	(86)	(85)
	66	82	66	71	68	95	115	80	96	99	110	109	108
)	(61)	(76)	(61)	(66)	(62)	(89)	(109)	(75)	(90)	(93)	(104)	(103)	(102)
	67	79	57	70	63	82	106	77	85	90	100	99	101
)	(63)	(74)	(53)	(65)	(59)	(78)	(100)	(72)	(81)	(85)	(95)	(94)	(96)
5	306	464	345	320	409	443	467	436	536	512	528	525	520
5)	(287)	(438)	(323)	(300)	(386)	(419)	(441)	(411)	(508)	(484)	(500)	(497)	(492)
5	253	432	289	268	379	396	421	353	476	457	470	458	458
5)	(234)	(407)	(268)	(249)	(355)	(372)	(396)	(331)	(449)	(431)	(444)	(432)	(432)
3	330	485	378	343	424	466	480	479	574	537	545	558	547
0)	(314)	(465)	(360)	(327)	(406)	(447)	(460)	(459)	(551)	(516)	(523)	(536)	(525)

n in parenthesis. [b] Measurements made on uncentrifuged samples containing M^{2+}(SDBS) colloids.

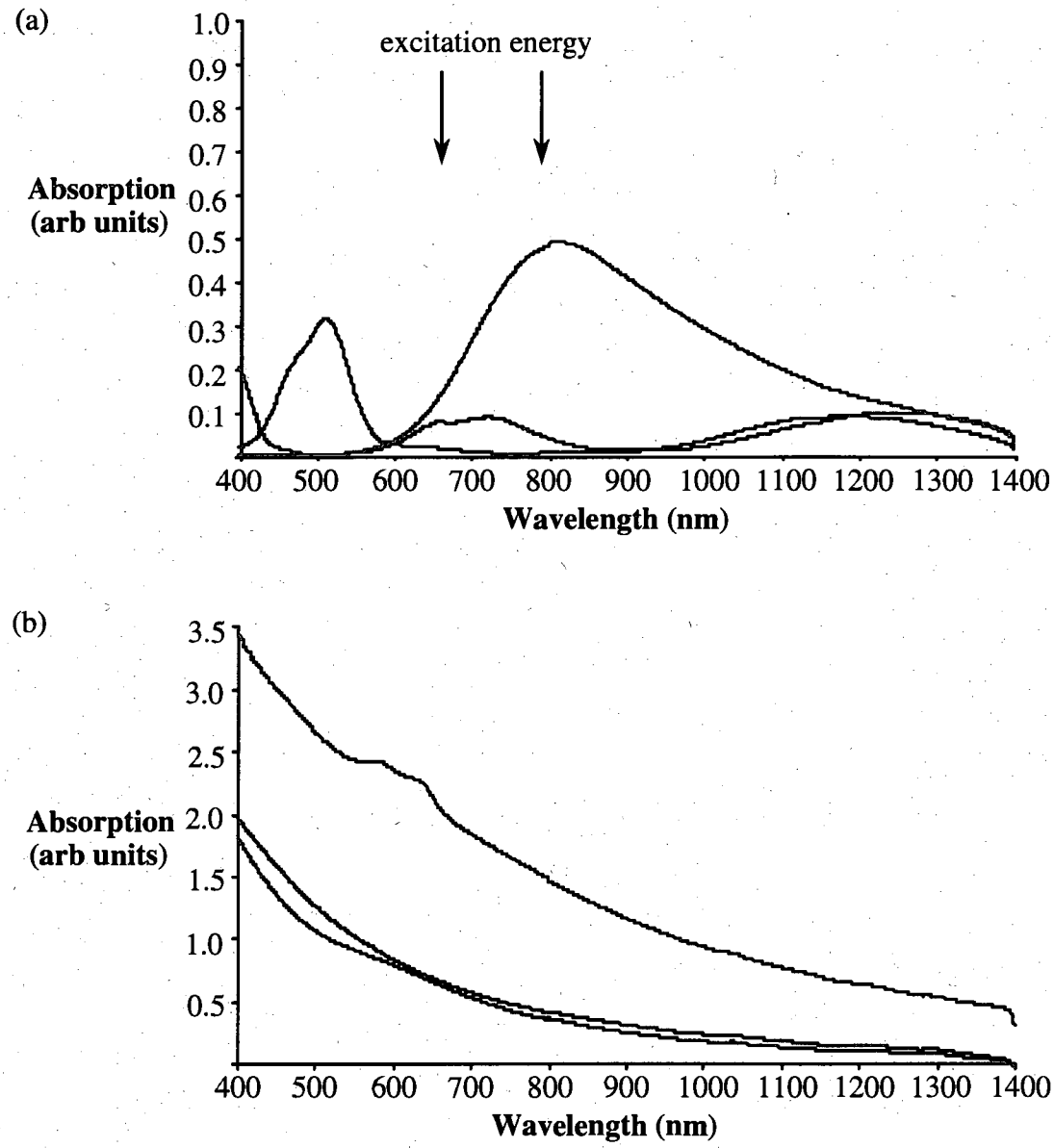

Figure 2.3. Absorption of $CuSO_4$ (—), $CoSO_4$ (—), and $NiSO_4$ (—) in (a) water and (b) in the presence of 1% SDBS. The 1% SDBS solution does not absorb in this spectral range. The excitation energies are shown for comparison.

in the presence of transition metals is at least partly due to the formation of a $M^{2+}\cdots$SDBS complex that filters the incident radiation and hence, reduces the observed

fluorescence intensity. The surfactant SDBS does not absorb in the 400 to 1400 nm range, but the colloidal precipitate has a different absorbance at each of the excitation energies, which should cause the quenching constants to vary whether they are calculated at 660 nm or 785 nm. This is in agreement with our observation.

Careful observation of the $Co(SO_4)$-SDBS solution shows the presence of a fine colloidal precipitate. This precipitate can be removed by centrifugation without precipitation of the SWNTs (see Experimental). UV-visible spectra show the concentration of SWNTs is unchanged after centrifugation. To insure that all absorbing colloid that could have an effect on the incident radiation has been removed, the absorption was monitored before and after centrifugation. Any remaining colloid that could have an effect would be evident in the absorption spectra. As can be seen in Figure 2.4, this was not observed. If the fluorescence of the Co^{2+}/SDBS-SWNT solution is

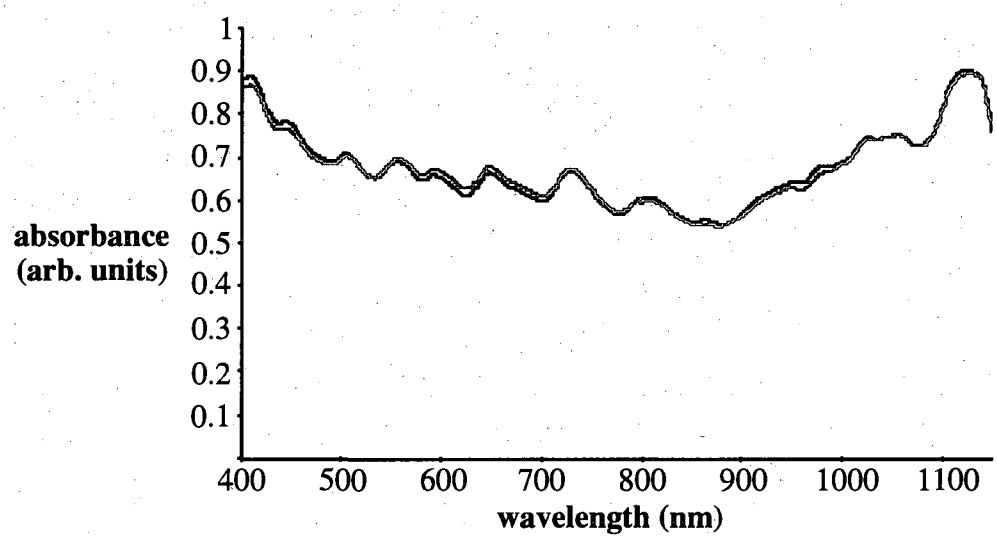

Figure 2.4. Absorbance spectra of SDBS SWNTs with 3.0 mM $CuSO_4$ after the colloidal precipitate has been removed by centrifugation (▬) and SDBS SWNTs with no treatment (▬).

enching constants for transition metal complexes from 660 nm irradiation.[a]

				SWNT	n.m								
2,4	9,7	13,2	8,7	10,5	9,5	8,6	7,6	8,4	9,4	10,2	7,5	6,5	8,3
48	322	284	376	234	192	208	225	77	120	148	187	141	141
33	407	259	334	289	247	252	269	210	196	208	230	223	212
9	352	182	260	267	107	94	85	97	26	58	78	61	42
3	106	53	107	101	81	94	125	104	90	100	115	112	106
4	100	44	98	98	76	94	123	98	86	96	110	104	96
1	117	74	127	109	90	105	127	108	95	104	120	112	108
72	443	578	449	424	387	378	366	393	389	358	410	423	405
24	423	566	461	412	400	383	370	421	402	377	430	392	414
70	396	479	353	369	294	282	257	276	316	274	315	305	304

termined by ICP AES. [b] Reliable quenching constants could not be obtained due to low peak intensities.

:nching constants for transition metal complexes from 785 nm irradiation.[a]

				SWNT	n.m								
2,4	9,7	13,2	8,7	10,5	9,5	8,6	7,6	8,4	9,4	10,2	7,5	6,5	8,3
48	322	284	376	234	192	208	225	77	120	148	187	141	141
33	407	259	334	289	247	252	269	210	196	208	230	223	212
9	352	182	260	267	107	94	85	97	26	58	78	61	42
3	106	53	107	101	81	94	125	104	90	100	115	112	106
4	100	44	98	98	76	94	123	98	86	96	110	104	96
1	117	74	127	109	90	105	127	108	95	104	120	112	108
72	443	578	449	424	387	378	366	393	389	358	410	423	405
24	423	566	461	412	400	383	370	421	402	377	430	392	414
70	396	479	353	369	294	282	257	276	316	274	315	305	304

:termined by ICP AES. [b] Reliable quenching constants could not be obtained due to low peak intensities.

measured after centrifugation, the apparent extent of quenching is significantly reduced. Moreover, the calculated quenching constants from both 660 and 785 are within experimental error of each other (Table 2.3 and Table 2.4).

Based upon the lowering of the metal ion concentration in solution, the precipitate is presumed to form from the interaction of Co^{2+} with SDBS (in the presence of NH_4OH). This is confirmed by the observation of identical precipitates from the direct reaction of $Co(SO_4)$ with SDBS at pH 10.5. In order to obviate the effects of the absorption by the precipitate, a series of samples were prepared in which an aliquot of MX_2 was added to SDBS-SWNT. The fluorescence was measured after addition, and the sample was centrifuged prior to re-collection of the fluorescence spectrum. Figure 2.5a shows the change in fluorescence intensity as a function of added $CoSO_4$ without removal of the metal-SDBS colloid, compared to the equivalent progression but after each sample had been centrifuged. It is important to note that these are overlaid decay graphs that occur over different concentration ranges. It is clear from Figure 2.5b that the actual quenching ability of $CoSO_4$ is significantly different than observed from the raw data. After removal of the absorbing colloids, both incident radiation and emission are no longer being absorbed by the colloids allowing higher emission intensity. The quenching constants depend on the incident and emissive radiation as well as the metal ion concentration in solution. When the colloid is removed by centrifugation, all three of these may change. For that reason, the metal concentrations are remeasured by ICP and emission intensities by fluorescence spectroscopy to calculate new Stern-Volmer quenching constants that may increase, decrease, or remain the same depending on how the three variables change. These "corrected" Stern-Volmer quenching constants are calculated from the data for all the centrifuged samples and are listed in Table 2.3 and Table 2.4.

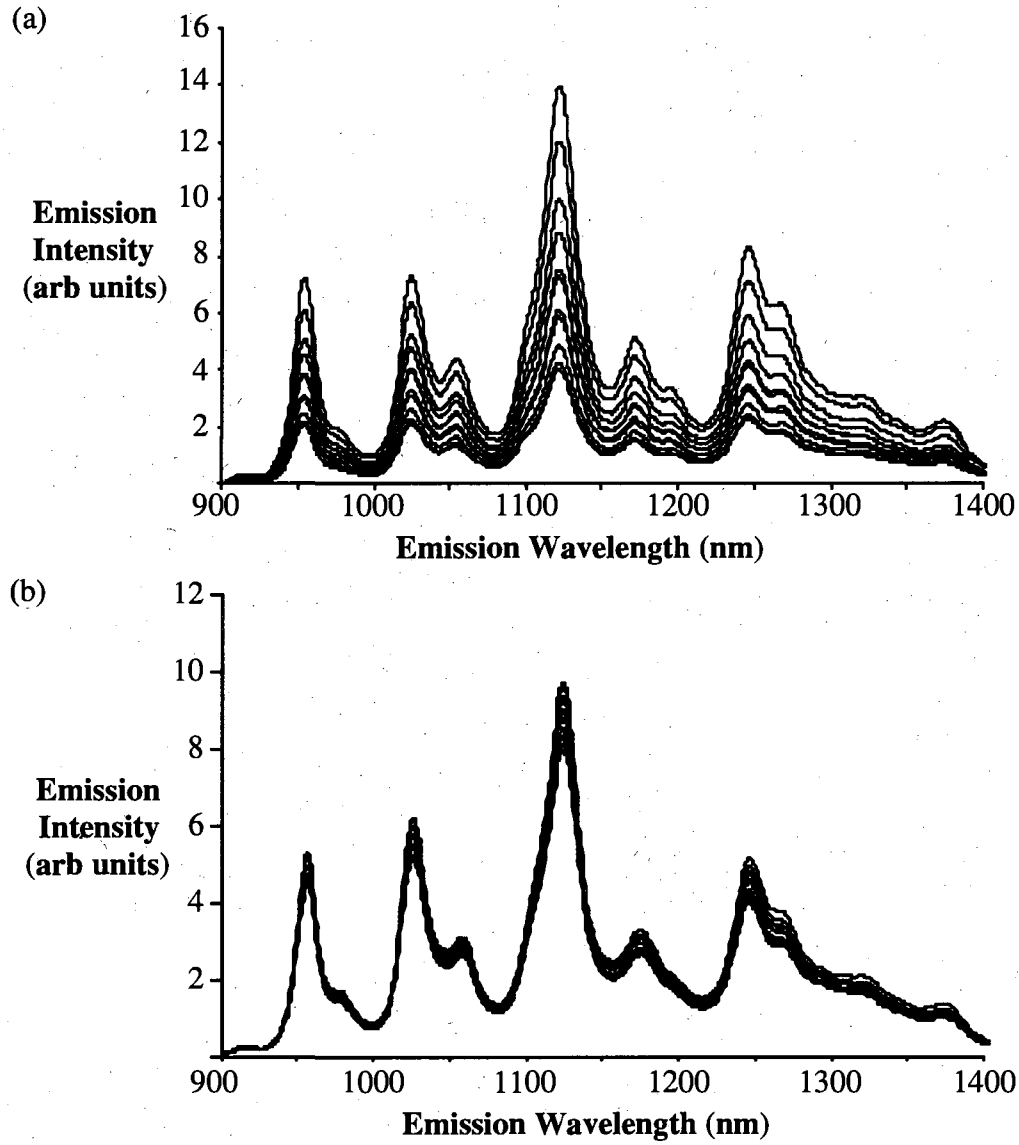

Figure 2.5. Fluorescence decay of SDBS-SWNTs due to the presence of $CoSO_4$ (a) before and (b) after the removal of $CoSO_4$ colloidal precipitate by centrifugation. The concentration range of (a) is 0 to 5.0 mM and (b) is 0 to 1.0 mM $CoSO_4$ in equal increments.

In the presence of colloidal precipitate, $CoSO_4$ acted as a much better quencher than its $CoCl_2$ and $Co(OAc)_2$ counterparts (refer to Table 2.2). With the correction, it

now exhibits a similar quenching ability to other Co^{2+} salts (Table 2.3 and Table 2.4). The differences after correction for Cu^{2+} and Ni^{2+} are less dramatic with only slight changes observed. However, it is important to note that removal of the absorbing colloidal species also eliminates the excitation energy dependence yielding the same quenching constants from both 660 nm and 785 nm excitation. Thus, while colloidal precipitates filter some of the incident radiation, a considerable quenching event still occurs.

Dependence on Metal. In our previous studies, the quenching constant for a particular *n,m* SWNT is highly dependant on the choice of group 2 or 12 metal ion. The same is true, to an even greater extent, for the transition metals. A comparison of the data for the acetate salts in Table 2.3 (eliminating counter ion effects) shows that the quenching efficiency follows the general trend $Ni^{2+} < Co^{2+} < Cu^{2+}$. The same is true for the sulfate and chloride salts. Comparing the data for all the *n,m* values, it is apparent that there is no correlation between the Stern-Volmer quenching constants and the atomic number, diffusion coefficient, or the reduction potential.

For diamagnetic Group 2 and 12 divalent metal salts, we have observed a strong correlation between the quenching constants and the ionic volume and charge density.[1] This correlation was explained by the interaction of the metal cation with the correlated electron-hole states in the exciton formed from the SWNT's light absorption. Where the attractive force is greater for the $M^{n+}\cdots e^-$ interaction than the hole$\cdots e^-$ interaction, the presence of the M^{n+} ion will cause the radiative recombination of the electron and hole less probable, resulting in a reduction in fluorescence. The excited electron is "pinned" by the charged sphere(s) of the metal ion(s). The larger the metal ion, the greater the volume of a SWNT's exciton can be affected by the charge of the metal ion.

If the quenching ability of the transition metal ions is due solely to the "charge

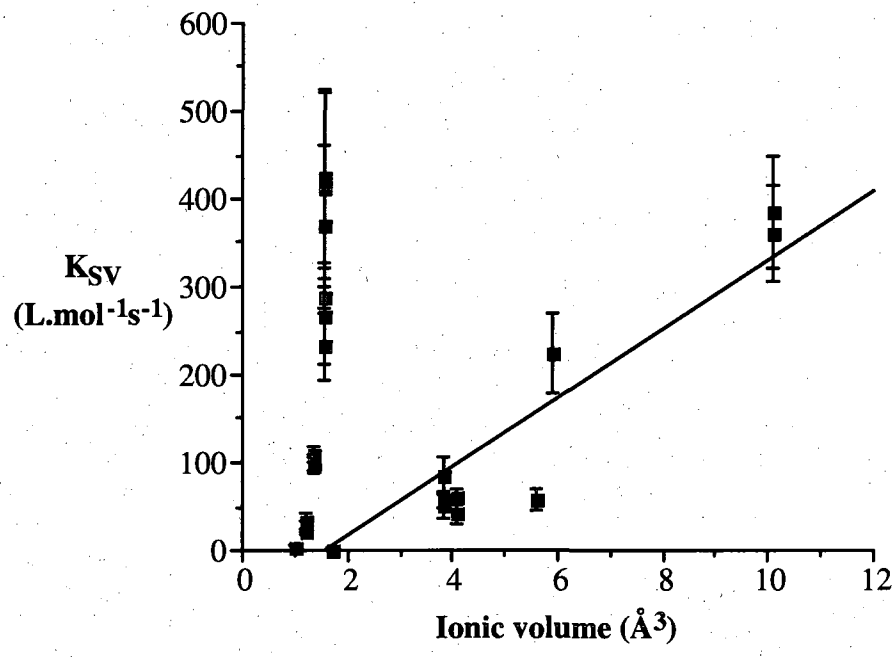

Figure 2.6. Corrected Stern-Volmer quenching constant for the 10,5 SDBS-SWNT using 660 nm excitation as a function of the M^{2+} ionic volume for CuX_2 (■), CoX_2 (■), NiX_2 (■) and Group 2 and 12 salts (■, $R^2 = 0.859$).

density effects," then the appropriate data for the transition metal ions should fit the same graph as for the Group 2 and 12 metals. In Figure 2.6, the transition metals (in particular Cu^{2+}, Co^{2+} and to a lesser extent Ni^{2+}) deviate considerably from the expected trend. The measured Cu^{2+} (r_{ionic} = 0.72 Å) shows a comparable Stern-Volmer quenching constant to that of Ba^{2+} (r_{ionic} = 1.34 Å),[5] while a consideration of its ionic radius would suggest a quenching efficiency similar to Zn^{2+} (r_{ionic} = 0.74 Å).

A decrease in fluorescence of a SWNT can be caused by any of several possible effects: inter-tube energy transfer from bundling, acid suppression of fluorescence, changes in the absorption (spectral bleaching), and quenching via either static or dynamic mechanisms. In our previous studies with Group 2 and 12 metal salts, we concluded that the decrease in fluorescence upon addition of the metal salt was not due to any of these

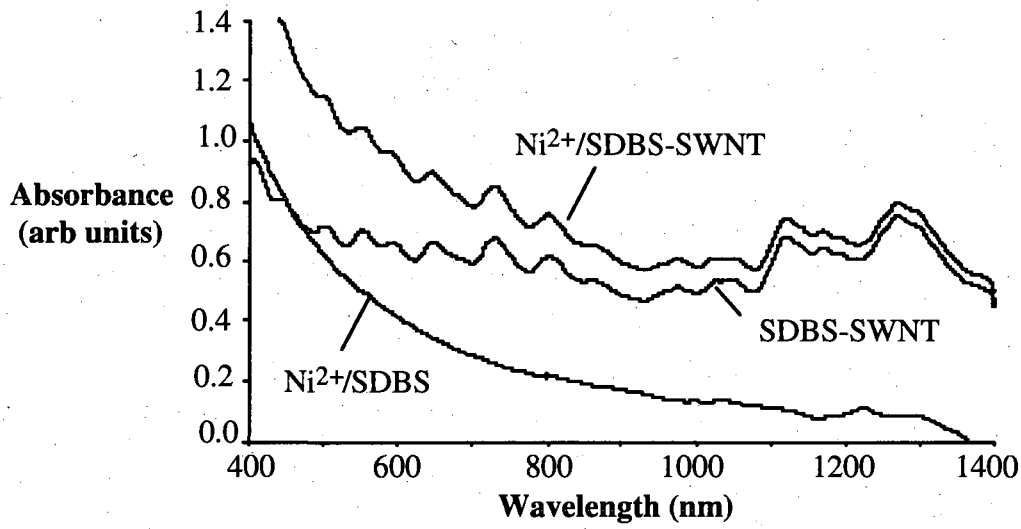

Figure 2.7. UV-Vis absorption spectra of SDBS-SWNTs, SDBS-SWNTs in the presence of $NiCl_2$ (2.5 mM), and $NiCl_2$ in the presence of SDBS.

effects but rather attributed to quenching.[1] Several key aspects suggest that transition metals quench the fluorescence of SDBS-SWNTs in a similar mechanism as the diamagnetic Group 2 and Group 12 metals.

A characteristic of bundling of SWNTs is a red shift and broadening of the bands in the UV-vis spectrum.[8] In Figure 2.7, no such effects occur with the addition of Ni^{2+}, suggesting that that the ground state electronic structure of the SWNTs is not perturbed. Further evidence for the lack of bundling is that fluorescence loss due to the presence of M^{n+} ions can be recovered by adding EDTA. For example, in Figure 2.8, the addition of 3.0 mM $CoCl_2$ to SDBS-SWNTs results in a reduction in fluorescence. Subsequent addition of an excess of EDTA results in the recovery of fluorescence. It is important to note that if the SWNTs did bundle, the binding energy of ~0.5 $eV.nm^{-1}$ of SWNT contact is difficult to overcome and treatment with EDTA would not separate them. In fact, bundling is generally irreversible without extreme physical treatment such as sonication.[9] As with our previous studies,[1] the suppression of SWNT fluorescence in an acidic

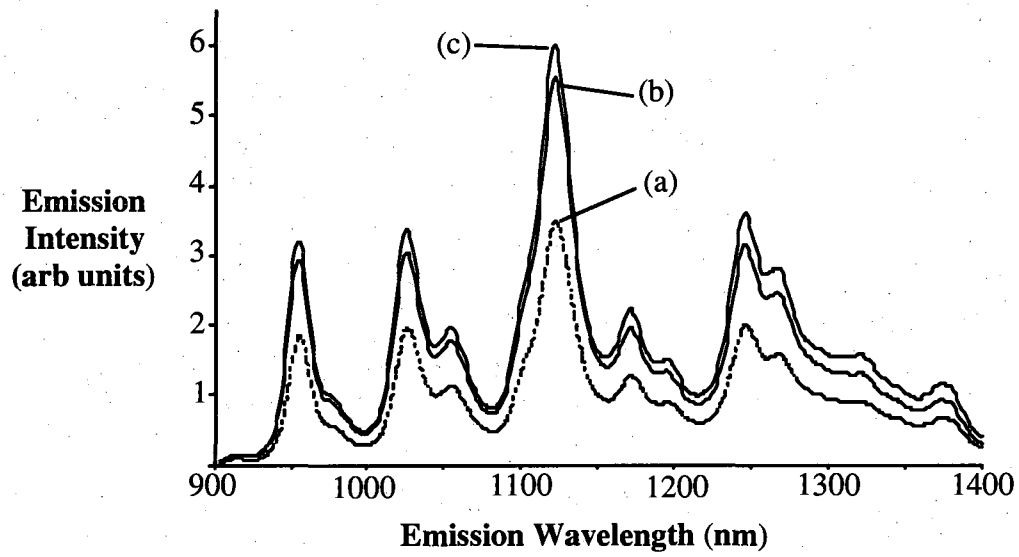

Figure 2.8. Fluorescence of SDBS-SWNTs using 660 nm excitation in the presence of $CoCl_2$ (3.0 mM) (a) before and (b) after the addition of EDTA (15 mM) showing the recovery of fluorescence with the addition of EDTA. The SDBS-SWNT fluorescence spectrum (c) in the presence of EDTA (15 mM), but absence of quencher is shown for comparison.

medium[10,11] is overcome by the use of basic conditions.

A loss of fluorescence can be caused by changes in the absorption properties of the fluorophore (i.e., the SDBS-SWNT). This process is ordinarily classified as "spectral bleaching." In Figure 2.7, there is no change in the absorbance spectra accompanying fluorescence decay with the addition of metal ions (c.f., Figure 2.8a), indicating that spectral bleaching is not the source of fluorescence decay; however, there is clearly a perturbation of the electronic structure of the SWNTs. The intensity of the radial breathing mode (RBM) is an indication of the electron density on the SWNT. As shown in Figure 2.9, the addition of Cu^{2+} shows a reduction in the radial breathing mode (RBM) at 236 cm^{-1} caused by a change in electron density in the nanotube.[12,13] The intensity of

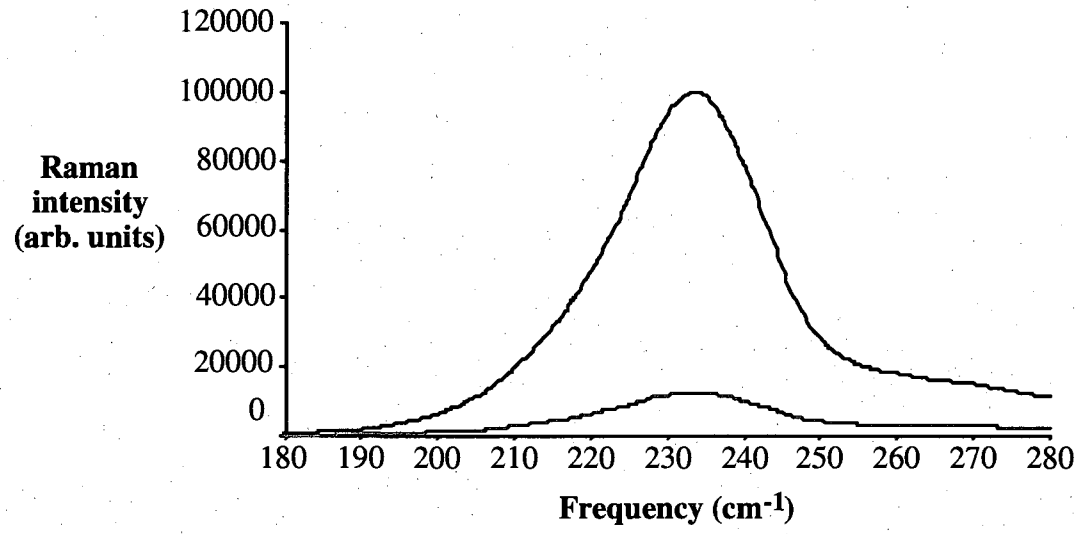

Figure 2.9. Intensity of the radial breathing mode for SDBS-SWNTs before (—) and after (—) the addition of 2.5 mM $CuSO_4$.

the RBM can be recovered upon the removal of the metal ions. The addition of EDTA promotes the formation of a M[EDTA] complex that is sterically hindered from being sufficiently close to the nanotubes, therefore, preventing the metal ions from having an effect.

Based upon the forgoing, we conclude that both diamagnetic and paramagnetic transition metal ions quench the fluorescence of SDBS surfacted SWNTs. While diamagnetic ions solely have an electronic character, transition metals possess possible electronic and paramagnetic properties. While there is no apparent effect of the paramagnetic center on the SWNT fluorescence quenching, the interaction of the transition metal ions with free surfactant (SDBS) results in the formation of a colloidal precipitate that absorbs in the ranges for fluorescence excitation (660 and 785 nm).[14] Removal of the colloid changes the fluorescence intensity such that $CoSO_4$ exhibits similar characteristics as those of $Co(OAc)_2$ and $CoCl_2$, and as a result the quenching efficiency follows the trend: $Ni^{2+} < Co^{2+} < Cu^{2+}$. It is worth noting that the trend is $d^8 <$

$d^7 < d^9$, which suggests that paramagnetic metal ions are better quenchers than diamagnetic ions. One could propose that this may account for the greater than expected reduction in fluorescence as was observed in previous work.[2,3] However, the magnetic moments (μ_{eff}), which were measured by the solution ^1H NMR Evans method,[15] of the metal salts at the pH used for the fluorescence measurements are in the order Co^{2+} (μ_{eff} = 3.72) > Ni^{2+} (μ_{eff} = 3.11) > Cu^{2+} (μ_{eff} = 1.83), which does not follow the trend of quenching efficiency. Thus, we conclude that the apparent enhanced quenching efficiency observed is not due to the paramagnetic nature of the metal ions and other pathways need to be explored.

Systems that utilize surfactant stabilized nanotubes and metal ions acting as quenchers have a variety of interactions that need to be considered in addition to the metal ion acting as a quencher. Most importantly, the SWNT···surfactant interaction needs to be maintained in order for the SWNTs to remain unbundled and hence fluoresce. A dramatic decrease in fluorescence is observed when the surfactant micelle is disrupted. In the present case the reversible nature of the transition metal quenching (i.e. upon addition of a metal chelating agent) precludes bundling that could be responsible for any quenching observed. The second important interaction is between the divalent, positively charged metal ion and the negatively charged surfactant head. A strong interaction (i.e., Cu^{2+} and Co^{2+}) leads to colloidal metal ion/surfactant precipitate, whereas a weak interaction that is observed for main group ions (e.g., Ba^{2+}, Ca^{2+}, etc.)[5] does not form the colloids.

Considering a strong M^{2+}···surfactant interaction first, we propose that excess surfactant in solution (not associated with a SWNT) will complex the metal ion added, resulting in metal···surfactant colloids. Once this excess surfactant is removed, any further addition of metal ions will still be drawn to the surfactant, the majority of which is complexing the SWNTs. Thus, the surfactant will concentrate the metal ions near the

nanotube surface. This in turn will cause increased quenching per unit concentration added. This is indeed observed. In contrast, for the consideration of the effect on the SWNT fluorescence in the case of a weak cation···surfactant interaction, we propose that the metal ions are evenly distributed in solution (and the solvent/surfactant cage around the SWNTs) eliminating their accumulation at the SWNT surface and following the trend of charge density established in Chapter 1. The nature of the increased quenching for copper and cobalt salts (as compared to their Group 2 and 12 analogs) lies in their electrostatic interaction with the SDBS surfactant that is immobilized on the surface of the nanotubes.

Dependence on SWNT *n,m* and Anion. In Chapter 1 we showed that for Group 2 and 12 metal salts the Stern-Volmer quenching constants (for a particular metal/anion combination) show a linear correlation with SWNT diameter. The correlation with SWNT diameter arises from the location of the electron/hole pair in the SWNT. The SWNTs with smaller diameters are quenched more efficiently that those with larger diameters because there is a greater likelihood of the metal ion finding an exciton in a smaller diameter tube. Main group metals that have high quenching efficiencies (i.e., those with large ionic radii such as Sr^{2+} and Ba^{2+}) show a strong inverse dependence of the quenching constants on the diameter of the SWNT. In contrast, main group metals that are less efficient (small ionic radii, e.g., Mg^{2+} and Ca^{2+}) show little defined variation between SWNT types. Given the relatively small size of the transition metals studied, it is expected that the quenching constants should show little difference as a function of SWNT diameter in a similar manner to that observed for smaller main group quenchers; this is indeed observed as illustrated in Figure 2.10. Thus, in regard to the *n,m* dependence of the quenching, the transition metals behave more in line with their ionic radii rather than their quenching ability.

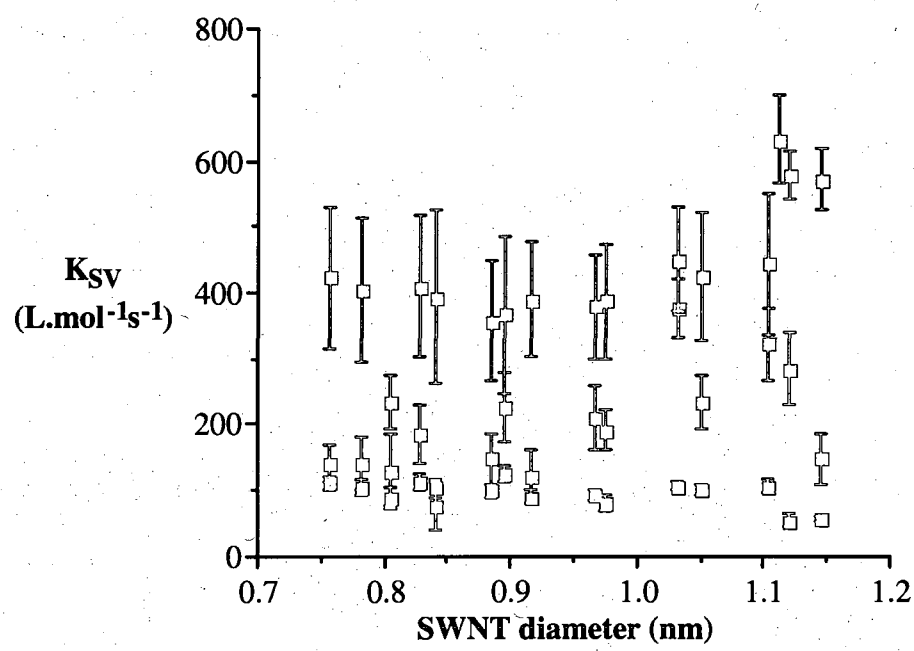

Figure 2.10. S-V quenching constants using MCl_2 for selected SDBS-SWNT (using 660 nm excitation) as a function of SWNT diameter. M = Cu (□), Ni (□), and Co (□).

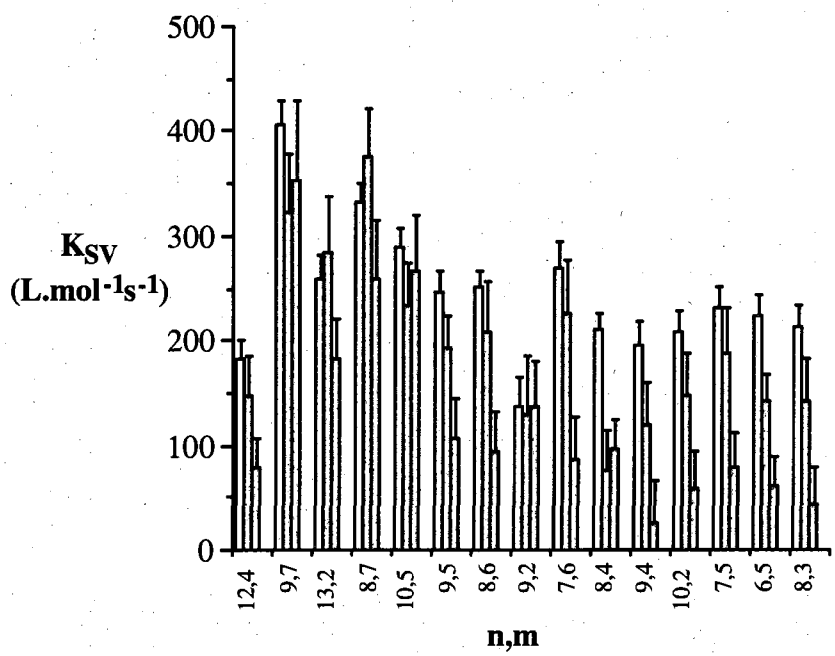

Figure 2.11. S-V quenching constants for SDBS-SWNT *n,m* values (using 660 nm excitation) as a function of CoX_n. X = Cl^- (□), SO_4^{2-} (□), and OAc^- (□).

As with the Group 2 and 12 metal salts, there is a dependence of the Stern-Volmer quenching constants on the identity of the anion, Figure 2.11. For the anions of the transition metals the quenching efficiency follows the trend of $Cl^- \approx SO_4^{2-} > OAc^-$. This order is opposite to that observed for ionic volume controlled quenching by Group 2 and 12 metal salts ($Cl^- \approx SO_4^{2-} < OAc^-$). In the latter case, we proposed the difference was due to the respective coordinative ability of the anions to the metals. The acetate···M^{2+} complex effectively had a larger ionic volume, making it a better quencher than the dissociating chloride and sulfate ligands. For the transition metals Cu^{2+} and Co^{2+}, the degree of quenching is more dependant on the ions' attraction to the SDBS's head than the ionic volume of the metal ion complex. We propose that the competition between the salt's counter ion and the surfactant is more important in defining the quenching ability of transition metal complexes as compared to that of main group metals.

Conclusions

We have demonstrated that both diamagnetic and paramagnetic transition metal ions quench SDBS surfacted SWNTs with varying degrees of efficiency. The identity of the anion has a lesser effect than that of the metal ion or the diameter of the SWNT. While all of the transition metal ions studied are relatively the same size, they quench the fluorescence of SDBS-SWNTs with varying efficiencies. We can preclude both the formation of a non-florescent ground state complex, spectral bleaching, or paramagnetic effects because even though the paramagnetic ions are better quenchers, their efficiency does not correlate with their magnetic moments. Instead, we propose that the SWNT excitons formed by light absorption are affected by the presence of the metal ion, facilitating non-radiative decay paths.

Unlike colorless Group 2 and 12 metal salts, there are two competing interactions occurring in solution for transition metals. The binding of the metal ions to the surfactant

results in the formation of colloidal species that filter the incident radiation in the fluorescence spectrometer and thus reduces the SWNTs absorbance. Photons that are not absorbed by the metal/surfactant colloid are absorbed by the SWNT. The SWNT then non-radiatively decays due to the presence of the metal ion. Even after the removal of the absorbent colloids, transition metals Cu^{2+} and Co^{2+} deviate (they are much better quenchers) from the trend expected from main group metals. We propose that the enhanced quenching observed in transition metal systems is due to the accumulation of metal ions near the surface of the micelle because of a strong $M^{n+}\cdots$SDBS interaction. This may not only be true for the SDBS-SWNT system but for any surfacted or polymer solubilized SWNT system where the free solvating species can complex with metal ions to yield a species that absorbs at the excitation wavelengths. If this happens, there may be an observed reduction in fluorescence of solubilized SWNTs without any quenching (or significant quenching) occurring. We therefore caution the use of fluorescence measurements of surfacted SWNTs as chemical sensors particularly in the presence of transition metals.

Experimental

All chemicals were obtained commercially and used without further purification. All solutions were prepared as described in Chapter 1. Metal salts used were $CuSO_4.5H_2O$ (Mallinckrodt Chemical), $Cu(OAc)_2.2H_2O$, $CuCl_2.2H_2O$, and $CoSO_4.7H_2O$ (J.T. Baker Chemical Company), $CoCl_2.6(H_2O)$, and $NiCl_2.6(H_2O)$ (Acros), $Co(OAc)_2$ (Alfa Inorganics) and $Ni(OAc)_2.4H_2O$ and $NiSO_4.6H_2O$ (Fisher Scientific Company). Technical grade sodium dodecylbenzensulfonate (SDBS), *tert*-butyl alcohol and 99.5% EDTA (Sigma-Aldrich), 99.9% deuterium oxide (Cambridge Isotope Laboratories Inc.), and 14.8 N NH_4OH (Fisher Scientific Company) were used as

received. Fluorescence, Raman, and UV-vis data were collected as described in the experimental section of Chapter 1.

^{1}H NMR spectra were recorded on a Bruker Avance-400 MHz spectrometer. A tube-in-tube apparatus was utilized with an inner reference solution consisting of 2% *tert*-butyl alcohol and 3-(trimethylsilyl)propane sulfonic acid in a 1 M NH_4OH H_2O/D_2O (80/20) solvent. The outer tube contained 2% *tert*-butyl alcohol and the paramagnetic compound (5 mM) in a 1 M NH_4OH H_2O/D_2O (80/20) solvent. The presence of D_2O in two different environments yielded two ^{2}H lock signals, either of which were used as the lock signal. The frequency shift of the two *tert*-butyl alcohol signals (methyl protons) were used to calculate the bulk magnetic susceptibilities and number of unpaired spins of the paramagnetic species.[15]

A Perkin Elmer Optima 4300 DV inductively coupled plasma atomic emission spectrometer (ICP-AES) was used to determine the metal ion concentrations. Each sample (0.5 mL) was treated with 90% HNO_3 (1.0 mL) for 48 hours to digest and/or bundle the nanotubes. The samples were diluted to 25.0 mL and the bundled nanotubes were removed by filtration. The metal ion concentrations were determined by ICP-AES. Preparation of SDBS surfacted SWNTs as well as all fluorescence recovery and Raman experiments were conducted as described in Chapter 1. Quenching experiments were conducted in a similar manner, but final metal concentrations were determined by ICP-AES to construct Stern-Volmer plots and calculate quenching constants.

References

1 J. J. Brege, C. Gallaway, and A. R. Barron, *J. Phys. Chem. C,* 2007, **111**, 17812.

2 B. Brocklehurst, *Radiat. Res. Rev.,* 1970, **2**, 149.

3 E. J. Marshall, N. A.Philipson, and M. J. Pilling, *J. Chem. Soc., Faraday Trans. 2,*

1976, **72**, 830.

4 *CRC Handbook of Chemistry and Physics,* 84th ed.; CRC Press: Boca Raton, FL., 2003.

5 R. Loscutova and A. R. Barron, *J. Mater. Chem.*, **2005**, *15*, 4346.

6 Applied NanoFluorescence, Houston TX.

7 J. E. Riggs, Z. Guo, D. L. Carroll, and Y.-P. Sun, *J. Am. Chem. Soc.,* **2000**, *122*, 5879.

8 M. J. O'Connell, S. M. Bachilo, C. B. Huffman, V. C. Moore, M. S. Strano, E. H. Haroz, K. L. Rialon, P. J. Boul, W. H. Noon, C. Kittrell, J. Ma, R. H. Hauge, R. B. Weisman, and R. E. Smalley, *Science,* 2002, **297**, 593.

9 Y. Tan and D. E. Resasco, *J. Phys. Chem. B,* 2005, **109**, 14454.

10 M. S. Strano, C. B. Huffman, V. C. Moore, M. J. O'Connell, E. H. Haroz, J. Hubbard, M. Miller, K. Rialon, C. Kittrell, S. Ramesh, R. H. Hauge, and R. E. Smalley, *J. Phys. Chem. B,* 2003, **107**, 6979.

11 G. Dukovic, B. E. White, Z. Zhou, F. Wang, S. Jockusch, M. L. Steigerwald, T. F. Heinz, R. A. Friesnew, N. J. Turro, and L. E. Brus, *J. Am. Chem. Soc.,* 2004, **126**, 15269.

12 L. Kavan, P. Rapta, L. Dunsch, M. J. Bronikowski, P. Willis, and R. E. Smalley, *J. Phys. Chem. B,* 2001, **105**, 10764.

13 K. Okazaki, Y. Nakato, and K. Murakoshi, *Phys. Rev. B,* 2003, **68**, 035434/1.

14 Similar colloids may also form with main group ions, but the resulting complexes do not absorb appreciatively at either 660 or 785 nm therefore their presence has little impact on the fluorescence intensity observed.

15 D. F. Evans, *J. Chem. Soc.,* 1959, 2003.

Chapter 3

Metal Ion Interactions with SWNT Fluorescence: The Role of the Surfactant

Introduction

In Chapters 1 and 2 we observed the effect of various metal ions on the fluorescence of sodium dodecylbenzene sulfonate (SDBS) surfacted single walled carbon nanotubes (SWNTs). The efficiency of quenching for Group 2 and Group 12 metal ions in Chapter 1 depends on the identity of the metal ion, the counter ion, and SWNT chirality.[1] As described in Chapter 2, the transition metal ions Ni^{2+}, Co^{2+}, and Cu^{2+}, exhibit increased quenching compared to the Group 2 and Group 12 analogs. We have assigned this difference to a greater interaction between the metal ions and the surfactant head group for the transition metals as compared to the Group 2 and 12 metal ions.[2] This suggests that the identity of the surfactant could also play a role in defining the extent of metal ion quenching of SWNTs. We are thus interested in comparing the effects of surfactant on the efficacy of metal ion fluorescence quenching of SWNTs.

Previous studies in the Barron Group have shown similarities as well as intriguing differences between the quenching of surfacted SWNTs with SDBS and sodium dodecyl sulfate (SDS). While coating SWNTs with CdS, it was observed that the fluorescence of SDS-surfacted SWNTs was quenched upon the addition of $Cd^{2+}/NH_4OH/TEA$ prior to the addition of the sulfur source (thiourea).[3] Upon addition of thiourea, and the formation of CdS coatings, the fluorescence returned to its original intensity. Thus, it would appear that Cd^{2+} quenches the SDS-SWNT fluorescence, and it is regained when the thiourea removes Cd^{2+}. This is much like our fluorescence quenching in Chapter 1, where the fluorescence is regained when EDTA treatment removes the metal ions from the vicinity of the nanotube. While this study suggests SDS behaves the same as SDBS during metal ion quenching, it was noted that there also seemed to be selectivity in that some peaks

appeared to be quenched significantly more than others. Other than reporting this observation, no attempt was made to determine its basis. It is clear, therefore, that a comprehensive study to determine the exact role of the surfactant identity in metal quenching of SWNTs is lacking.

Carbon nanotubes have been dispersed in a wide variety of surfactants for different applications.[4] Cationic and anionic surfactants provide good dispersibility and a long shelf life for individualizing SWNTs, making them attractive precursors for SWNT based sensors. Regardless whether the surfactant head group is positive or negatively charged, ionic surfactants disperse nanotubes in the same way. It is reasonable to propose that the hydrophobic tail adsorbs onto the highly hydrophobic surface of the nanotube and the hydrophilic charged head group extends into the water. The hydrophilic termini is often depicted as forming a layer around the SWNT,[5] however, the exact structure of the surfactant layer is unclear. It is reasonable to assume that each nanotube that is wrapped in surfactant electrostatically repels other similar nanotubes and thus prevents bundling. Certainly the presence of a charged surface is known to debundle SWNTs in solution,[6,7,8] and it is within reason to assume a similar effect is prevalent with charged surfactants.

The structures of four commonly used ionic surfactants are shown in Figure 3.1. While both types of surfactants should interact with the SWNT in a similar manner (hydrophobic interactions), it is likely that they will interact differently with positively charged metal ions. The cationic surfactants cetyltrimethylammonium bromide (CTAB) and dodecyltrimethylammonium bromide (DTAB) should electrostatically repel metal ions and thus fluorescence quenching should not be observed.[9] The anionic surfactants SDS and SDBS should both attract metal ions in a similar manner given the sulfate end group, however, does the structure of the surfactant hydrophobic tail have an indirect effect of the quenching of SWNTs by metal ions? The presence of the benzene in SDBS should provide a strong hydrophobic π-stacking interaction that will not be present for the SDS···SWNT conjugate; the structure of the surfactant layer should be distinct. Based

upon our previous results in Chapters 1 and 2, it should be possible to observe this phenomenon through fluorescence experiments.

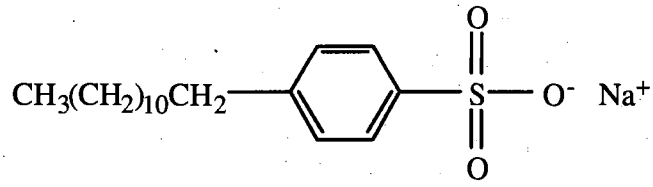

(SDBS)

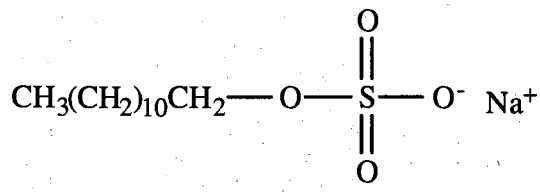

(SDS)

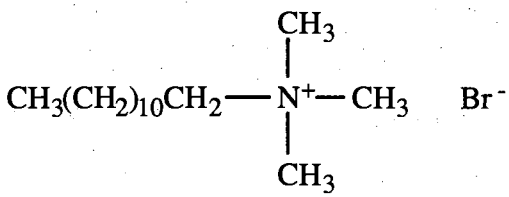

(DTAB)

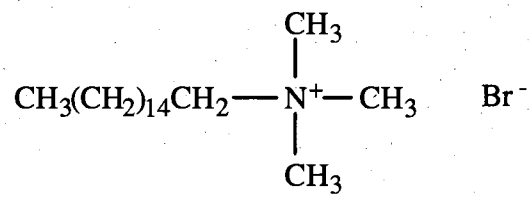

(CTAB)

Figure 3.1. Structure of common anionic surfactants used to disperse SWNTs.

Results and Discussion

Our initial studies (Chapters 1 and 2) focused on the quenching of SDBS surfacted nanotubes by various metal ions, which exhibit Stern-Volmer behavior.[1,2] This allowed for a quantitative assessment of the quenching and assignment of a mechanism as a basis of comparison for other surfactant systems. To understand the role of the

surfactant in fluorescence quenching, we varied the surfactant molecules while keeping the fluorophore (SWNT) and quencher (metal ion) constant.

Group 2 Metal Ions. The treatment of SDS-SWNTs with the Group 2 metal ions Mg^{2+}, Ca^{2+}, Sr^{2+}, and Ba^{2+} causes quenching of the SWNT's fluorescence. A representative plot is shown in Figure 3.2. The Group 2 metal ions quench SDS surfacted nanotubes in the same manner as they quench SDBS surfacted nanotubes; all *n,m* nanotubes are quenched to varying degrees and no spectral shifts occur. This type of behavior is consistent with the SDBS-SWNT with Group 2 metal ion system studied in Chapter 1 and the extent of quenching can be quantified. Table 3.1 lists the calculated Stern-Volmer quenching constants for all the Group 2 metal ions with SDS and SDBS surfacted nanotubes.

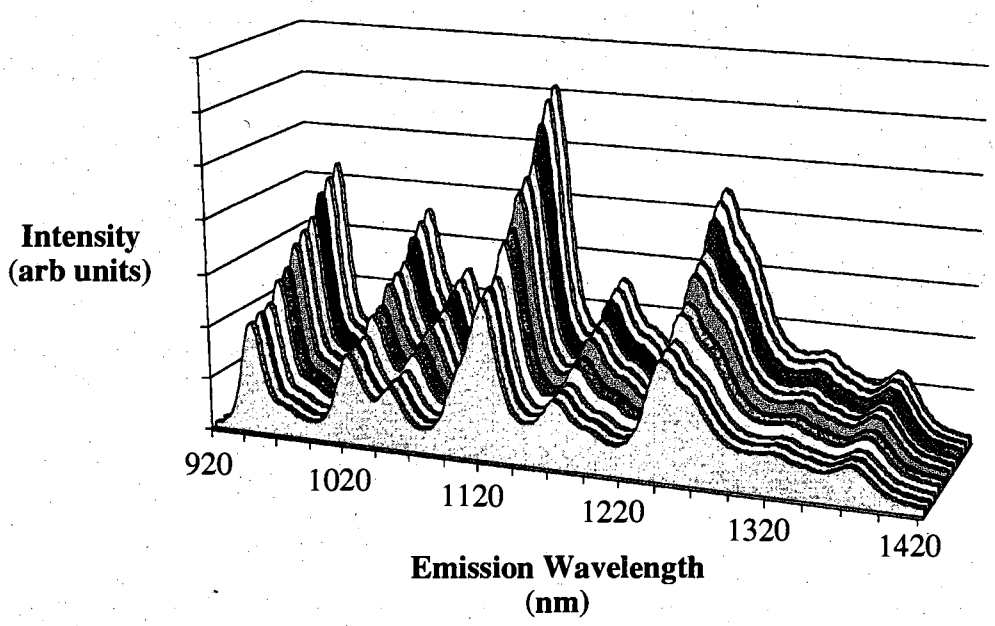

Figure 3.2. Decay graph of SDS-SWNTs excited at 660 nm treated with $BaCl_2$ from 0 to 5.0 mM in 0.5 mM increments.

Given the association of transition metal ions with SDBS surfactant,[2] we wanted to ensure that the main group ions are simply removing the surfactant from the nanotube causing a reduction of the fluorescence intensity (Chapter 2). For this to occur, the M^{2+}···surfactant interaction must be greater than the SWNT···surfactant interaction. McDonald et al. found the desorption activation energy for SDBS surfacted tubes to range between 84.3 and 148.8 $kJ.mol^{-1}$ while SDS surfacted tubes range between 54.8 and 166.8 $kJ.mol^{-1}$.[10] Indirect quenching by surfactant removal would predict that SDS tubes would be more greatly affected than SDBS tubes through this mechanism. We do not observe this trend confirming that the M^{2+}···SWNT interaction is the controlling factor in the quenching (Table 3.1) and not the SWNT···surfactant interaction.

Quenching interactions are limited by the ability of metal ions to come in close proximity of the SWNT surface. While it may be tempting to envision a surfacted SWNT as a cylindrical micelle with a nanotube core,[11] a random adsorption of surfactant molecules on the nanotube surface is the more realistic model,[12] although there has been experimental evidence for a "grease spot" type distribution of small aggregated micelles.[13,14]

A comparison of the quenching by a particular metal salt (BaOAc, $BaCl_2$, or $SrCl_2$) reveals that SDS-surfacted nanotubes are quenched to a lesser extent (lower K_{sv}) than the SDBS-surfacted nanotubes. This is apparent in Figures 3.3 and 3.4 (as well in the comparison of the data in Table 3.1). Here for a constant metal ion and nanotube n,m value, K_{sv} SDBS > K_{sv} SDS. A surfactant desorption model, as observed by Niyogi et al.[15], would predict that K_{sv} SDS > K_{sv} SDBS because the E_a of surfactant desorption is greater for SDBS than SDS. Clearly this is not observed; thus, the extent of fluorescence must be due to the accessibility of the metal ion to the SWNT surface. The head groups of both surfactants are the same, resulting in similar interactions with the metal ions, i.e., M^{2+}···$O{=}S(O)_2$-R. However, the tails of the two surfactants have the potential to act in a slightly different manner.

quenching constants for Group 2 metal complexes with SDBS-SWNTs and SDS-SWNTs from 660 nm
DS-SWNTs given in parenthesis).

	SWNT n.m													
4	9,7	13,2	14,0	8,7	10,5	9,5	8,6	7,6	8,4	9,4	10,2	7,5	6,5	8,3
	a	11	19	30	27	6	24	31	35	26	28	31	a	30
)	a	a	(12)	(7)	(5)	a	(6)	(5)	a	(8)	(10)	(1)	a	(6)
	a	22	18	21	21	14	30	43	20	26	33	38	a	36
)	a	(4)	(7)	(6)	(5)	(2)	(8)	(9)	a	(15)	(16)	(7)	a	(15)
	a	34	33	27	33	32	43	54	34	42	47	50	a	54
)	a	(3)	(6)	(5)	(4)	(1)	(8)	(8)	a	(11)	(13)	(4)	a	(12)
	40	40	13	32	41	26	43	61	26	39	43	51	48	51
7)	(113)	(87)	(231)	(206)	(220)	(21)	(54)	(69)	(47)	(37)	(73)	(60)	(85)	(57)
	67	30	19	55	61	19	43	51	53	39	39	46	46	44
5)	(109)	(92)	(253)	(217)	(192)	(27)	(63)	(83)	(51)	(42)	(82)	(71)	(101)	(66)
3	203	295	244	211	224	258	313	377	293	385	382	398	402	392
5)	(216)	(240)	(225)	(275)	(168)	(180)	(227)	(261)	(279)	(216)	(251)	(246)	(270)	(217)
4	323	460	363	294	361	431	481	611	464	603	596	637	613	640
9)	(192)	(223)	(151)	(197)	(195)	(200)	(208)	(227)	(241)	(236)	(234)	(223)	(202)	(216)
5	352	577	413	344	385	508	568	661	483	683	669	710	688	688
5)	(269)	(248)	(225)	(256)	(258)	(238)	(247)	(264)	(310)	(281)	(280)	(266)	(240)	(255)

stants could not be obtained due to low peak intensities.

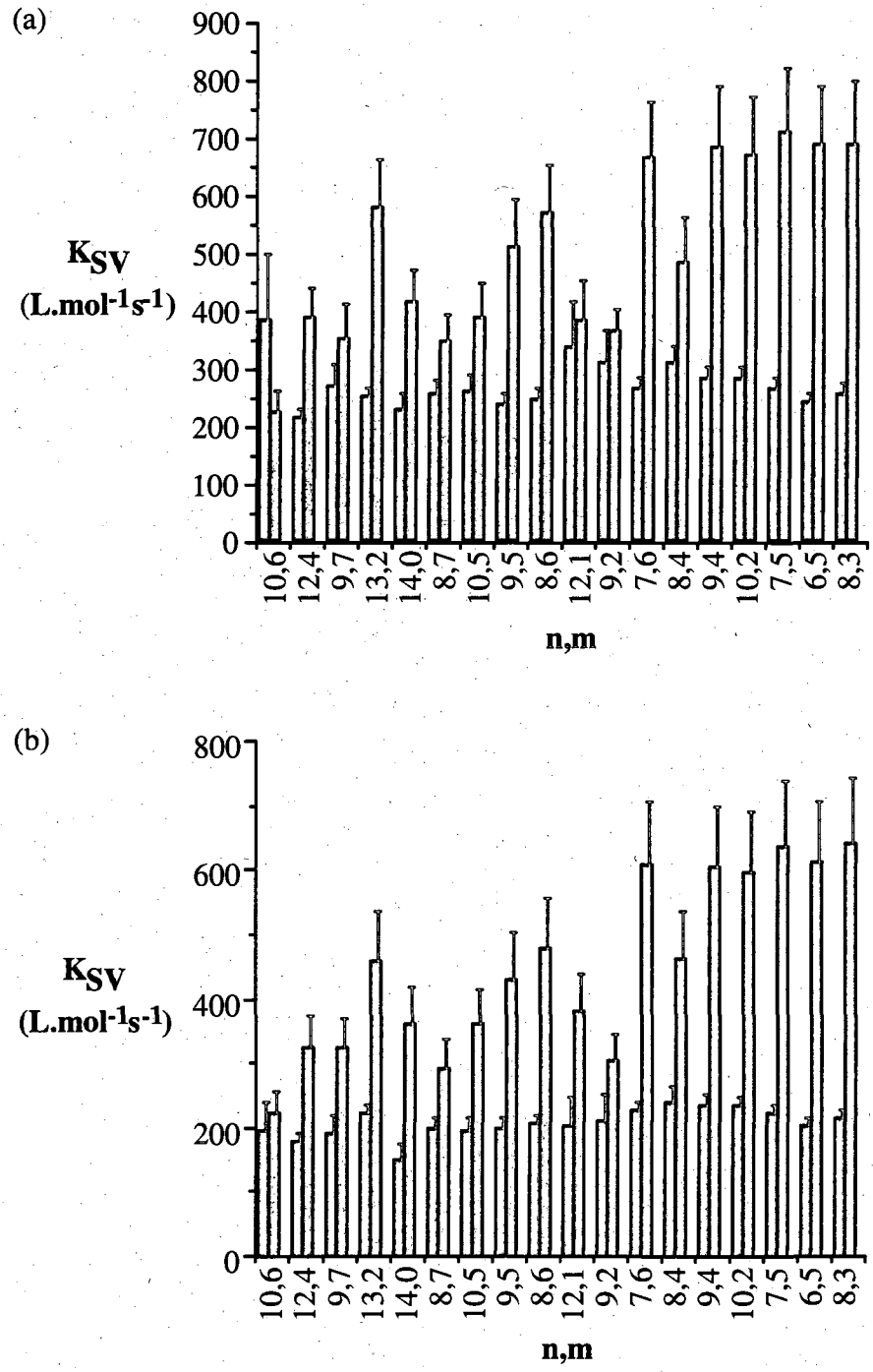

Figure 3.3. SDS-SWNTs (□) and SDBS-SWNTs (□) quenched by (a) BaOAc and (b) $BaCl_2$.

The interaction of the hydrocarbon tail of SDS with a SWNT is limited to van der Waal interactions, and as such, the hydrocarbon tail would randomly adsorb onto the nanotube surface with no preferred orientation. Furthermore, it is reasonable to expect the

hydrophilic anionic sulfate group will be oriented away from the hydrophobic SWNT surface (Figure 3.5). Thus, the metal ions are also randomly distributed along the nanotube as individual charges.

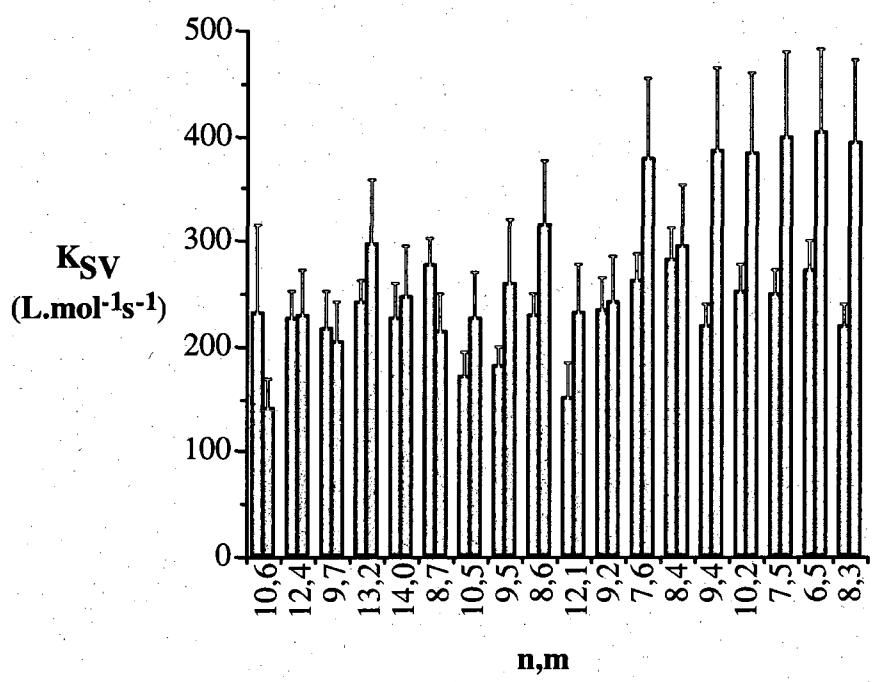

Figure 3.4. SDS-SWNTs (□) and SDBS-SWNTs (□) quenched by $SrCl_2$.

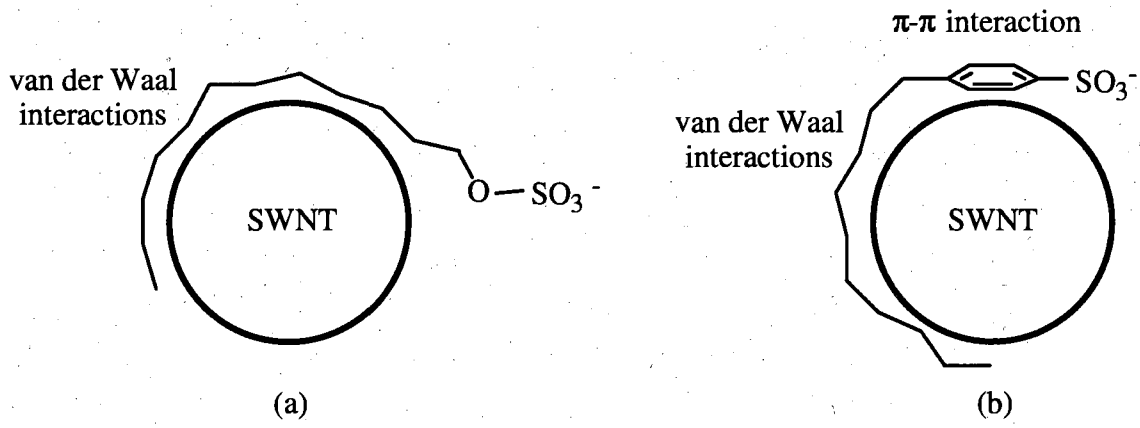

Figure 3.5. Schematic of the proposed interaction of (a) SDS and (b) SDBS with an individual SWNT.

In addition to the same $C_{12}H_{25}$ hydrocarbon tail, SDBS has a benzene group that will bind more strongly with the nanotube due to π-π stacking interactions, which stabilizes the surfactant on the nanotube.[16] If a strong π-π stacking interaction is present, the sulfate group, and hence the metal ion, will be closer to the SWNT surface (Figure 3.5). Given the quenching effect per metal ion is dependant on the $M^{2+}\cdots$SWNT distance, the extra π-π stacking will result in the metal ion being forced closer to the surface of the SWNT, and therefore a greater quenching being observed per metal ion. This is in–line with our observed fluorescence quenching results (see Figures 3.3 and 3.4).

Group 12 Metals. After investigating the differences between the Group 2 metal ion quenching of SDS and SDBS-SWNT fluorescence, we went on to look at how Group 12 metal ions differentiate between the two anionic surfactants. Our previous results (Chapter 1) showed that for SDBS-SWNTs, Group 2 and 12 metals both follow Stern-Volmer behavior.[1] Given the similar behavior between Group 2 and 12 metals for SDBS-SWNTs, it would be reasonable to propose that the quenching constant (K_{sv}) for Group 12 quenched SDS-SWNTs should be less than observed for their SDBS counterparts. Surprisingly, a very different scenario is observed. As may be seen from Figure 3.6, the quenching of SDS-SWNTs by Cd^{2+} does not follow a simple Stern-Volmer behavior. It appears that some tubes are quenched to a great extent while others are barely affected, as can be observed in the overlay plot in Figure 3.7. The same type of decay occurs for both Zn^{2+} and Hg^{2+}. Weisman and co-workers have shown that the fluorescence spectra may be fitted for the contributions from each particular n,m SWNT.[17] Each individual spectrum was therefore fitted to determine the intensity contributions of 43 different fluorescing tubes. Deconvolution of the spectra shown in Figure 3.6 gives the individual components for each SWNT n,m value. This suggests there is selectivity with regard to the quenching. There have been previous reports of selectivity with regard to those

SWNTs with band gaps above/below threshold values,[18] but this is clearly another phenomenon.

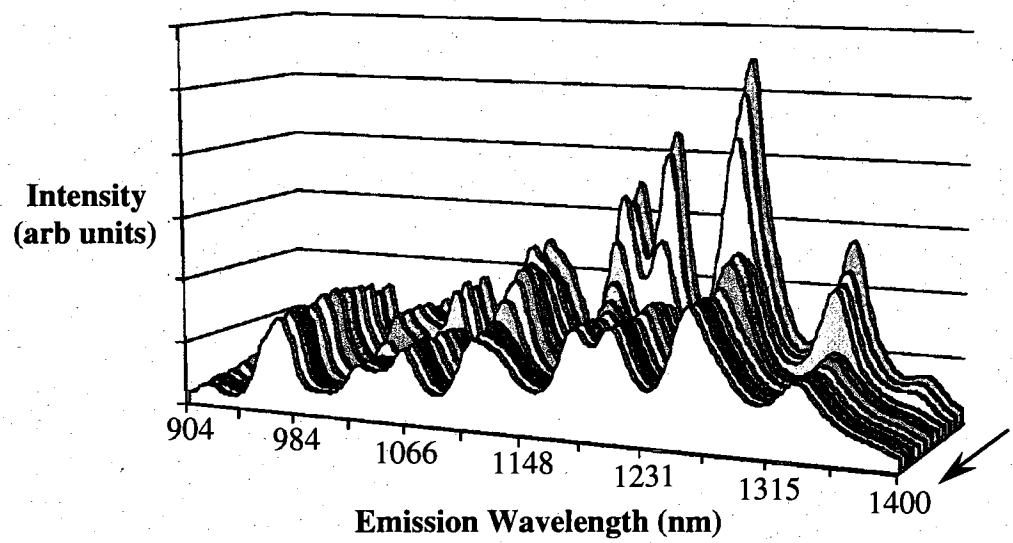

Figure 3.6. Decay graph of SDS-SWNTs excited at 785 nm treated and with $CdCl_2$ from 0 to 5.0 mM in 0.5 mM increments. The arrow indicates increasing M^{2+} concentration.

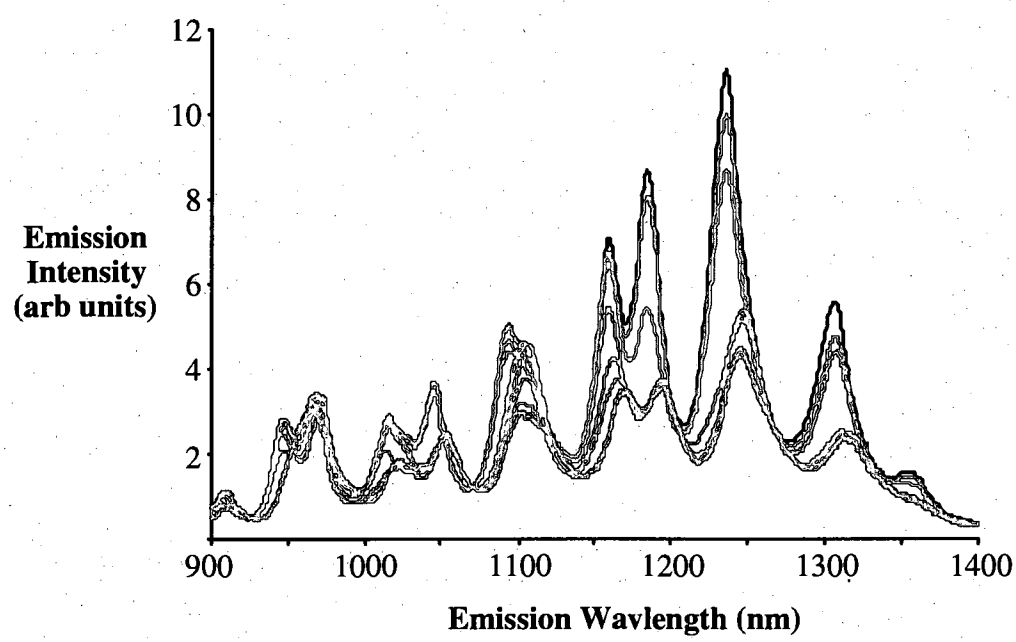

Figure 3.7. Overlay plot of SDS-SWNTs excited at 785 nm and treated with $CdCl_2$ from 0 to 5.0 mM in 0.5 mM increments.

In attempts to understand this observation, we focus on two SWNTs with similar diameters and emission wavelengths. The 10,5 tube has a diameter of 1.050 nm and emits at 1252 nm, while the 8,7 tube is 1.032 nm in diameter and emits at 1270 nm. The difference between them is that 10,5 is a mod 2 tube while 8,7 is a mod 1 SWNT.[19] Given their similarities in electronic properties, it follows that they would be expected to exhibit similar fluorescence quenching in the presence of Cd^{2+}. Surprisingly, careful observation of Figures 3.6 and 3.7 shows that the two tubes act differently. It appears that the emission contribution of the 10,5 tube at 1252 nm is completely eliminated in the presence of Cd^{2+} while the 8,7 tube follows a decay similar to that found in SDBS quenching, i.e., the greater the metal concentration the greater the decrease in fluorescence. Upon further inspection, it appears that the emission of other mod 2 nanotubes also completely ceases in the presence of Group 12 metal ions while the mod 1 nanotubes follow a more normal diminishing of the fluorescence intensity. This apparent distinguishment between mod 1 and mod 2 should be very unlikely since there is no reason for there to be any difference, therefore there must be an alternative rationalization.

As was discussed in Chapter 2, transition metal ions formed aggregates with the surfactant however, no evidence for a similar precipitate is observed here. The bundling of SWNTs results in the loss of fluorescence intensity.[20] Adding 3.0 mM Cd^{2+} to the SDS-SWNTs causes a reduction in fluorescence (61% of its original intensity), Figure 3.8. Subsequently adding ethylenediaminetetraacetic acid (EDTA) restores the fluorescence to 93% of its original intensity and shifts the peaks to their original position. Thus bundling is unlikely. A similar effect was observed during CdS coating of SDS-solubilized SWNTs.[21] The fluorescence of the SDS-SWNTs was quenched in the presence of Cd^{2+}. Upon addition of the sulfur source (thiourea), formation of CdS removes the free Cd^{2+} and the fluorescence is regained. Furthermore, the apparent selectivity (or shift) observed during the addition of Cd^{2+} is overcome after the SWNTs

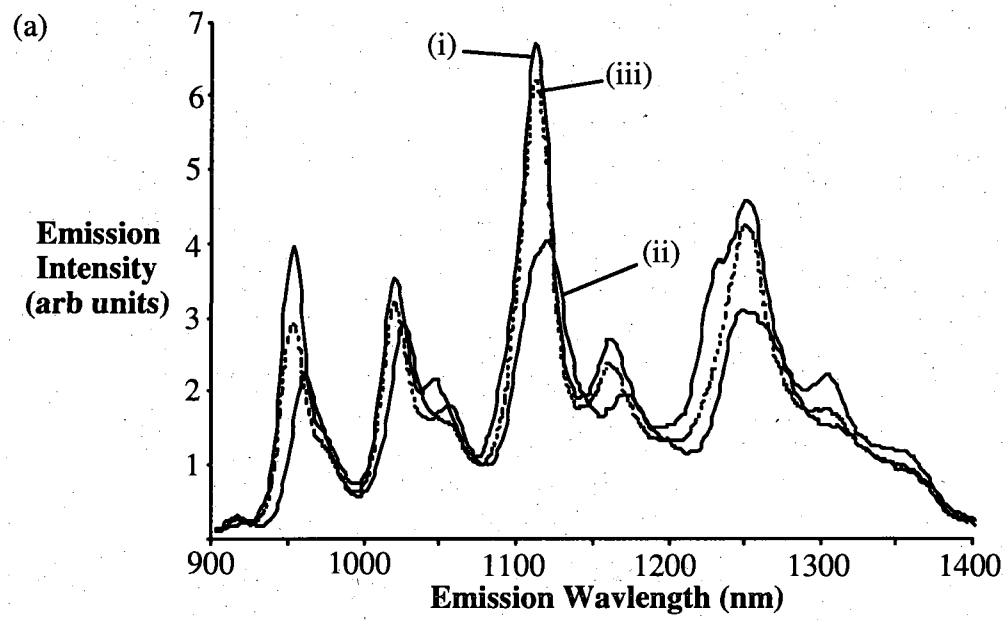

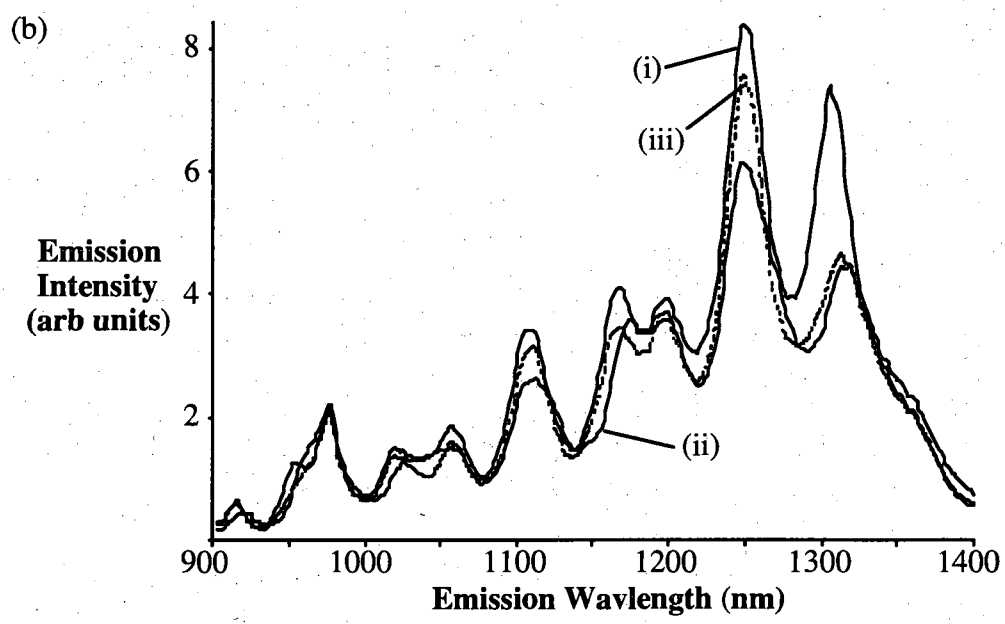

Figure 3.8. The emission spectra of SDS-SWNTs from (a) 660 nm and (b) 785 nm excitation. The (i) SDS-SWNTs, (ii) SDS-SWNTs quenched from Cd^{2+}, and (iii) recovered from EDTA treatment are shown.

are coated with CdS. Thus, we can exclude any bundling effects causing ground state changes.

In the absence of SWNT bundling and metal salt aggregation, the changes in fluorescence must be due to either a ground state or excited state process. To distinguish between the two possible mechanisms, we have looked at the absorption region of the nanotubes. As may be seen from Figure 3.9, the absorbance spectra of SDBS-SWNTs remains unchanged upon the addition of Cd^{2+}, although the fluorescence is quenched. In contrast, the electronic structure of SDS-SWNTs is disrupted as indicated by the significant shift in the bands in the 900 - 1400 nm region.[22] Thus, even though the cadmium salts do not absorb at 660 or 785 nm, the presence of ions in solution affect the ground state of the SDS surfacted nanotubes, shifting their absorption energies. This seems contradictory, however, because the emission data we have obtained is due to excitation at 660 or 785 nm.

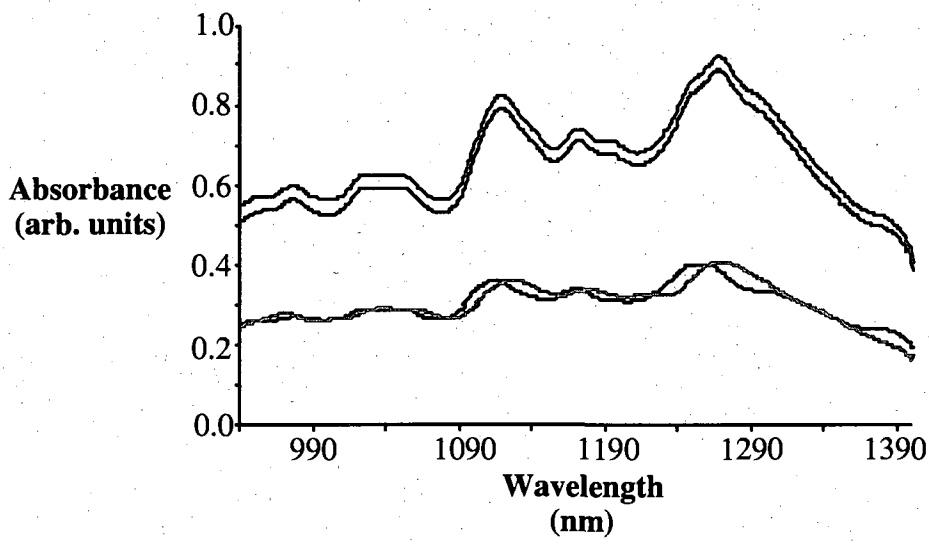

Figure 3.9. The absorbance spectra of SDS-SWNTs in H_2O (—) and SDS-SWNTs with Cd^{2+} (—). Shown for comparison are SDBS-SWNTs in H_2O (—), and SDBS-SWNTs with Cd^{2+} (—).

It is clear that the ground state of the SDS-SWNTs is altered in the presence of Group 12 metal ions. When the ground state is affected, we would expect the excitation wavelength for each individual n,m SWNT to change. To determine if this is occurring, the change in both excitation and emission wavelength for individual SWNTs can be probed by constructing a photoluminescence map as shown in Figure 3.10.[23] In considering the 10,5 and 8,7 SWNTs discussed above, the addition of 5 mM $CdCl_2$ to SDS-SWNTs results in a significant shift of the excitation wavelength of each SWNT. The resulting shift in the emission wavelengths are different for each n,m value, and thus, the apparent "selectivity" observed in the fluorescence spectra from 660 and 785 nm excitation is actually a result of different shifts in the emission spectrum that cannot be fitted using commercial software. The resulting combined peaks happen to look like there is selective quenching!

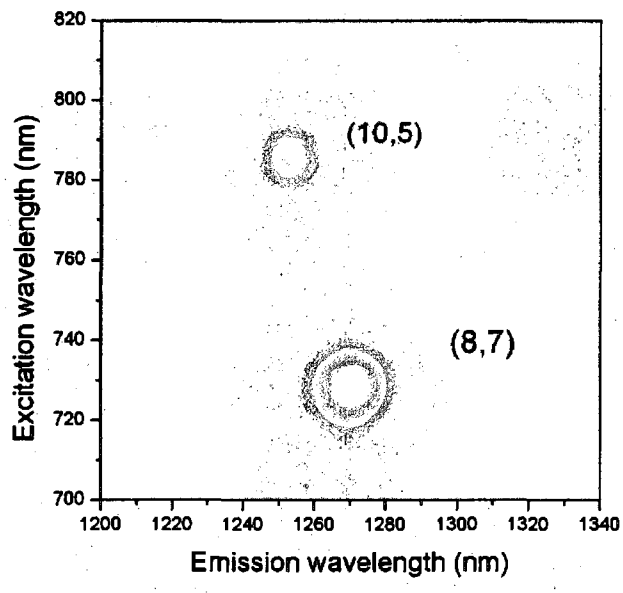

Figure 3.10. The 2D excitation and emission plot of the 10,5 and 8,7 SWNTs for (a) SDS-SWNTs and (b) SDS-SWNTs in the presence of 5 mM $CdCl_2$.

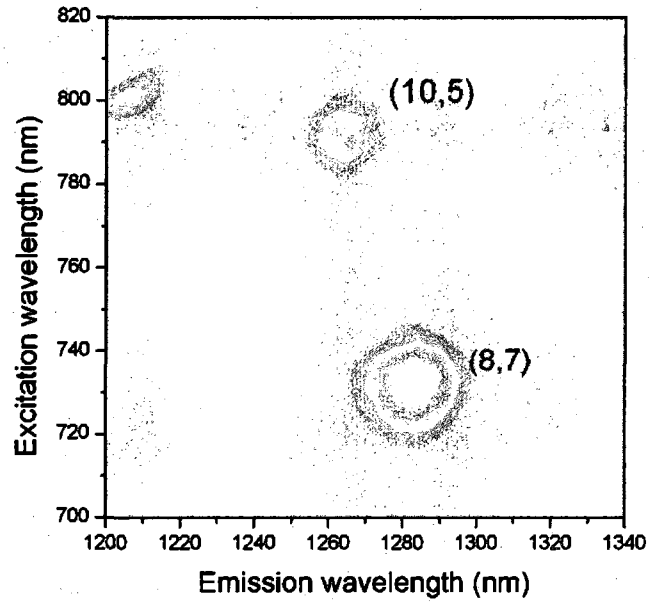

Figure 3.10, contd. The 2D excitation and emission plot of the 10,5 and 8,7 SWNTs for (a) SDS-SWNTs and (b) SDS-SWNTs in the presence of 5 mM $CdCl_2$.

Careful observation of the spectra (Figure 3.7) shows that the different chirality nanotube's emission wavelengths are shifted by all metals but to varying degrees, Figure 3.11. This is expected, however, because the different chirality nanotubes have different electronic structures (bandgaps) and diameters. The plots of the emission wavelength shifts in relation to the bandgap and diameter of the SWNT are very similar, Figure 3.12. This is not surprising given the near inverse relationship between the diameter and bandgap. Both variables correlate well with the observed shifts, and the interdependency of the two makes it impossible to assign the effect to one variable or another.

With an understanding that the peaks in the fluorescence spectrum are shifted when Zn^{2+}, Cd^{2+} and $Hg^{2+}$are added, it is still possible to measure the intensity of 11 (n,m) values as a function of metal concentration. As may be seen from Figure 3.13, the corrected decreases in fluorescence intensity of 4 representative nanotubes do not follow

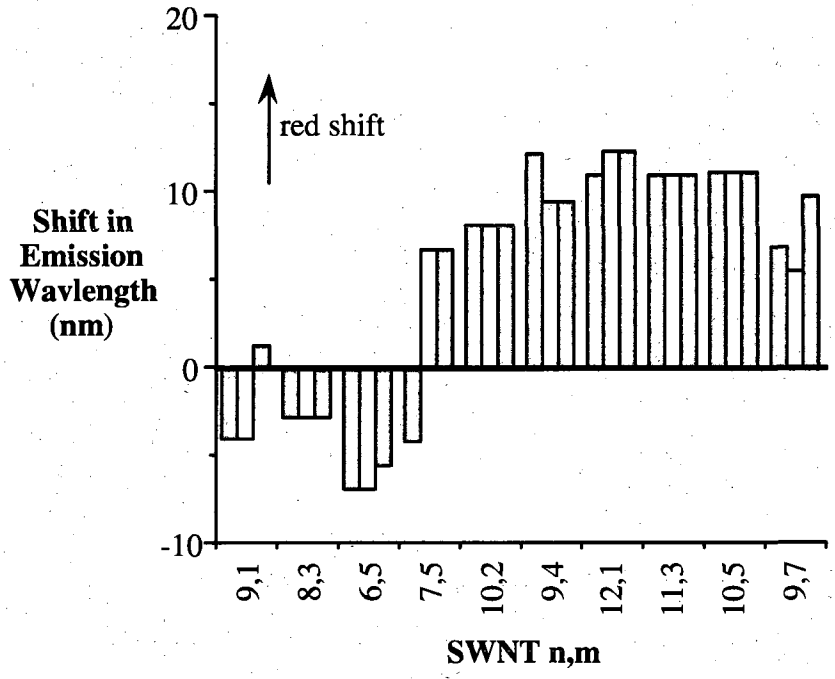

Figure 3.11. Shift (red = +ve, blue = -ve) of the emission wavelength for selected SWNT n,m values for the addition of 5 mM of $ZnCl_2$ (□), $CdCl_2$ (□), and $HgCl_2$ (□) for 785 nm irradiation showing the dependence on both the SWNT, n,m and the metal cation.

the trend expected from Stern-Volmer behavior. Instead there appears to be a critical concentration of metal ion, $[M^{2+}]_c$, that causes a step change in fluorescence intensity. Above this concentration there appears to be no significant further reduction in fluorescence intensity. An important observation is that the critical concentration is not the same for each SWNT (n,m) value, i.e., it is chirality dependent. Notice in Figure 3.13 that the 10,5 and 12,1 nanotubes have a critical concentration at 1.0 mM while the 7,5 nanotube is at 1.5 mM and the 9,1 tube is closer to 2.0 mM. To better assess this event, the critical concentration, ($[M^{2+}]_c$), was determined for each of the n,m nanotubes to determine if there were any trends present. There is no apparent relationship between the $[M^{2+}]_c$ and the band gap or the diameter of the SWNTs, as is evident in Figure 3.14. A distinct relationship between the identity of the metal ion and the critical concentration

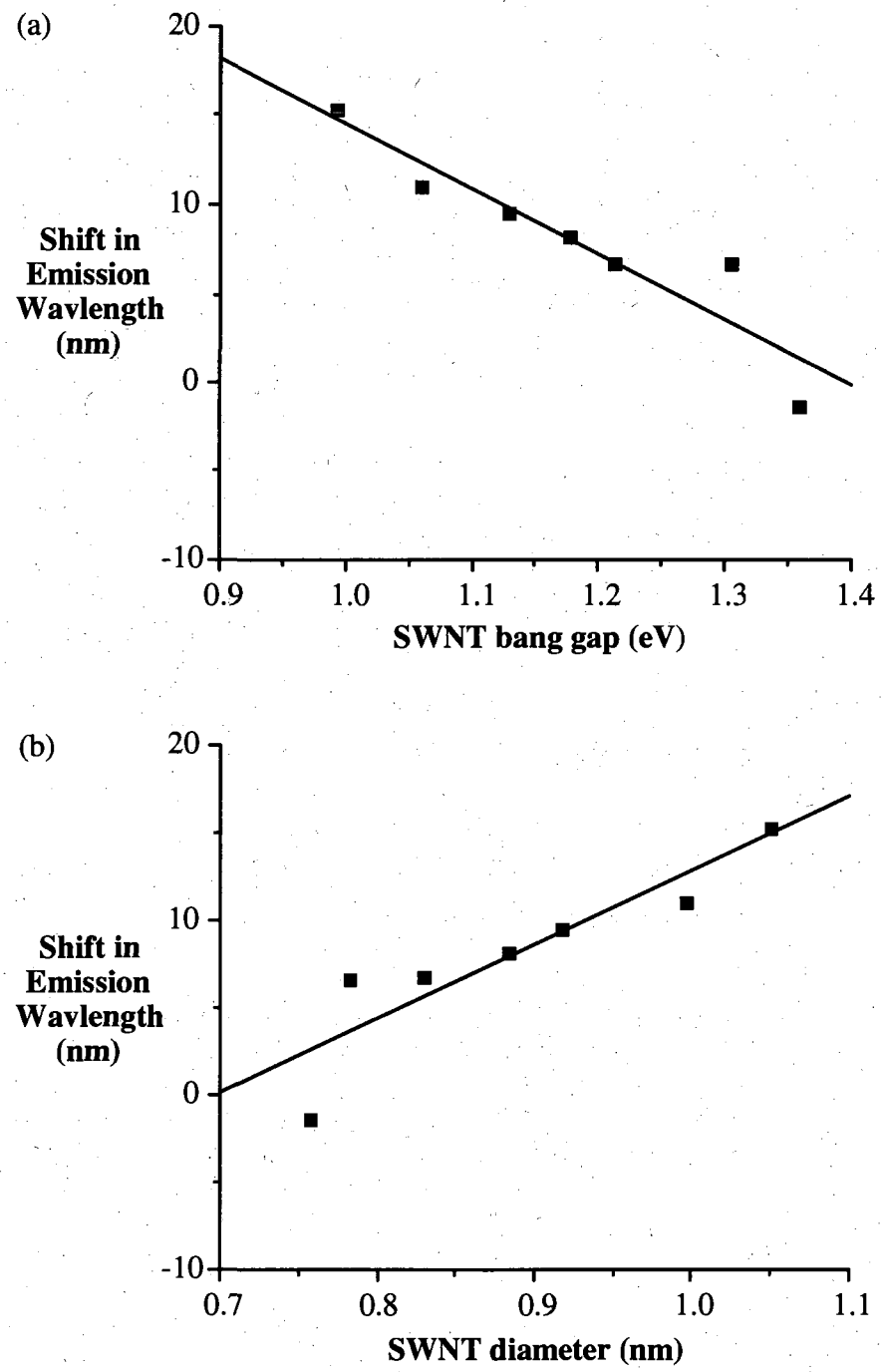

Figure 3.12. Plot of shift in emission wavelength as a function of (a) SWNT band gap ($R^2 = 0.870$) and (b) SWNT diameter ($R^2 = 0.814$).

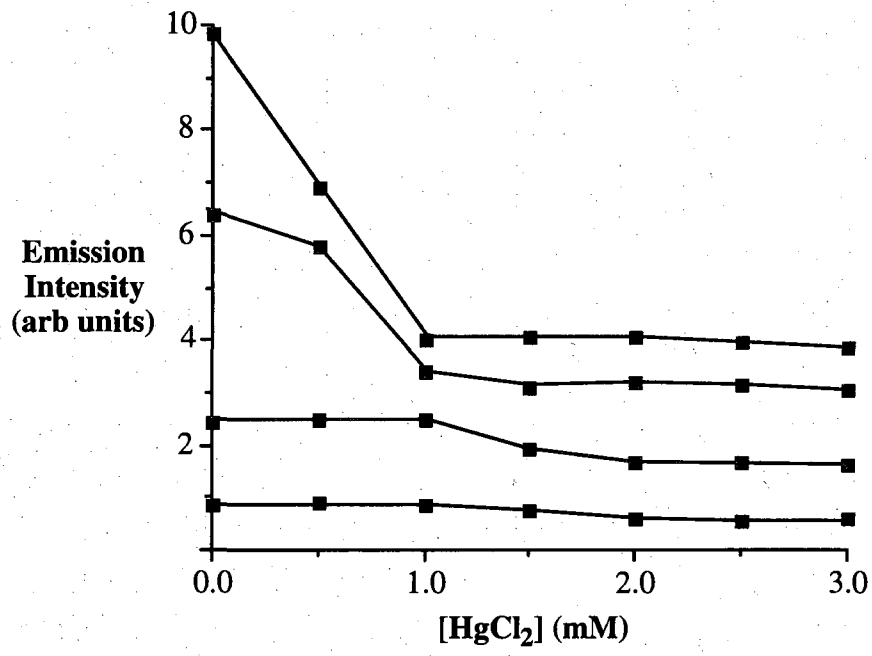

Figure 3.13. Plot of fluorescence intensity as a function of concentration of $HgCl_2$ for 10,5 (■), 12,1 (■) 7,5 (■), and 9,1 (■) SWNTs showing the dependence on the SWNT chirality of the step-change in fluorescence intensity. All intensities are corrected for shifts in the emission spectra.

exists in Figure 3.15. The general trend follows that $[Zn^{2+}]_c > [Cd^{2+}]_c > [Hg^{2+}]_c$ for a given n,m chirality nanotube.

Previous examples of abrupt changes in fluorescence intensity that are not associated with SWNT bundling involve changes in the dielectric constant or changes in the surfactant wrapping of the SWNT. The addition of acid to SWNT solutions reacts reversibly with preadsorbed oxygen to protonate the sidewalls of the SWNTs.[24] This change in dielectric constant bleaches the fluorescence of the nanotubes. DNA wrapped SWNTs were shown to undergo a conformation change when exposed to $HgCl_2$ in

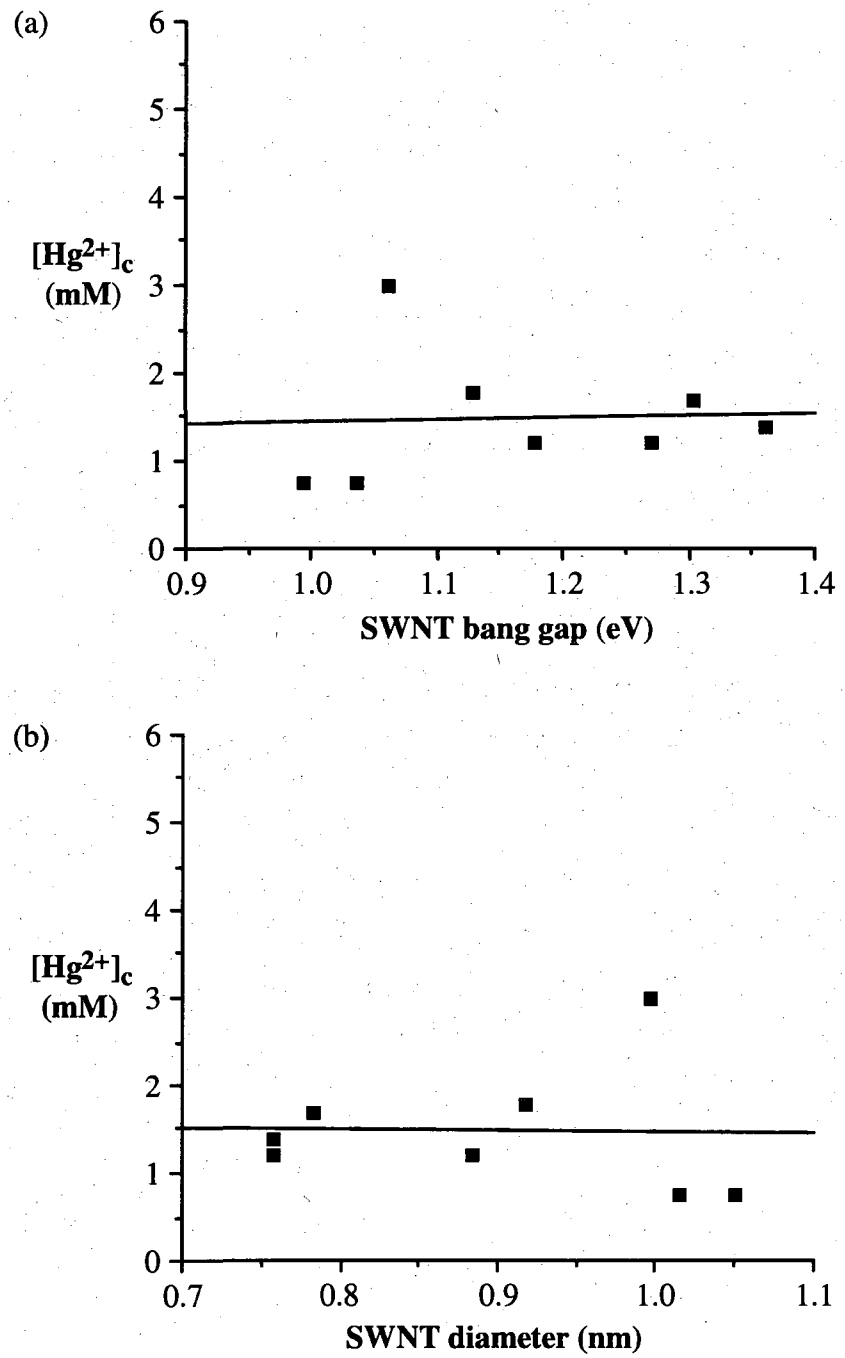

Figure 3.14. Critical concentration of $HgCl_2$ as a function of (a) SWNT bang gap and (b) SWNT diameter.

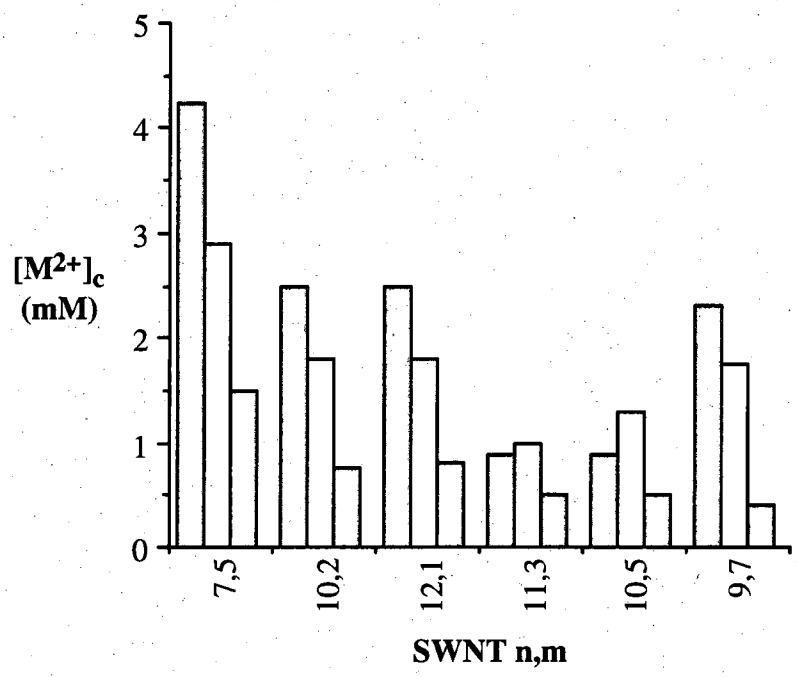

Figure 3.15. Critical concentration of M^{2+} (mM) as a function of SWNT n,m value for $ZnCl_2$ (□), $CdCl_2$ (□), and $HgCl_2$ (□) for 785 nm irradiation.

solution.[25] The transition from a B configuration to a Z structure simultaneously caused an abrupt decrease in the fluorescence intensity due to the rearrangement of the surfactant around the nanotubes. This presumably also induced a change in the dielectric constant near the surface of the nanotube.

For SDBS-surfacted SWNTs, the interaction of the metal ions with the surfactant (M^{2+}···SDBS) is weaker than the interaction of the surfactant with the SWNT (SDBS···SWNT). Thus, the addition of either Group 2 or 12 metals does not appear to alter the surfactant micellular structure around the SWNT. Instead, the fluorescence of the SWNTs is decreased due to the localized presence of the metal ion's charge. In contrast, in the case of SDS, the interaction of the surfactant with the SWNT is limited by van der Waal interactions and the structure of the SDS-SWNT conjugate is overcome by the addition of the Group 12 metal but not by Group 2 metals. This differentiation can be

rationalized by a consideration of the relative hardness of the metal ions and the sulfonate and sulfate "ligands".

Group 2 metals can be considered to be hard Lewis acids, will be mostly solvated in solution, and will form primarily ionic interactions with the surfactants. The closeness of the metal ion to the SWNT surface will solely depend on the surfactant···SWNT interaction (i.e., Figure 3.5). Group 12 metals will essentially form covalent bonds to the surfactants. With SDBS, this results in the forcing of the Group 12 metal ion close to the surface of the SWNT but without overcoming the π-π interactions between the SDBS and the SWNT surface. Based upon known crystal structure data for sulfonate and sulfate "ligands" complexes,[26] we propose that the Group 12 metal ions will form strong covalent complexes with the surfactant, which with SDS causes a rearrangement of the surfactant···SWNT conjugate structure. As the metal concentration reaches a critical level we propose it forces the restructuring of the micelle (Figure 3.16). The rearrangement of the solvation environment around the SWNT results in a change in the dielectric constant around the SWNT.[24] Further support for this surfactant rearrangement is evident in the lack of observed quenching. It follows that surfactant binding to the metal ion rearranges the surfactant and lifts the metal ion away from the surface of the nanotubes such that no quenching can occur. Thus, a constant fluorescence intensity is achieved as observed in Figure 3.13.

The general trend observed in Figure 3.15 is in line with the size and relative coordinative ability of the metal ions causing disruption of the micelle. The small size of Zn^{2+} limits the number of surfactant head groups to which it can coordinate while the larger size of Hg^{2+} permits the disruption of more surfactant molecules. Thus, it follows that the amount of Hg^{2+} needed to disrupt the same number of surfactant molecules as Zn^{2+} is less.

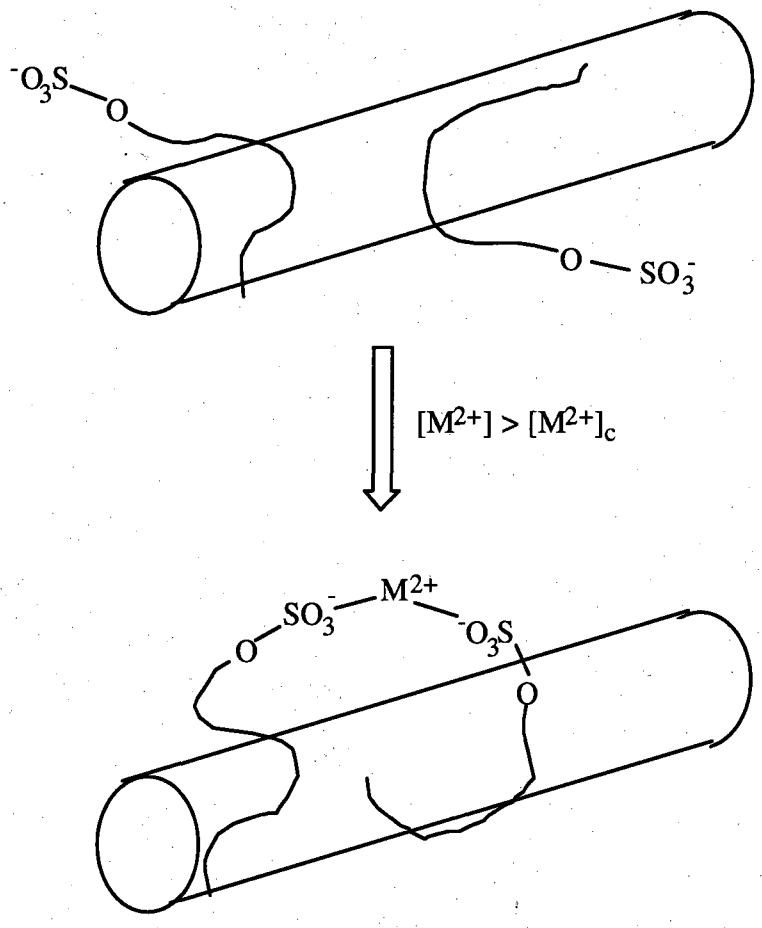

Figure 3.16. Schematic representation of the reorganization of the SDS surfactant micellular structure around a SWNT promoted by the addition of a Group 12 metal ion.

Conclusions

The solubilization of unfunctionalized SWNTs into aqueous solution is going to be increasingly important especially in regard to both biological and environmental issues.[27] It is therefore imperative to understand how various solubilization agents interact with the SWNT. Based upon the above results, we propose that an investigation of the quenching of fluorescence of anionic surfacted SWNTs by Group 2 metals allows for an indirect observation of the structure of the surfactant-SWNT conjugate. For example, the greater quenching (higher K_{SV}) observed for SDBS-SWNTs as compared to

SDS-SWNTs is consistent with the metal being held closer to the SWNT surface; the ground state changes observed for SDS-SWNT conjugates are consistent with a rearrangement of the surfactant micelle. We propose that future studies on additional anionic surfactants will offer insight into both the structure and stability of surfactant···SWNT conjugates.

Experimental

All chemicals were obtained commercially and used without further purification. All solutions were prepared as described in Chapter 1. Sodium dodecyl sulfate (SDS) wa obtained from Sigma-Aldrich and used as received. Fluorescence, Raman, ICP and UV-vis data were collected as described in the experimental sections of Chapters 1 and 2. Photoluminescence data was collected using a J-Y Spex Fluorolog 3-211 spectrofluorometer equipped with a liquid N_2-cooled InGaAs detector. All emission intensities were corrected for the wavelength dependencies of the instrument's excitation and detection systems.

References

1 J. J. Brege, C. Gallaway, and A. R. Barron, *J. Phys. Chem. C,* 2007, **111**, 17812.

2 J. J. Brege, C. Gallaway, and A. R. Barron, *J. Phys. Chem. C,* 2008, in press.

3 R. Loscutova, and A. R. Barron, *J. Mater. Chem.*, 2005, **15**, 4346.

4 V. C. Moore, M. S. Strano, E. H. Haroz, R. H. Hauge, and R. E. Smalley, *Nano Lett.*, 2003, **3**, 1379.

5 V. V. Didenko, V. C. Moore, D. S. Baskin, and R. E. Smalley, *Nano Lett.*, 2005, **5**, 1563.

6 P. K. Rai, A. N. G. Parra-Vasquez, J. Chattopadhyay, R. A. Pinnick, F. Liang, A. K. Sadana, R. H. Hauge, W. E. Billups, and M. Pasquali, *J. Nanosci. Nanotechnol.*, 2007, **7**, 3378.

7 R. E. Anderson and A. R. Barron, *J. Nanosci. Nanotechnol.*, 2007, **7**, 3436.

8 J. Chattopadhyay, A. K. Sadana, F. Liang, J. M. Beach, Y. Xiao, R. H. Hauge, and W. E. Billups, *Org. Lett.*, 2005, **7**, 4067.

9 Treatment of cetyl trimethylammonium bromide (CTAB) and dodecyltrimethyl ammonium bromide (DTAB) surfacted SWNTs with either Group 2 and Group 12 metal ions showed no reduction in fluorescence in the range of 0 to 5.0 mM of quencher. J. J. Brege and A. R. Barron, unpublished results.

10 McDonald, T. J.; Engtrakul, C.; Jones, M.; Rumbles, G.; Heben, M. J. *J. Phys. Chem. B.,* **2006**, *110*, 25339.

11 V. V. Didenko, V. C. Moore, D. S. Baskin, and R. E. Smalley, *Nano Lett.*, 2005, **5**, 1563.

12 K. Yurekli, C. A. Mitchell, and R. Krishnamoorti, *J. Am. Chem. Soc.,* 2004, **126**, 9902.

13 H.-P. Hentze, S.R. Raghavan, C.A. McKelvey, and E.W. Kaler, *Langmuir,* 2003, **19**, 1069.

14 A. Whitsitt and A. R. Barron, *J. Coll. Interf. Sci.*, 2005, **287**, 318

15 S. Niyogi, S. Boukhalfa, S. B. Chikkannanavar, T. J. McDonald, M. J. Heben, and S. K. Doorn, *J. Am. Chem. Soc.,* 2007, **129**, 1898.

16 H. Adams, C. A. Hunter, K. R. Lawson, J. Perkins, S. E. Spey, C. J. Urch, and J. M. Sanderson, *Chem. Eur. J.*, 2001, **7**, 4863.

17 Applied NanoFluorescence, Houston TX.

18 M. J. O'Connell, E. E. Eibergen, and S. K. Doorn, *Nature Mater.* 2005, **4**, 412.

19 R. B. Weisman and S. M. Bachilo, *Nano Lett.,* 2003, **3**, 1235.

20 Y. Tan and D. E. Resasco, *J. Phys. Chem. B,* 2005, **109**, 14454.

21 R. Loscutova, and A. R. Barron, *J. Mater. Chem.*, 2005, **15**, 4346.

22 It should be noted that no shift in the absorption spectra is observed for either SDBS-SWNTs or SDS-SWNTs in the presence of Group 2 metal ions.

23 S. M. Bachilo, M.S. Strano, C. Kittrell, R. H. Hauge, R. E. Smalley, and R. B. Weisman, *Science,* 2002, **298**, 2361.

24 M. S. Strano, C. B. Huffman, V. C. Moore, M. J. O'Connell, E. H. Haroz, J. Hubbard, M. Miller, K. Rialon, C. Kittrell, S. Ramesh, R. H. Hauge, and R. E. Smalley, *J. Phys. Chem. B,* 2003, **107**, 6979.

25 D. A. Heller, E. S. Jeng, T. – K. Yeung, B. M. Martinez, A. E. Moll, J. B. Gastala, and M. S. Strano, *Science*, 2006, **311**, 508.

26 A. Keys, T. Barbarich, S. G. Bott, and A. R. Barron, *J.Chem. Soc., Dalton Trans.*, 2000, 577.

27 C. M. Sayes, F.e Liang, J. L. Hudson, J. Mendez, W. Guob, J. M. Beach, V. C. Moore, C. D. Doyle, J. L. West, W. E. Billups, K. D. Ausman, and V. L. Colvin, *Toxicol. Lett.*, 2006, **161**, 135.

Chapter 4

Ultra-Small Copper Nanoparticles from a Hydrophobically Immobilized Surfactant Template

Introduction

Nanotechnology has dominated chemical research in the past decade because unlike bulk materials, properties at the nanoscale can be controlled by altering the size of the material. Copper and copper oxide nanoparticles are of great interest because they have potential in a wide variety of areas including optical, catalytic, electronic, and antifouling applications.[1] Copper nanoparticles have been produced using many methods such as using supercritical carbon dioxide,[2,3] water-in-oil microemulsions,[4] high temperature decomposition of organometallic precursors,[5] and a polyol reduction method.[6] Polymer composites containing copper nanoparticles have been shown to possess antibacterial and antifungal properties.[7,8,9] Copper particles can also be used to fabricate other useful nanomaterials. For instance, they are used as catalysts for the growth of single walled carbon nanotubes.[10]

Even as nanofabrication methods have become routine in the last few decades, several challenges still persist. First, producing small nanoparticles (i.e., less than 10 nm) can be daunting. As the diameter of particles decreases, the positive attribute of surface area increases (relative to volume), but the surface energy also increases which favors the aggregation of small particles, or ripening, into larger particles. When successful production of small nanoparticles is achieved, they are often accompanied by large nanoparticles yielding a polydisperse sample. It may be possible to extract the small particles that are of interest, however, the overall yield is low. Thus, it is advantageous to produce a narrowly disperse product that does not require complicated separation techniques.

A second desirable goal is to be able to produce nanomaterials in an environmentally friendly way. Green syntheses are not only categorized as those who use environmentally friendly solvents but are also extended to those processes that have low energy consumption and simplified experimental techniques. Therefore, it is advantageous to develop new synthetic procedures that are more efficient, use less energy, and produce the desired product with little or no side products. When dealing with nanomaterials, a synthetic route to produce small, narrowly dispersed particles that do not require complicated or harsh chemical treatments is paramount.

For many applications, small nanoparticles are better than larger ones because they have a higher surface area to volume ratio. In order for small particles to exist, a limited number of ions need to be restricted to an area before reduction. Reverse micelle systems fix the number of ions that can be reduced by trapping them in the water core of the micelle forming small particles. A reverse micelle systems is limited, however, because the structure of the micelle is dynamic and the surfactant molecules are free to move in solution. Furthermore, not all the micelles are exactly the same size, therefore, each micelle will have a different number of metal ions and produce different size particles. In search of a more rigid system where nanoparticle formation can be guided during reduction, it is no surprise that several groups have turned to carbon nanotubes as templates for nanoparticle growth.[11,12,13]

Multi walled carbon nanotubes (MWNTs) have been used as templates for the synthesis of copper oxide nanoparticles.[14] The nanotubes were first filled with copper ions and then calcinated at 450 °C for 5 hours. The rigorous treatment however only produces rod-like CuO particles that are 20 - 90 nm in diameter and up to 700 nm long. Furthermore, destruction of the template is required to obtain the particles. The advantage of having a nanotube template to control size is offset by the extreme synthesis required. In another report, carbon nanotubes with diameters between 5 and 10 nm were used as a template to produce copper nanoparticles and nanofibers.[12] This high temperature

method (>773 K) revealed that the size of the particles obtained by hydrogen reduction was restricted by the diameter of the nanotube; therefore all the particles were less than 10 nm.

Wang et al. have used single walled carbon nanotubes (SWNTs) dispersed in poly(styrene-alt-maleic acid) (PSMA) to form a nanotube and metal nanoparticle assembly.[13] Particles (3 - 6 nm) are formed on the PSMA that is adhered to the nanotube, forming a rigid assembly that is stable for weeks; however there is no mention of being able to separate the particles for uses other than in a SWNT assembly. To our knowledge, there are no reports of using SWNTs as templates to form small (<2 nm) metallic nanoparticles that can be used for subsequent processing. The diameter of SWNTs ranges from 0.7 nm to 2 nm. Carefully exploiting the templating nature of the SWNTs, one should be able to obtain nanoparticles less than 2 nm in diameter.

Results and Discussion

In Chapters 2 and 3, it was found that positively charged copper ions interact with the adsorbed surfactant head groups causing large local concentrations of copper ions near the nanotube surface. Local metal ion concentration is enhanced in the vicinity of the nanotube causing fluorescence quenching. In that study, the large local concentrations caused increased fluorescence quenching as compared to their Group 2 analogs, Figure 4.1. In the current study, we introduced SWNTs as a scaffold to limit the mobility of the metal ions in solution; therefore, the physical aspect of SWNTs is used to our advantage. Single walled carbon nanotubes are individualized in solution with sodium dodecylbenzene sulfonate (SDBS). The SWNT immobilizes the hydrophobic tails of the surfactant onto the nanotube, leaving the hydrophilic negatively charged sulfonate groups extending into the solution. Copper chloride ions are electrostatically fixed near the surfactant head groups. Reduction with N,N,N',N'-tetramethyl-*p*-phenylenediamine

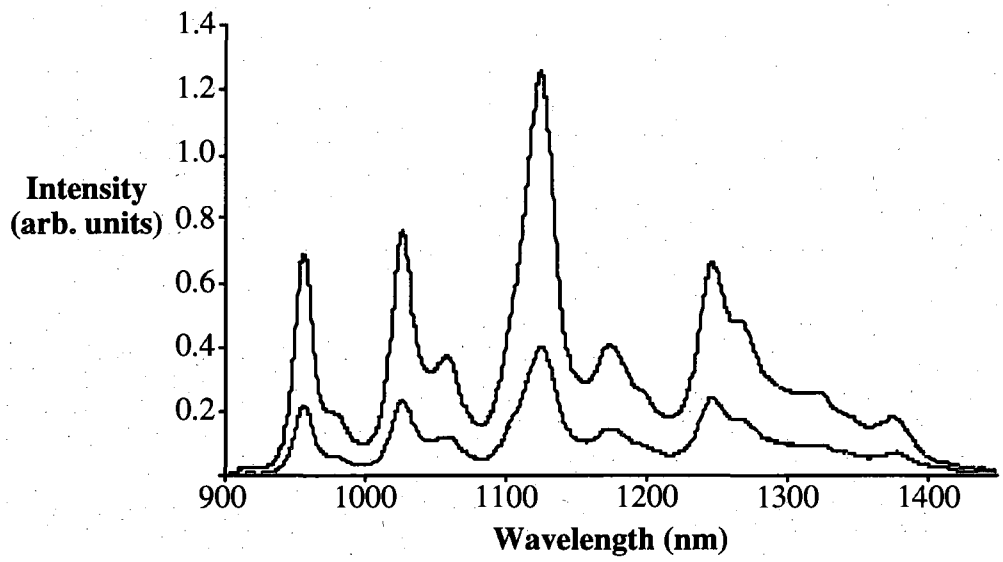

Figure 4.1. The fluorescence of SDBS-SWNTs (—) in solution and (—) in the presence of 5 mM $CuCl_2$.

(TMPDA) in the presence of citrate at room temperature produces ultra-small copper particles. The size of the nanoparticles is restricted by the number of copper ions concentrated in one area as observed by Wang et al.[13] The number of ions in close proximity to each other is dictated by the size of the scaffold i.e., the <2 nm carbon nanotube. Analyzing the particles using AFM reveals that a narrowly dispersed sample is produced where all the particles are less than 2 nm in diameter, Figure 4.2. Particle size analysis shows the plurality of the particles have diameters between 0.60 and 0.79 nm, Figure 4.3. This is precisely what is predicted using a SWNT template. Unlike other SWNT scaffold methods,[13] the particles do not adhere to the sidewalls of the tube, which allows them to be used in further processing.

It has been reported that carbon nanotubes are capable of spontaneously reducing metal ions on their sidewalls to produce particles as small as 2 nm.[15] In particular, Au and Pt easily form particles because their reduction potentials fall below the Fermi level of SWNTs. In agreement with these studies, we do not observe spontaneous formation of

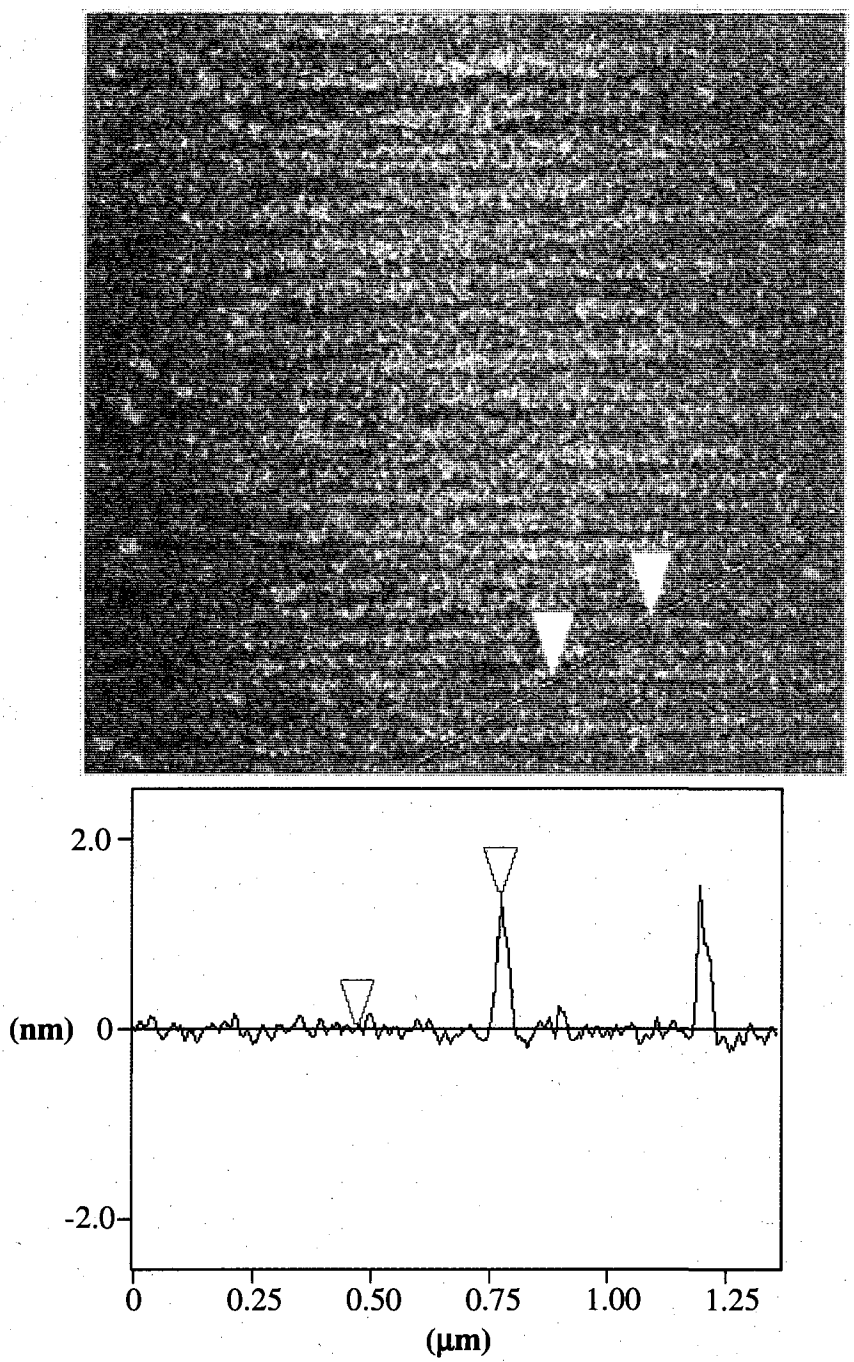

Figure 4.2. Representative AFM image (2 μm x 2 μm) and associated height profile of copper nanoparticles formed using SDBS-SWNT templates spin-coated on mica.

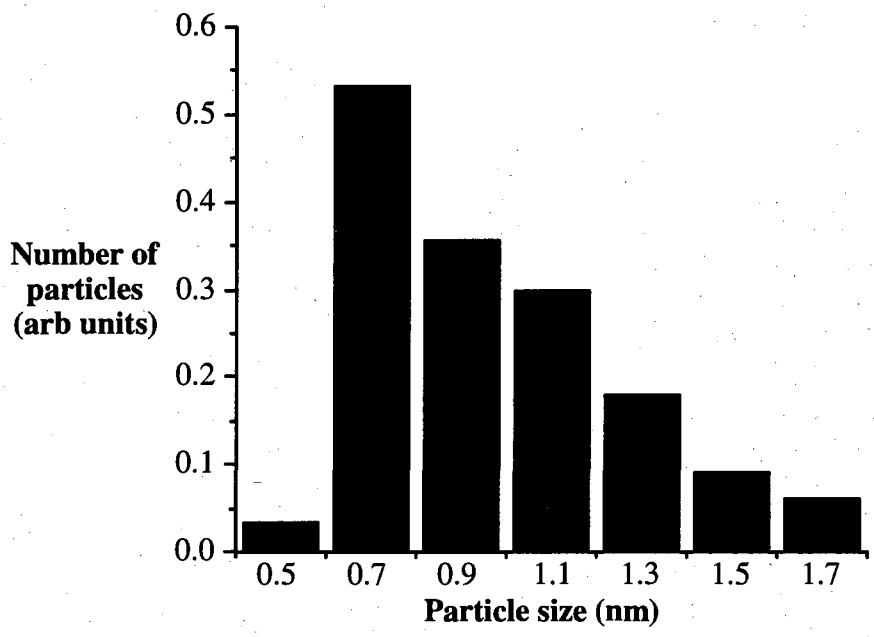

Figure 4.3. Particle size distribution of ultra-small copper nanoparticles analyzed by AFM height data.

copper particles. A control experiment was conducted with SDBS-SWNTs, citrate, and copper ions (in absence of reducing agent) and no particle formation was observed.

Similar to other phenylenediamine reducing agents, copper nanoparticle formation occurs from a single electron donation from each of the amine groups of TMPDA leaving $TMPDA^{+}$-Cl^{-} as the oxidized byproduct.[16,17] To ensure that the complete reduction of copper was achieved, X-ray photoelectron spectroscopy was conducted on a dried sample as shown in Figure 4.4. The major contribution of the Cu $2p_{3/2}$ peak (932.4 eV) is that associated with zero valent copper,[18] consistent with the electron diffraction data. However, the smaller contribution in Figure 3 (934.2 eV) along with additional peaks at 941.6 and 943.7 eV are consistent with CuO. The indicated Cu:CuO ratio of 2.8:1 suggest the Cu nanoparticles have a CuO shell. Attempts to minimize the CuO

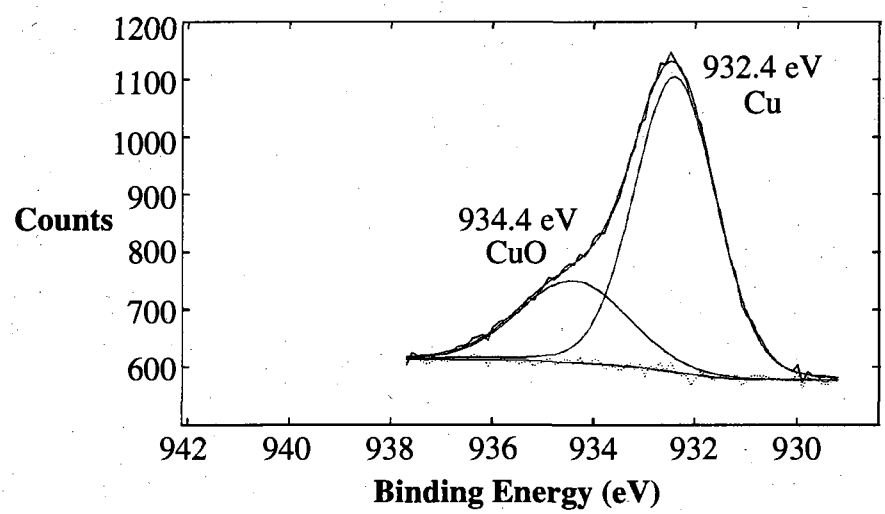

Figure 4.4. High-resolution Cu $2p_{3/2}$ X-ray photoelectron spectra of the Cu nanoparticles confirming the presence of Cu^0.

component through the use of excess reducing agent were not successful suggesting the oxide shell is formed upon exposure to the atmosphere.

Small diameter nanoparticles tend to aggregate in solution in order to lower the surface energy on the particles. In this synthesis, citrate was added to stabilize the particles and prevent them from aggregating together. In Figure 4.5, TEM images show the particles separated and without aggregation. Further, the crystallinity of the particles is clear based upon the observed lattice fringes at high resolution as well as the selected area electron diffraction (SAED) pattern consistent with metallic copper (Figure 4.6).

It has been reported that copper nanoparticles have a characteristic absorption plasmon peak around 570 nm.[19,20] Observation, or lack thereof, of this absorption peak can depend on several factors. For instance, when a copper chloride or copper oxide layer is present on the particles the absorption is not observed. In addition, it has been shown that as the particle size decreases, the prominent band at 570 diminishes. In fact, it is predicted that particles of less than 2 nm diameter will not exhibit a peak at all. This is

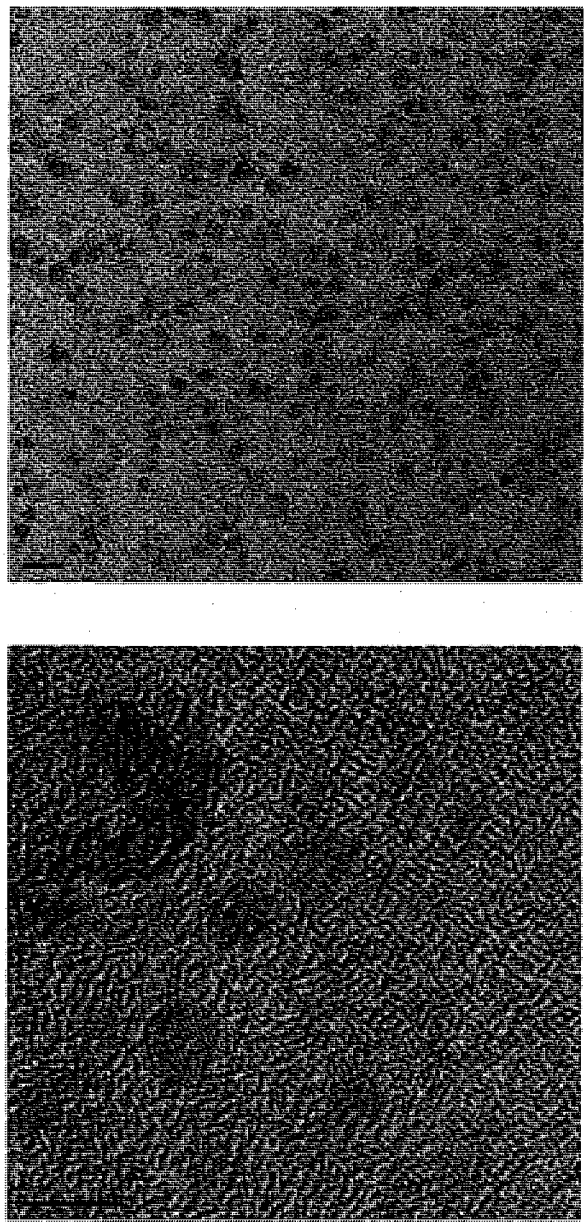

Figure 4.5. TEM images of ultra small copper nano particles. The top scale is 20 nm and the bottom scale is 5 nm.

in agreement with our studies where the absorption near 570 nm from the plasmon band is absent (Figure 4.7). Thus, the lack of plasmon absorption for our particles is due to a

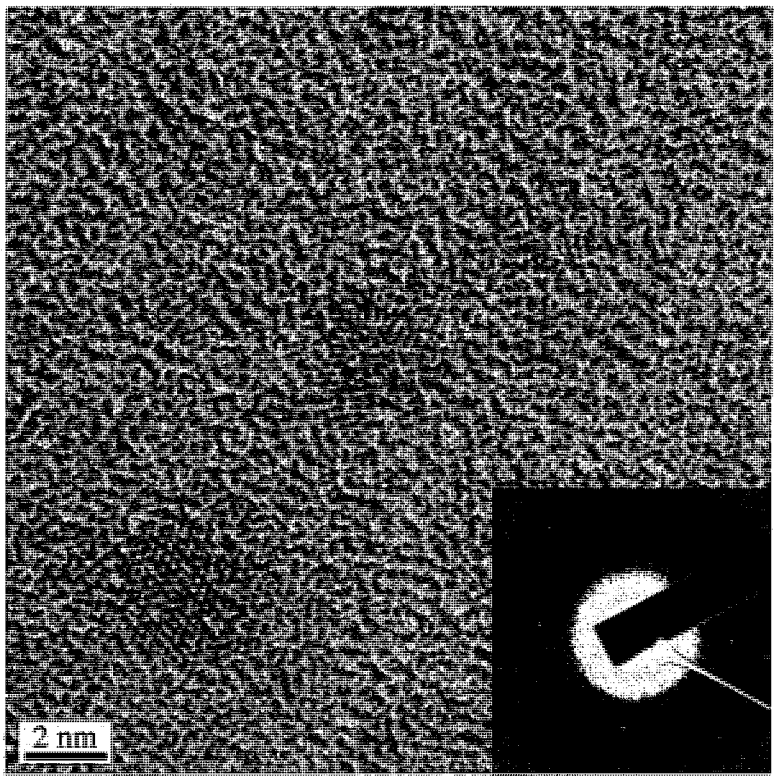

Figure 4.6. TEM image of ultra small copper nano particles including the selected area electron diffraction (inset).

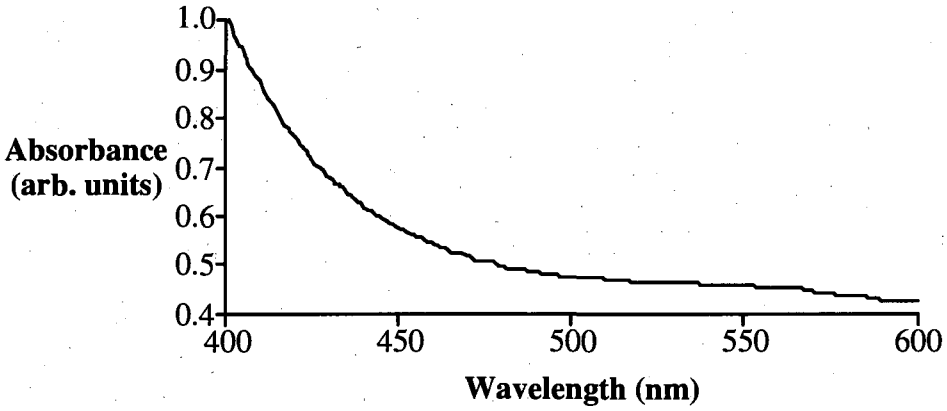

Figure 4.7. UV-vis absorption spectrum of ultra-small copper nanoparticles.

combination of small particle size and a thin copper oxide layer around the particles (c.f., Figure 4.4 and 4.6).

It is important to note that regular surfactant solutions are not sufficient to provide large concentrations of copper ions near each other to form small particles because the SDBS is not immobilized. The dynamic nature of surfactants in aqueous solutions and the hydrophillic nature of metal ions make it difficult to form uniform micellar reactors to produce metal nanoparticles. The dynamic nature of micelles can be restricted by using them in an organic solvent forming a reverse micelle system. The use of supercritical carbon dioxide affords the benefits of using a green solvent with tunable sizes, but the particles are relatively large and the method is cumbersome.[21] We have developed a method to make "static" micelles in aqueous solution for the synthesis of a few nanometer copper particles.

A number of control experiments were performed to confirm the interdependency of the SWNT/SDBS/Cu^{2+} system. It has been reported that carbon nanotubes are capable of spontaneously reducing metal ions on their sidewalls to produce particles.[22] A control experiment was therefore conducted with SDBS-SWNTs, sodium citrate, and $CuCl_2$ (in absence of reducing agent). No particle formation was observed indicating that the SWNTs do not act as a reducing source but as a template for the surfactant···metal interaction. To confirm the templating role of the SWNT, a control experiment was conducted where copper ions were reduced with TMPDA in the presence of SDBS surfactant and citrate, but without the SWNTs as a template to facilitate small particle formation. The TEM image in Figure 4.8 shows that some small nanoparticles are produced that are near 2 nm but a plethora of other diameter particles are also present. Without the SWNT template present to immobilize the surfactant and restrict the number of copper ions confined to an area, uncontrollable reduction proceeds, forming a wide dispersity sample. AFM confirms this very wide particle size distribution where particles can be as small as 2 nm but as large as 150 nm in diameter in Figure 4.9.

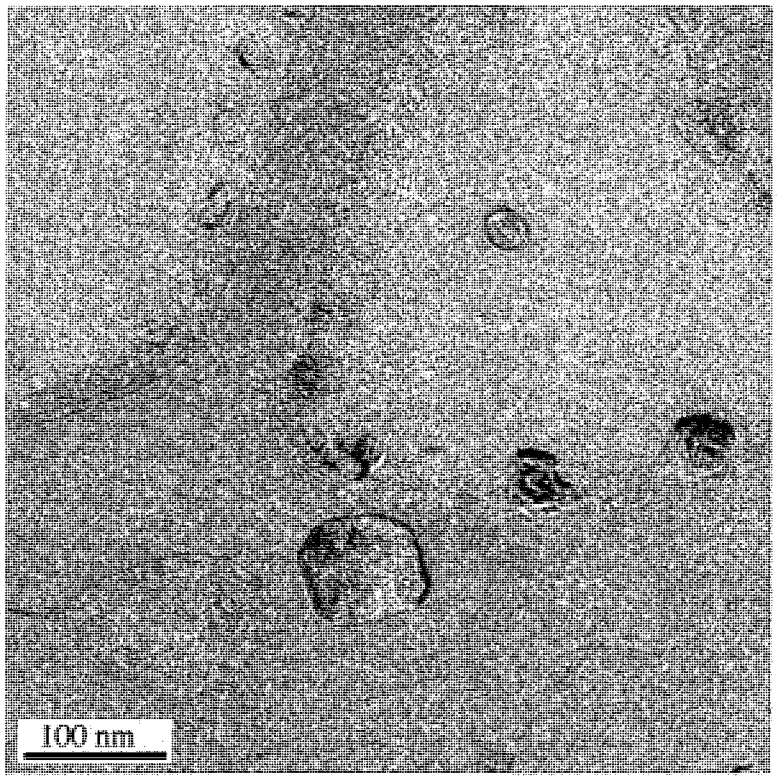

Figure 4.8. TEM image of copper nanoparticles produced in the absence of SWNTs.

The monodispersity of the copper particles produced can be attributed to the size of the SWNTs. The nanotube solution is a mixture of different chirality nanotubes, but they are all roughly the same diameter (0.7 to 1.4 nm). The small size of the copper particles can be ascribed to the templating nature of the SWNTs. The hydrophobically immobilized surfactant tails force the cupric ions to be in close proximity, which reduces their mobility. Upon reduction, the particle size is confined to the small number of copper ions in close proximity to each other.

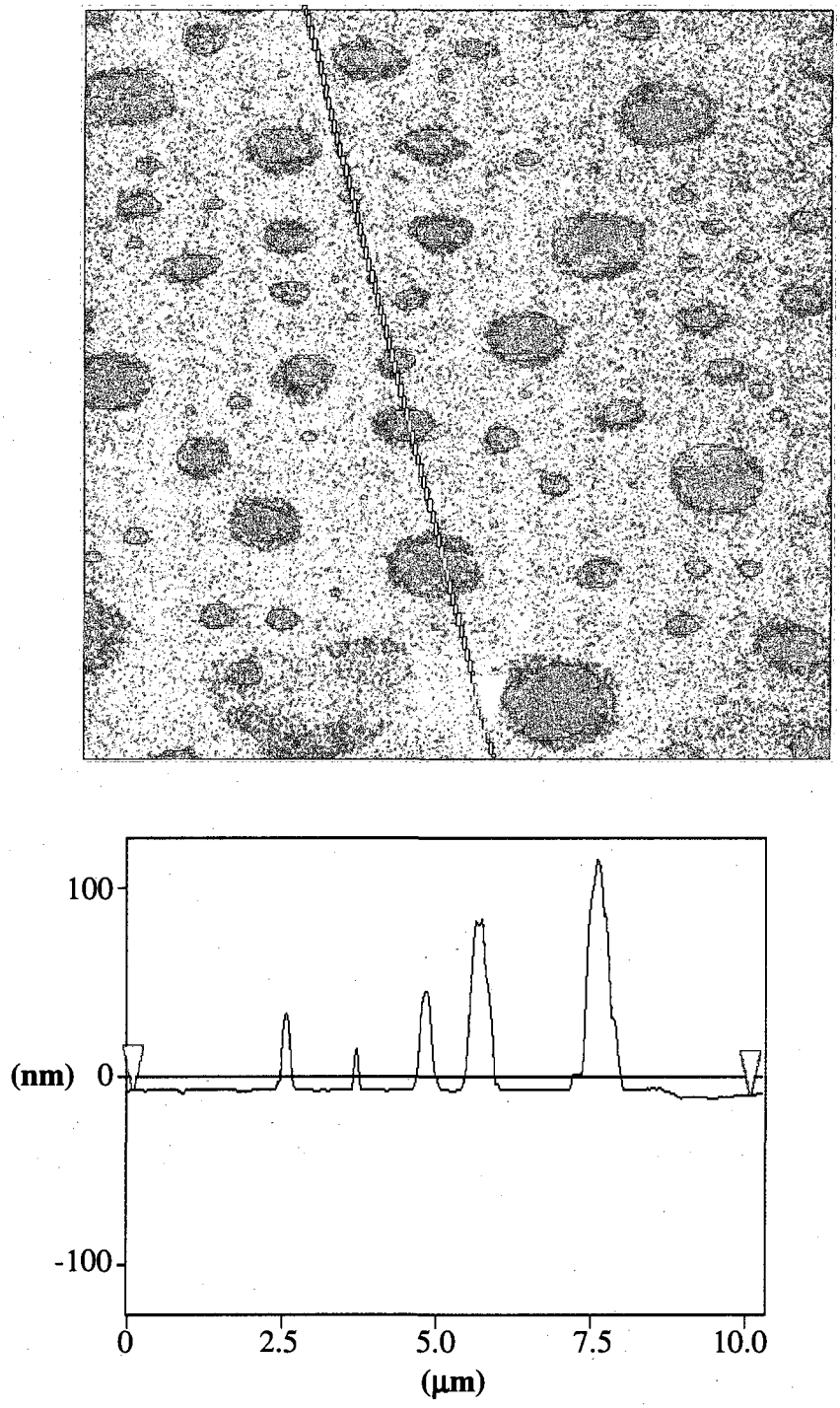

Figure 4.9. Representative AFM image (10 μm x 10 μm) and associated height profile of copper nanoparticles produced in the absence of SWNTs spin-coated on mica. Heights range from 2 nm to > 100 nm.

Conclusions

In conclusion, we have developed a method to make "static" micelles in aqueous solution for the synthesis of metal nanoparticles. We have demonstrated that the formation of a SWNT-surfactant conjugate modifies the size and templating effect of the surfactant as compared with the surfactant alone. As a result ultra-small (< 5 nm) copper nanoparticles may be prepared. The SWNT template technique should be applicable to other nanoparticle syntheses where a reduction in size and narrowing of dispersity is desired. We propose that the concept of using a hydrophobically immobilized SWNT template may be extended to other carbon materials with the potential for creating a range of size and shaped nanoparticles with a high degree of control and unlike those made by other methods.

Experimental

All chemicals were obtained commercially and used without further purification. All solutions and surfacted nanotubes were prepared as described in Chapter 1. The metal salt $CuCl_2$, technical grade sodium dodecylbenzene sulfonate (SDBS), and 99% N,N,N',N'-tetramethyl-p-phenylenediamine (TMPDA) was used as received from Sigma Aldrich. Absorption spectra were collected on a Varian Cary 400 spectrophotometer and all measurements were taken at room temperature (298 K). XPS data was recorded on a Physical Electronics Phi Quantera instrument. The base pressure was 5×10^{-9} Torr, with an Al cathode as the X-ray source set at 100 W with a pass energy of 40.00 eV for the survey scan and 26.00 eV for the high-resolution scan, 45° take off angle, and a 100 μm beam size. Atomic force microscopy (AFM) was performed using tapping mode on a Nanoscope V system. TEM images and SAED diffraction patterns were obtained on a Jeol-2100F field emission gun transmission electron microscope operated at 200 kV. Images were obtained using a CCD camera. Samples were prepared by drop drying a

dilute aqueous nanoparticle solution onto a 400 mesh copper grid with an ultra-thin holey carbon film (Ted Pella, Inc.).

Synthesis of 2 nm copper particles. In a round bottom flask, 3 mL of 1% SDBS-SWNTs was combined with 2 mL of 40 mM $CuCl_2$ (0.08 mmol) and stirred for 30 minutes. Next, 4 mL of 20 mM sodium citrate (0.08 mmol) was added dropwise and stirred for 30 minutes. The copper was reduced with 4 mL of 40 mM TMPDA (0.16 mmol) and stirred for 24 hours. Extraction and purification of the particles proceeded as follows. The reaction mixture (5 mL) was combined with 7 mL 1-butanol and stirred for five minutes. It was then centrifuged at 4400 rpm for 5 minutes. The aqueous layer was removed for characterization. An excess of ethanol was added and the solution was centrifuged at 4400 rpm for 5 minutes to crash the particles out of solution. The procedure was repeated several times to wash the particles in preparation for XPS and microscopy analysis.

References

1 K. C. Anyaogu, A. V. Fedorov, and D. C. Neckers, *Langmuir,* 2008, **24**, 4340.

2 H. Ohde, F. Hunt, and C. M.Wai, *Chem. Mater.*, 2001, **13**, 4130.

3 G. L. Williams, J. K. Vohs, J. J. Brege, and B. D. Fahlman, *J. Chem. Ed.*, 2005, **82**, 771.

4 L. Qi, J. Ma, and J. Shen, *J. Colloid Interface Sci.,* 1997, **186**, 498.

5 C. Crouse and A. R. Barron, *J. Mater. Chem.*, 2008, **18**, 4146.

6 B. K. Park, S. Jeong, D. Kim, J. Moon, S. Lim, and J. S. Kim, *J Colloid Interface Sci.,* 2007, **311**, 417.

7 N. Cioffi, N. Ditaranto, L. Torsi, R. A. Picca, E. De Giglio, L. Sabbatini, L. Novello, G. Tantillo, T. Bleve-Zacheo, and P. G. Zambonin, *Anal. Bioanal. Chem.,* 2005, **382**, 1912.

8 A. Esteban-Cubillo, C. Pecharroma´n, E. Aguilar, J. Santare´n, and J. Moya, S. *J. Mater. Sci.*, 2006, **41**, 5208.

9 N. Cioffi, L. Torsi, N. Ditaranto, G. Tantillo, L. Ghibelli, L. Sabbatini, T. Bleve-Zacheo, M. D'Alessio, P. G.; Zambonin, and E. Traversa, *Chem. Mater.*, 2005, **17**, 5255.

10 W. Zhou, Z. Han, J. Wang, Y. Zhang, Z. Jin, X. Sun, Y. Zhang, C. Yan, and Y. Li, *Nano Lett.*, 2006, **6**, 2987.

11 H.-Q. Wu, X.-W. Wei, M.-W. Shao, J.-S. Gu, and M.-Z. Qu, *Chem. Phys. Lett.*, 2002, **364**, 152.

12 P. Chen, X. Wu, J. Lin, and K. L. Tan, *J. Phys. Chem. B,* 1999, **103**, 4559.

13 D. Wang, Z.-C. Li, and L. Chen, *J. Am. Chem. Soc.,* 2006, **128**, 15078.

14 H.-Q. Wu, X.-W. Wei, M.-W. Shao, J.-S. Gu, and M.-Z. Qu, *Chem. Phys. Lett.*, 2002, **364**, 152.

15 H. C. Choi, M. Shim, S. Bangsaruntip, and H. Dai, *J. Am. Chem. Soc.,* 2002, **124**, 9058.

16 R. Munday, *Chem.-Biol. Interactions,* 1988, **65**, 133

17 Williams, G. L.; Vohs, J. K.; Brege, J. J.; Fahlman, B. D. *J. Chem. Ed.*, 2005, **82**, 771.

18 B. K. Park, S. Jeong, D. Kim, J. Moon, S. Lim, and J. S. Kim, *J Colloid Interface Sci.,* 2007, **311**, 417.

19 J. A. Creighton, and D. G. Eadon, *J. Chem. Soc., Faraday Trans.,* 1991, **87**, 3881.

20 E. Anno, M. Tanimoto, and T. Yamaguchi, *Phys. Rev. B,* 1988, **38**, 3521.

21 G. L. Williams, J. K. Vohs, J. J. Brege, and B. D. Fahlman, *J. Chem. Ed.*, 2005, **82**, 771.

22 H. C. Choi, M. Shim, S. Bangsaruntip, and H. Dai, *J. Am. Chem. Soc.,* 2002, **124**, 9058.

Conclusion

The extraordinary physical and chemical properties of SWNTs continue to make them attractive candidates for sensing applications, especially where harsh environments are encountered. While the list of potential applications for SWNTs in sensing roles grows, the need to fully understand basic interactions remains. Our research has revealed that the dominating interactions in surfactant···SWNT conjugates can be quite complex and unpredictable. For example, knowing the effect of a Group 12 metal ion on SDBS···SWNT conjugates may lead one to believe the interaction governs the quenching of the similar anionic SDS···SWNT conjugate, yet they yield profoundly different outcomes. While the two surfactants are often used interchangeably to disperse nanotubes, our results show that caution needs be taken in choosing due to the differences in their response to the presence of Group 12 metal ions.

We have shown that by monitoring fluorescence of SWNTs during metal ion interactions it is possible to gain insight into the physical and chemical aspects of surfactant···SWNT conjugates. The fundamental interactions of the conjugates with their environment must be understood before the material can be used in sensing applications. Applying this method and conducting studies on additional anionic surfactants will offer insight into both the structure and the stability of surfactant···SWNT conjugates, adding crucial information to our knowledge base.

In addition to the insight gained about SWNT···surfactant conjugates, the application of our research has lead us to the development of a method of making "static" micelles in aqueous solution for the synthesis of metal nanoparticles. We have demonstrated that the formation of a SWNT···surfactant conjugate modifies the size and templating effect of the surfactant as compared with the surfactant alone. As a result, ultra-small (< 2 nm) copper nanoparticles can be prepared. The SWNT template technique should be applicable to other nanoparticle syntheses where a reduction in size

with narrow dispersity is desired. We propose that the concept of using a hydrophobically immobilized SWNT template may be extended to other carbon materials with the potential for creating a range of size and shaped nanoparticles with a high degree of control and unlike those made by other methods.

The research presented in this thesis reiterates the need for an understanding of basic chemical interactions. We have shown that valuable information about the physical and chemical aspects of surfactant···SWNT conjugates may be gained through a series of experiments. This knowledge in itself is of great value to the scientific community, with the added benefit of utilizing the data to develop a novel synthesis technique to produce ultra small nanoparticles. We believe the template can be expanded to produce a broad range of other new nano-structures. As scientists, we must treat new discoveries with caution and never forget to look at the basic underlying principles that govern their glamour. At times this understanding may lead to new discoveries just as in our work.